GEOCHEMISTRY

A Translation of

ГЕОХИМИЯ

No. 7 1959

CONTENTS

Vinogradov, A. P., L. S. Tarasov, and S. I. Zykov. Isotopic composition of leads from the ores of the Baltic shield 689
Gerling, E. K., and Yu. A. Shukolyukov. Accumulation of A^{38} in uranium minerals 750
Baranov, V. I., and L. A. Khristianova. Radioactivity of the waters of the Indian Ocean 765
Borisenko, L. F. On the distribution of scandium in igneous rocks on the example of some massifs of the Soviet Union . . 770
Solodov, N. A. Geochemistry of rare-metal granite pegmatites 778
Ozerova, N. A. The use of primary dispersion halos of mercury in the search for lead-zinc deposits 793
Gerasimovskii, V. I., M. M. Kakhana, L. M. Rodionova, and V. A. Venkina. On the geochemistry of niobium and tantalum in the Lovozero alkalic massif 803
Frank-Kamenetskii, V. A. Discussion. Discussion of the position of alkali metals in the structure of beryl 813

Published by

The Geochemical Society

Translated and Produced by Royer & Roger, Inc.

GEOCHEMISTRY

A translation of the journal of the Academy of Sciences, U. S. S. R., devoted to geochemistry

A publication of the Geochemical Society, supported financially by a grant from the National Science Foundation.

Officers of the Society, 1961

Harold C. Urey, President
University of California
La Jolla, California

Robert M. Garrels, Vice President
Harvard University
Cambridge 38, Massachusetts

Konrad B. Krauskopf, Secretary
Department of Geology
Stanford University, California

George T. Faust, Treasurer
U. S. Geological Survey
Washington 25, D. C.

Tom F. W. Barth, Past President
Mineralogisk Museum
Oslo 45, Norway

Councilors

F. G. Houtermans, 1959-1961
University of Bern
Bern, Switzerland

A. E. J. Engel, 1959-1961
California Institute of Technology
Pasadena 4, California

Thure G. Sahama, 1960-1962
University of Helsinki
Helsinki, Finland

Ralph S. Cannon, Jr., 1960-1962
U. S. Geological Survey
Denver 14, Colorado

Franz E. Wickman, 1961-1963
Riks Museet
Stockholm 50, Sweden

O. Frank Tuttle, 1961-1963
Pennsylvania State University
University Park, Pennsylvania

Translation
Editor........Earl Ingerson
Managing
Editor.. John W. Winchester
Board of Associate Editors: Leason H. Adams, F. R. Boyd, Paul E. Damon, Michael Fleischer, Jack Green, T. S. Lovering, Duncan McConnell, Donald McGannon, Jr., Brian Mason, Jack Vallentyne, D. E. White.

Subscription Prices

Per year (eight issues). $20.00

To members of the Geochemical Society and to educational institutions $10.00

Single copies . . . . . . $2.00 and $4.00

Subscriptions and orders should be addressed to the Geochemical Society and sent to

Prof. Earl Ingerson
Dept. of Geology
The University of Texas
Austin 12, Texas

TRANSLITERATION

There is no ideal system of transliterating Russian; each has its advantages and disadvantages. For the translation of Geokhimiya we have chosen the system used by Chemical Abstracts, partly because of its wide acceptance by other journals and partly because of certain advantages in alphabetization of names. The principal differences between this system and others in common use are as follows:

Russian	Chem. Abs.	Others
Х	kh	h
Ц	ts	tz
Щ	shch	sch
Ю	yu	iu
Я	ya	ia

Translated by

ROYER and ROGER, Inc.

ISOTOPIC COMPOSITION OF LEADS FROM THE ORES OF THE BALTIC SHIELD

A. P. VINOGRADOV, L. S. TARASOV, and S. I. ZYKOV
V. I. Vernadskii Institute of Geochemistry
and Analytical Chemistry
Academy of Sciences USSR, Moscow

(ABSTRACT)

The isotopic composition of the galena lead and of the lead impurities from various ores of different genetic types and of different age from the whole territory of the Baltic shield has been determined. All together about 100 samples have been investigated. According to the isotopic lead composition two evolutional branches of leads stand out: the svekofennian and the karelian type. The svekofennian leads are more monotonous and are characteristic of higher values of all three isotopes with regard to Pb^{204} than the karelian leads. Besides leads corresponding to the age of their formation, a series of considerably more ancient leads than the ores and rocks including them has been found. A graph is proposed for calculating the age of leads according to their isotopic composition basing on ideas about the differentiation of terrestrial matter and empirical regularities of variations in the isotopic composition of synchronous leads (Table 7, Fig. 8). Some age groups of leads typical of the whole territory are singled out. Assumptions are made regarding the geological history of the shield on the basis of data on the isotopic compositions of leads.

1. GEOLOGICAL CHARACTERISTICS AND THE ISOTOPIC COMPOSITION OF LEAD FROM THE ORES OF THE BALTIC SHIELD

In an earlier paper, using the Hercynian ore deposits of Altai and Kalba [1] as examples, we showed that the isotopic composition of admixed lead in different ores can be used as a marker of geologic time and as an indicator of the character of ore genesis and of the source of the ore substance.

In the present work we extended these investigations to the oldest Precambrian ores and rocks.

At present it is possible to distinguish within the Baltic shield a number of large regions (zones) sharply differing from each other in geologic history and present day structure (Fig. 1).

There are no isotope data for the Caledonian zone of the northwestern part of the shield nor for its extreme southwestern part (the zone of Gothides, I, Fig. 1), and they will not be discussed here.

The Central and eastern parts of the shield are occupied by the Svecofennide zone and by the Fenno-Karelian (III) and Kolskian (V) belts of the Karelides, until recently regarded as younger than the Svecofennides. The two belts are separated by the pre-Karelian Marealbian zone (IV), which is older than the Svecofennian zone, and the Kolskian belt is bounded on the northwest by the ancient Murmansk block (VI) containing the oldest known rocks of the Baltic shield [2]. *

The variation in the isotopic composition of lead and its causes were discussed by A. P. Vinogradov in reference [3], and the application of the phenomenon to the problems of the present work, in our earlier papers [1, 4]. In the present work, for comparison and analysis, we used also the graphs of Pb^{207}/Pb^{204} -- Pb^{206}/Pb^{204} and Pb^{208}/Pb^{204} -- Pb^{206}/Pb^{204}. As before, we shall refer to them simply as the 207/206 and 208/206 graphs.

A detailed description of the ores is given in Tables 2 -- 6, where individual deposits are grouped into larger regional zones. The tables give also the absolute ages computed from the isotopic composition of the leads. The method of calculating ages, the accuracy of the results and an analysis of all this material will be discussed below.

The Svecofennides of Sweden and Finland. ** All ore deposits of the Svecofennian zone of Sweden and Finland are in the areas of the oldest rocks of the leptite series (Fig. 1, Table 1) containing ferruginous rocks (magnetite quartzites) in addition to the metamorphosed acid effusives and sedimentary rocks.

These supracrustal deposits are represented now by separate remnants preserved among the extensive exposures of gneisses and granites. They may be united into belts beginning in Sweden and continuing into Finland. All ore deposits of the Svecofennian zone of Sweden and Finland lie in these belts. The principal types of deposits are various iron ores (from metamorphosed sedimentary ores to metasomatic and migmatitic ores) and polymetallic ores [5, 6].

The series of leads from the central region of Sweden shows a remarkable uniformity of isotopic composition (Table 2) in the samples from Utö (No. 1)***, Långban (No. 2, 116) and Falun (No. 7), in spite of the mineralogical difference of the ores (hematite, galena). The ores of Utö and Långban differ greatly in the degree of metamorphism but belong to the primary sedimentary type. The Falun ores, although deposited by a more

---

*By the kind permission of A. A. Polkanov and E. K. Gerling, we used in this paper a number of ages reported at the VIII meeting of the Committee for Determination of Absolute Age of Geological Formations, which met in Moscow in May of 1959.

**The geological descriptions are based entirely on published data. References are given to the principal sources only.

***Number of sample as given in Tables 2 -- 6 and Figs. 1 and 2.

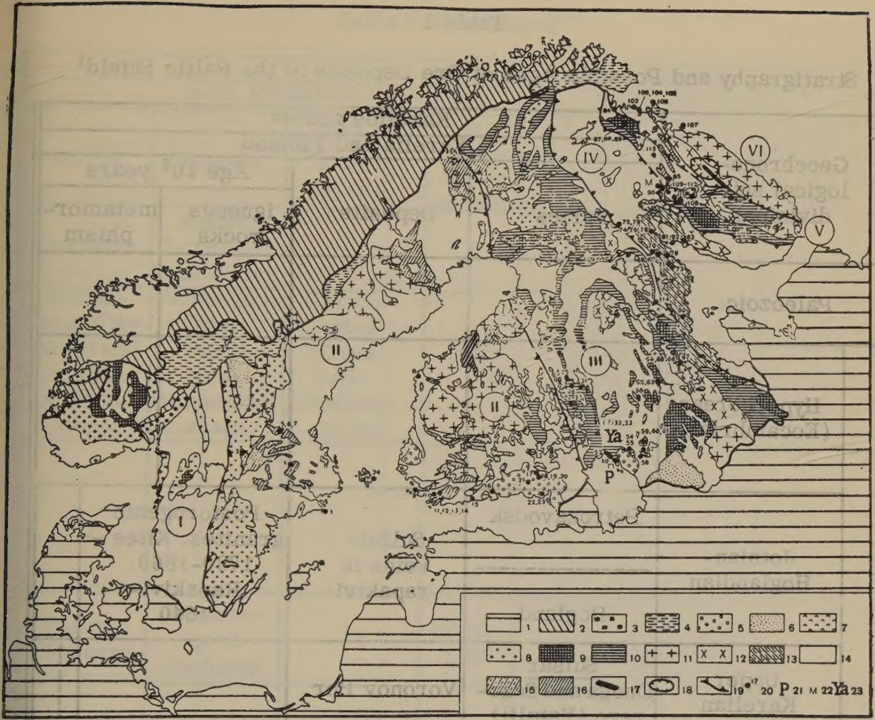

Fig. 1. Geological structure of the Baltic shield and location of lead samples analyzed for isotopic composition

Symbols: 1 - Mesozoic- Cenozoic, Paleozoic and Eocambrian platform deposits; 2 - Swedish and Norwegian Caledonides; 3 - alkalic intrusives, Paleozoic (Oslo region, Khibiny, Lovozero etc) and Precambrian (some intrusives of Karelia and Kola Peninsula); 4 - Hyperborean (sparagmitic) formations; 5 - rapakivi granites and porphyries; 6 - Jotnian and Hoglandian rocks; 7 - alkalic granites of Kola Peninsula; 8 - post-Karelian granites; 9 - late Karelian deposits; 10 - early Karelian deposits; 11 - granites, mainly microcline and oligoclase: in Sweden and Finland, Svecofennian syn- and late - orogenic; largely palingenetie; 12 - granite gneisses; mainly oligoclase (in Karelia and on Kola Peninsula); 13 - Marealbian gneisses; 14 - gneisses and migmatites of different ages; granite gneisses; locally, especially in Sweden there are younger granites not differentiated on the map; 15 - different schists in Sweden and Finland, similar to or contemporaneous with leptite formations; 16 - leptites of Sweden, Finland and Karelia carrying iron ores and ferruginous schists and gneisses of Kola zone; 17 - gneisses and schists of Polmos and Poros including ferruginous schists; 18 - the area of distribution of the oldest migmatized supracrystal rocks; 3000 - 3500 million years old; 19 - boundaries of Svecofennian and older zones and of Karelides (triangles point in the direction of Svecofennian areas); 20 - sample localities and numbers; 21 - P - Pitkyaranta, samples Nos. 41, 42, 43, 44, 45, 46, 47, 48, 49, 50, 51, 52; 22 - M - Nittis-Kumuzh'e, Monchetundra, samples Nos. 90, 91, 92, 93, 94, 95, 96, 97, 98, 99, 100; 23 - Ya - Yalonvara, samples Nos. 34, 35, 36, 37, 38, 39.

Regional zones: I - Gothides of southern Norway and southwestern Sweden; II - Svecofennides of central and northern Sweden and central Finland; III - Karelides of Karelia and eastern and northern Finland; IV - Marealbian block; V - Karelides of Kola Peninsula; VI - Murmansk block

Table 1

Stratigraphy and Possible Ages of Ore Deposits of the Baltic Shield[1]

Geochronological subdivisions			Karelide zones[5] — Karelia and Finland: Series	Deposits	Age 10^6 years: igneous rocks	Age 10^6 years: metamorphism
Paleozoic						
Precambrian	Hyperborean (Eocambrian)					
	Jotnian-Hoglandian		Petrozavodsk	Sulfide veins in rapakivi	Postorogenic granites. Kitee - 1780-1860. Rapakivi- 1640	
			Hogland			
	Upper Karelian		Suisar Onega and Segozero (Yatulii)	Voronov Bor		1700 – 1800
	Lower Karelian	Upper part of section	Tunguda	Shuezersk Voitsk Nadvoitsk	Granites of group III	
			Kalevii (in Finland)	Outokumpu Panjavara Keiasiioki Nunnalakhti Kinon-Koznala (?)	Granites. Maarianvaara, 1810-1860. Pegmatites, 1845	
			Ladoga	Impilakhti Pegmatites	Pegmatites 1800	
		Lower part of section	Sortavali	Pitkyaranta	Late orogenic granites; migmatization and granitization; early orogenic granites 1790-1860	
			Parandovo and its analogues	Khautovara Nyalmozero Ulyalegi Parandovo Sondala (?)		
			Gimoli	Gimoli		
			Gneisses, granite gneisses	Faddein-Kelja[2]	Pegmatites 2400-2500. Granite gneisses 2500	
	Katarchean					

Table 1 (Continued)

Kola Peninsula				Pre-Karelian rocks			
				White Sea region			
Series	Deposits	Age 10^6 years		Series	Deposit	Age 10^6 years	
		Igneous rocks	metamorphism			Igneous rocks	metamorphism
Devonian	Khibiny Lovozero Sebl'-Yavr						
Formations of Rybachii and Srednii peninsulas	Vaida-guba (Bazarnaya guba-Murmansk coast	Glauconites from sedimentary rocks	720-1030		Quartz-carbonate veins with sulfides	Porphyritic rapakivi-like granites	
Varzug Pechenga	Monchegora Pechenga		1720-1700		Kemi	Granites, group III 1860-1890	
Imandra							
Tundra							
Keivi	Galena from alkalic granite pegmatites	Pegmatites alkalic granites 1720	1690-1700				
Iron Ore	Olenegorsk Varanger fjord	2000-2450					
Kola Poros Polmos		1700-2600	2300-2700	Loukh* Kh.-L, K	White Sea pgmtites	1950 (1850-2000)	1830-2100
Granite gneisses migma.		1840-3250	2820-3480	Gran.-gneis.		Age of about 2500 has been suggested	

Table 1 (Continued)

Geochronological subdivisions		Svecofennide zone[4]			
		Sweden and Finland			
		Series	Deposits	Age 10^6 years	
				igneous rocks	metamorphism
Paleozoic				Alkalic intrusives Oslo 300	
Hyperborean	Jotnian-Hoglandian	Sparagmites Jotnian		Postorogenic granites 1540-1670. Rapakivi 1610-1670	
Svecofennian time		In some areas there are analogues of upper and late lower Karelian of the eastern part of the Baltic shield			
	Late orogenic intrusions, migmatization granitization		Pernaiö, Pukkila, Lemi (?) Ommeberg, Shellefteo (?)	Late orogenic granites 1820-1830, 1630-1690 (?)	Tampere schists 1790
	Syn-orogenic intrusions Sedimentation	Leptite-iron ore series	Orijarvi, Korsnas, Ajala, Atto, Falun, Langban, Sala, Ytterby pegmatites, etc. Kirunas, Uto	1760-1845 synorogenic granites. Pegmatites 1700-1810	Utö schists 1700
			Varutresk pegmatites	2100	2090-2130

Note: Footnotes to Table 1.

[1] Age data in this Table are taken from reference [2] and others. Kouvo's potassium-argon ages [7] have been recalculated to the new constants $\lambda_K = 5.50 \cdot 10^{-11}$ year^{-1}; $\lambda_\beta = 4.72 \cdot 10^{-10}$ year^{-1}.

[2] The Faddein-Kel'ya deposit lies in granite gneisses but is most likely contemporaneous with polymetallic ores of the Pitkyaranta, Nyalmozero etc. type.

[3] According to the opinion of Swedish geologists Kirunavaara deposit is almost synchronous with supracrustal deposits.

[4] Only the data most important for our purpose have been noted for Sweden and Finland. The data on strata later than the leptite series are not given for these formations lack material for lead analyses and cannot be used in further discussion.

[5] Interrupted lines separate formations belonging to different structural-facies zones.

* Loukh

Kh.-L, K represents: Loukh
Kheto-Lambinsk, Keret'

Table 2

Isotopic Composition of Leads from the Ores of the Svecofennian Areas of the Western Half of the Baltic Shield

Sample No.	Locality	Sample[1]	Description of deposit and country rock	Isotopic composition of lead			Absolute age in 10^6 years according to the graph		Reference
				$\frac{Pb^{206}}{Pb^{204}}$	$\frac{Pb^{207}}{Pb^{204}}$	$\frac{Pb^{208}}{Pb^{204}}$	207/206	208/206	
			1. Swedish zone						
1[1]	Utö	Hematite from magnetite schists	Magnetite-bearing schists of the leptite formation	15.92	15.61	35.89	1830	1810	
2	Långban	Native lead from iron ore	Metamorphosed iron deposit in leptite, bordered by magnetite-bearing skarns	15.83	15.45	35.60	1800	1800	[10][2]
116	"	"	"	15.84	15.55	35.68	1840	1820	[9]
3	Kiruna	Magnetite from massive fine-grained magnetite ore	Massive tabular magnetite body in quartz porphyries, analogues of the leptite formation. The ores contain apatite (up to 2% P) decreasing in amount with depth. Magmatic deposit	61.73	19.60	134.05	1400[3]	-	
4	Sala	Galena	Diopside-tremolite skarns with sphalerite and galena, in dolomite	15.40	14.95	34.90	1810	1990	[8]

Table 2 (Continued)

Sample No.	Locality	Sample[1]	Description of deposit and country rock	Isotopic composition of lead			Absolute age in 10^6 years according to the graph		Reference
				$\frac{Pb^{206}}{Pb^{204}}$	$\frac{Pb^{207}}{Pb^{204}}$	$\frac{Pb^{208}}{Pb^{204}}$	207/206	208/206	
5	Falun	Magnetite in large octahedral crystals	Massive ore body in dolomite. Contains pyrite and less chalcopyrite, pyrrhotite, sphalerite, galena and magnetite. Ores in tremolite, cummingtonite and anthophyllite skarns. The enclosing leptite is cut by granites and partially granitized	–	–	–	–	–	[9]
6	"	Galena		15.34	14.99	33.84	1870	1800	
7	"	Galena		15.89	15.61	35.86	1850	1820	
			2. Central Finnish zone						
			a) Svecofennian deposits						
8	Korsnas	Galena	Mineralization in skarns among carbonate beds and pyroxene gneisses in rocks similar to the leptites of southern Finland[2]	15.95	15.57	36.26	1790	1860	[7]

Table 2 (Continued)

Sample No.	Locality	Sample[1]	Description of deposit and country rock	Isotopic composition of lead			Absolute age in 10^6 years according to the graph		Reference
				$\frac{Pb^{206}}{Pb^{204}}$	$\frac{Pb^{207}}{Pb^{204}}$	$\frac{Pb^{208}}{Pb^{204}}$	207/206	208/206	
9	Attu	Galena	Mineralization in tremolite-bearing quartzose rocks of the leptite formation. The ores consist of pyrite, pyrrhotite, sphalerite, galena and chalcopyrite. Locally there are later coarse-grained galenas	15.82	15.47	35.89	1820	1870	[7]
10	Ajala	Galena	In the same rocks as the Orijärvi deposit (see below)	15.95	15.64	36.24	1820	1850	[7]
11	Orijärvi	Galena	Deposit is in the schists of the leptite formation and is related to tremolite-actinolite skarns. Polymetallic ores. Besides the main type of ore there is also tetrahedrite and other sulfosalts associated with galena (evidently later mineralization)	15.74	15.46	34.08	1860	1580	[11]
12	"	Galena		15.80	15.46	35.88	1840	1900	[7]
13	"	Galena		16.09	15.56	36.17	1700	1730	[7]
14	"	Galena		16.50	15.70	36.80	1500	1530	[8]

Table 2 (Continued)

Sample No.	Locality	Sample[1]	Description of deposit and country rock	Isotopic composition of lead			Absolute age in 10^6 years according to the graph		Reference
				$\frac{Pb^{206}}{Pb^{204}}$	$\frac{Pb^{207}}{Pb^{204}}$	$\frac{Pb^{208}}{Pb^{204}}$	207/206	208/206	
15	Pukkila	Galena	Galena occurs in biotite gneisses in quartz-galena and quartz-sphalerite veins	15.73	15.36	35.30	1820	1830	[7]
16	Pernaiö	Galena	Veins with argentian galena, sphalerite, chalcopyrite, pyrrhotite and also arsenopyrite, loellingite and tetrahedrite. Not far from rapakivi granite.	15.85	15.51	36.00	1810	1880	[7]
17	Lemi	Galena	Impregnations and segregations of pyrrhotite ores with sphalerite, galena and chalcopyrite in amphibole schists, 0.5 km from contact with rapakivi. It is believed that the ores are older than rapakivi (?)	16.13	15.60	36.42	1690	1750	[7]

Table 2 (Continued)

Sample No.	Locality	Sample[1]	Description of deposit and country rock	Isotopic composition of lead			Absolute age in 10^6 years according to the graph		Reference
				$\frac{Pb^{206}}{Pb^{204}}$	$\frac{Pb^{207}}{Pb^{204}}$	$\frac{Pb^{208}}{Pb^{204}}$	207/206	208/206	
			b) Deposits related to rapakivi						
18	Tyulisenlampi, Lemi	Pegmatitic feldspar	Pegmatite veins in rapakivi	16.39	15.52	36.42	1480	1560	[7]
19	Metalaluoto Lemi	Pegmatitic feldspar	Pegmatite veins in rapakivi	16.63	15.39	36.26	1250	1330	[7]
20	Pyhtää	Feldspar ovoid from vyborgite	Rapakivi	17.09	15.83	37.47	1260	1190	[7]
21	Lyuyumyaki	Galena	Quartz-feldspar veinlets with galena and chalcopyrite in rapakivi	19.33	16.31	39.61	anomalous		[7]
22	Säkkijarvi	Galena	Veinlets with galena and chalcopyrite in rapakivi	19.50	16.09	39.87	anomalous		[7]
23	"	"	"	19.15	15.80	39.13	anomalous		[7]
24	Sottunga	Galena	Quartz-feldspar veins in rapakivi with chalcopyrite, pyrite and galena	22.30	16.42	40.50	anomalous		[7]

[1] Samples Nos. 1, 3, 5 and 6 received from the A. E. Fersman collection of the Mineralogical Museum, Academy of Sciences USSR.

[2] References at the end of the paper.

[3] From the $\Delta Pb207/\Delta Pb206$ ratio, see text.

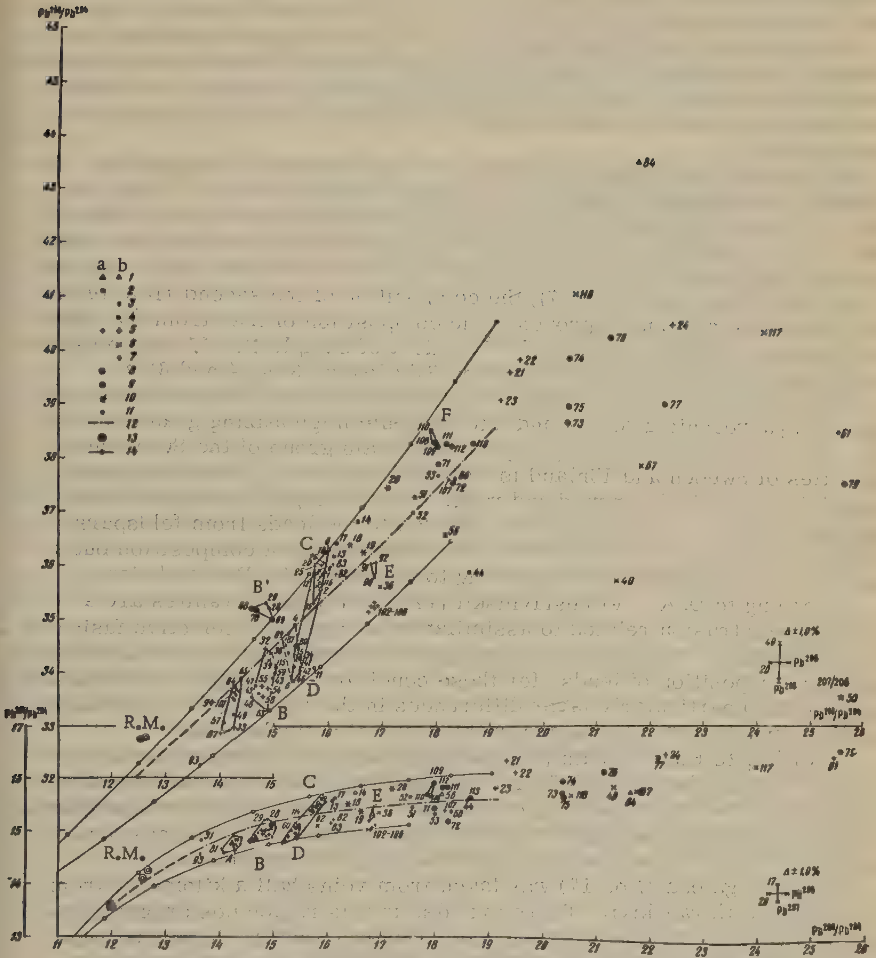

Fig. 2. Isotopic composition of leads and isotope contours of the Baltic shield

Numbers of samples within contours on 207/206 graph: A - 33, 49, 52, 64, 65, 81, 94, 95, 96, 97, 98, 99, 100; B - 28, 29, 38, 39, 43, 45, 47, 48, 54, 55, 58, 59, 63, 68, 69, 70, 118; C - 1, 2, 7, 8, 9, 10, 11, 12, 15, 16, 25, 26, 116; D - 4, 6, 34, 35, 41, 42, 46, 49, 60, 80, 87, 88, 89, 114; E - 36, 90, 91, 92; F - 102, 103, 104, 105, 106.

a) for Svecofennian and older areas; b) for Karelian areas; 1 - iron deposits; 2 - polymetallic ores related to skarns or sulfide deposits; 3 - magnetite ores and sulfides in skarns of the Pitkyaranta type; 4 - sulfide deposits; 5 - veins with galena; 6 - veins with chalcopyrite and molybdenite and galena from these veins; 7 - copper-nickel deposits; 8 - pegmatites of the White Sea region; 9 - alkalic pegmatites and carbonatites; 10 - feldspars from rapakivi granites and their pegmatites; 11 - rocks; 12 - boundary between Svecofennian (above) and Karelian (below) types of lead; 13 - leads from galenas of Rosetta Mine (R. M.), Africa; 14 - reference curves of Precambrian calculated graph of Fig. 8.

active process of iron-magneisum metasomatism, have the same composition of lead. Some of the ores, No. 6 (Falun) and No. 4 (Sala), are evidently related to a different source. Their composition, as we shall see later, is characteristic of the ores of the Karelian zone (Table 2, Fig. 2).

The lead from the Kiruna deposit, which has undergone remelting, is distinctly anomalous. The cause of anomaly may be either a strong enrichment of the magmatic source of these ores (syenite porphyry) in uranium and thorium or the enrichment in these elements of the ores themselves during fusion.

The leads of the Finnish localities are more varied in composition. The principal Svecofennian group of these leads (Table 2, Nos. 8, 9, 10, 12, 15, 16) is also very uniform and identical with the Swedish leads (Table 2, Nos. 1, 2, 7 and 116). But within the Orijarvi deposit there are two other types of lead besides that of sample No. 12. The first (No. 13) is similar to the lead from Lemi (No. 17); the composition of the second (No. 14) is still more different and approaches the composition of lead from the rapakivi granites. The anomalous Pb^{208} content of sample No. 11 may be similar to the anomalies noted in Falun and Sala leads (Nos. 4 and 6). *

The main type of ore of Sweden and Southern Finland is geologically related to synorogenic granites and late orogenic migmatizing granites [5, 6, 7]. The most reliable average age for the main group of the Svecofennian localities of Sweden and Finland is 1800 million years. The leads from rapakivi are markedly varied and range from the highly anomalous leads of galenas (Table 2, Nos. 21, 22, 23, and 24) to the leads from feldspars (Table 2, Nos. 18, 19, 20), which should have modern composition but actually have composition corresponding to the end of the Precambrian.

According to D. A. Velikoslavinskii [12] the rapakivi granites are a multiphase intrusion related to assimilation at depth and selective fusion of the substratum. This interpretation agrees very well with the data on the isotopic composition of leads, for these conditions (multiple intrusions and assimilation) particularly favor differences in the U/Pb and Th/Pb ratios in different intrusive phases and in the rocks of a single phase.

According to Kouvo's data [7], the lead content in different varieties of rapakivi varies sharply: 68-72 g/t in vyborgite, 58-64% in dark rapakivi, 19-22, 60, 100-108, 200-215 g/t in rapakivi granite (in different samples). The same author notes a more uniform lead content in the oldest granodiorites: 70-75 g/t in one sample and 100-114 g/t in two others.

The Lemi galena (No. 17) was taken from veins half a kilometer from the contact with rapakivi. There are also in this region postorogenic intrusions very near rapakivi in age (see Tables 1 and 2). It may be supposed that the Lemi galenas are related either to the postorogenic intrusions of the Onas type or to the earliest rapakivi phases. According to their isotopic composition, the Orijärvi galenas, Nos. 17 and 14, may be placed in genetic relationship with the postorogenic granites and rapakivi granites, respectively (Table 1).

The eastern part of the Baltic shield. The supracrustal Karelian rocks are erosional remnants of deposits of the deep troughs of the Karelian geosyncline separated by anticlinal folds in the pre-Karelian basement. They form the west, central and east Karelian and the central Kola zones

---

* Possibly this anomaly is due to experimental error, for these leads were analyzed in the first series of analyses [11].

(Pechanga, Imandra-Varzug and Keiv areas). In the lower part of the Karelide section several series may be distinguished characterized by different sections in different structural-facies zones, but all composed of typical geosynclinal sediments [13]. Sulfide deposits are related mainly to the volcanic Parandovo series and its analogues (Parandovo, Ulyalegi, Khautovara, Yalonvara). The Pitkyaranta magnetite skarn deposit lies at the contact with the overlying Ladoga series (according to K. O. Krats [14]) and the Outokumpu deposit lies in the analogues of the Ladoga series in Finland.

On the Kola Peninsula, similar rocks occur in the Pechenga and Imandra-Varzuga series. The latter is evidently somewhat younger than the Parandovo series but the age of the Pechenga series is still debatable (it is referred to the Proterozoic or to the Paleozoic). It contains the Pechenga copper-nickel deposit. The Monchegora copper-nickel deposit, on the other hand, is related to the interformational intrusion in the rocks of the Imandra-Varzug series.

The rocks of the lower part of the Karelian section contain numerous quartz veins with chalcopyrite and sometimes with molybdenite and outcroppings of lead ore. In the Ladoga Lake region there are extensive fields of pegmatites. In central Karelia and on the Kola Peninsula, in a setting similar to that of the Svecofennides, there are widespread leptites and magnetite quartzites of ore quality (Gimoli, Olenegorsk deposits, Varanger fiord). On the Kola Peninsula these rocks are referred by A. A. Polkanov [2] to pre-Karelian time.

In the more ancient pre-Karelian rocks of the White Sea region, pegmatites are common, and to the north, in the vicinity of Kandalaksha Bay, there are quartz-carbonate veins with sulfides.

According to K. O. Krats [14] and V. A. Perevozchikova [15], the entire continental-volcanic series represents deposits of the initial stage in the development of the Karelian geosyncline (Lower Proterozoic, according to these authors). The Gimoli, Parandovo and Yalonvara series lie with a strong unconformity upon pre-Karelian granite and other gneisses. In all zones these early Karelian series are overlain by continental carbonate sequences of the Onega and Segozero series contemporaneous with the final stage of Karelian folding (Middle Proterozoic). The last, platform, stage in the development of this territory is represented by the Hogland-Jothnian deposits in the south of Karelia and the Hyperborean deposits of Rybachii and Srednii peninsulas and of the Kil'din island on the Murmansk coast (Upper Proterozoic).

The supracrustal Karelian rocks have been repeatedly cut by orogenic, late orogenic and postorogenic granite intrusions. The intrusions of the first two types and their pegmatites [16] are considered responsible for the formation of skarns [17] and even of the Pitkyaranta magnetite ores [18]. The age of these intrusives is 1790-1860 million years [2] and we conclude that the magnetite deposit at Pitkyaranta is 1800 million years old, i. e., contemporaneous with the main type of Svecofennian deposits.

The variation in the isotopic composition of lead in the Karelides and on the eastern part of the Baltic shield with its included pre-Karelian zones is much more complex (Tables 3-6, Fig. 2), than in the Svecofennian zone. The Pitkyaranta mineralized area (Fig. 3) alone contains several types of lead. It is most remarkable that in the ores of the first stage of mineralization, magnetites (Nos. 42, 46) carrying admixed lead with the isotopic

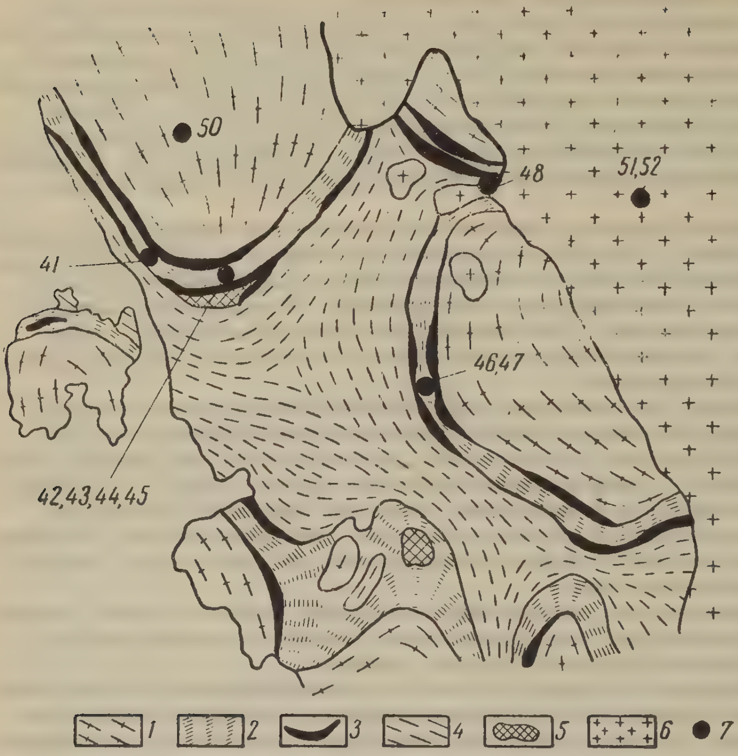

Fig. 3. Sketch map of the Pikyaranta region after K. A. Shurkin [16]

1 - gneisses, granite gneisses (>2500 million years); 2 - hornblende schists and schistose amphibolites; 3 - limestones and skarns; 4 - biotite and quartz-biotite schists (Ladoga series); over 1700 - 1800 million years old; 5 - post-Ladoga granites and granodiorites; 6 - rapakivi granites (1620-1650 million yrs.); 7 - location of samples and their numbers.

composition of the 15.48, 15.07, 34.11 type* there are veinlets of galena and sphalerite with lead of an older isotopic composition (Nos. 48, 47, 43) of the 14.66, 14.88, 33.75 type (Table 3). Moreover, both the sequence of lead types and the isotopic composition of lead in each of them (Fig. 4) is the same in different areas of the mineralized region. The earliest molybdenites intimately associated with skarns have admixed lead of the same

---

* The isotopic composition of lead is given in the same order as in Tables 2-6.

Table 3

Isotopic Composition of Ores of the West-Karelian Zone

Sample No.	Locality	Sample[1]	Description of deposit and country rock	Isotopic composition of lead			Absolute age in 10^6 years according to the graph		Reference
				$\frac{Pb^{206}}{Pb^{204}}$	$\frac{Pb^{207}}{Pb^{204}}$	$\frac{Pb^{208}}{Pb^{204}}$	207/206	208/206	
			3. West-Karelian zone a) Finnish area						
25	Paniiavara	Galena	Carbonate-barite veins in Karelian schists	15.74	15.45	35.98	1850	1980	[7]
26	Keiyasiioki	Native lead	Grains of lead in soil associated with detrital carbonates. Evidently from veins similar to those at Paniiavara (No. 25)	15.92	15.70	36.06	1860	1840	[7]
27	Outokumpu	Chalcopyrite from massive chalcopyrite-pyrrhotite ore	The deposit is in the schists of the Karelian formation, a northwestern extension of pre-Ladoga schists. The sulfides lie in a sequence of quartzites, dolomites and schists. Intrusions of serpentine in the hanging wall.	-	-	-	-	-	

Table 3 (Continued)

Sample No.	Locality	Sample[1]	Description of deposit and country rock	Isotopic composition of lead			Absolute age in 10^6 years according to the graph		Reference
				$\frac{Pb^{206}}{Pb^{204}}$	$\frac{Pb^{207}}{Pb^{204}}$	$\frac{Pb^{208}}{Pb^{204}}$	207/206	208/206	
28	Outokumpu	Galena from chalcopyrite-rich veins cutting the main orebody	The deposit is in the schists of the Karelian formation, a northwestern extension of pre-Ladoga schists. The sulfides lie in a sequence of quartzites, dolomites and schists. Intrusions of serpentine in the hanging wall.	14.90	15.23	35.21	2270	2440	[7]
29	"			14.84	15.21	35.29	2310	2520	[7]
30	"	Galena. Small grains from small fractures with pyrrhotite. 20 m. below main orebodies	" "	120.44	28.32	33.64	1930[2]	-	[7]
31	Nunnan-lakhti	Galena from amphibole skarns	Ore in amphibole skarns developed in Karelian strata similar to the country rock at Outokumpu	13.64	14.81	34.14	2870	3200[3]	[7]
32	Kinon-Koznala	Galena	Deposit not described	14.85	14.99	34.44	2190	2300	[11]
33	"	Galena	" "	14.27	14.64	32.96	2370	2370	[8]

Table 3 (Continued)

Sample No.	Locality	Sample[1]	Description of deposit and country rock	Isotopic composition of lead			Absolute age in 10^6 years according to the graph		Reference
				$\frac{Pb^{206}}{Pb^{204}}$	$\frac{Pb^{207}}{Pb^{204}}$	$\frac{Pb^{208}}{Pb^{204}}$	207/206	208/206	
			b) Northern Ladoga region						
			1. Yalonvara mineralized area						
34	Yalonvara	Pyrrhotite from pyrite-pyrrhotite ores	Graphitic schists and quartzites of the Yalonvara series (analogue of Parandovo series) with lenses of pyrite-pyrrhotite ore (Nos. 34 and 35). This zone is cut by quartz veins with molybdenite, No. 36. The latter are cut in their turn by quartz veins with galena (Nos. 37-39)	15.48	15.11	34.29	1840	1800	
35	"	Pyrite ore		15.43	15.05	34.28	1850	1830	
36	"	Quartz from quartz veins with molybdenite		16.95	15.35	35.61	1040 (anomalous)	940	
37	"	Galena from quartz veins	" "	-	-	-	-	-	
38	"	" "	" "	14.95	15.04	34.35	2150	2200	
39	"	" "	" "	14.90	15.02	34.24	2160	2210	

Table 3 (Continued)

Sample No.	Locality	Sample[1]	Description of deposit and country rock	Isotopic composition of lead			Absolute age in 10^6 years according to the graph		Reference
				$\frac{Pb^{206}}{Pb^{204}}$	$\frac{Pb^{207}}{Pb^{204}}$	$\frac{Pb^{208}}{Pb^{204}}$	207/206	208/206	
40	Impilakhti "Seraya Gorka"	Molybdenite from pegmatites	The pegmatites in hornblende schists are related to the third post-Ladoga granites (according to K. A. Shurkin [16])	21.32	15.80	35.74	(anomalous)		
			2. Pitkyaranta mineralized area						
41	Old deposit, Omel'yanov I	Molybdenite from diopside skarn	Skarns at the base of Ladoga formation K. O. Kratts' Sortavali formation) with magnetite ores and other mineralogically very varied mineralization. Sulfide mineralization is older than skarns and magnetite ores. Formerly the deposit was believed to be genetically related to rapakivi intrusion	15.46	15.09	34.25	1840	1800	
42	Old deposit, Klee 6	Magnetite from magnetite ores and skarns		15.48	15.07	34.11	1820	1760	
43	"	Sphalerite from magnetite ores (same sample as No. 42)		14.97	14.89	33.90	2060	2100	
44	"	Chalcopyrite from diopside skarn		18.62	15.58	35.93	(anomalous)		

Table 3 (Continued)

Sample No.	Locality	Sample[1]	Description of deposit and country rock	Isotopic composition of lead			Absolute age in 10^6 years according to the graph		Reference
				$\frac{Pb^{206}}{Pb^{204}}$	$\frac{Pb^{207}}{Pb^{204}}$	$\frac{Pb^{208}}{Pb^{204}}$	207/206	208/206	
45	Old deposit, Klee 6	Galena from chalcopyrite No. 44 (same sample)	Skarns at the base of Ladoga formation K. O. Kratts' Sortavali formation) with magnetite ores and other mineralogically very varied mineralization. Sulfide mineralization is older than skarns and magnetite ores. Formerly the deposit was believed to be genetically related to rapakivi intrusion	14.72	14.96	33.61	2250	2200	
46	Lyupikko	Magnetite from magnetite ore in skarn		15.48	15.04	34.04	1810	1750	
47	"	Galena from carbonate veinlets in magnetite ore No. 46 (same sample)		14.66	14.88	33.75	2250	2280	
48	vaara Koskelo	Galena in cleiophane veins cutting hematite ore	" "	14.60	14.86	33.54	2280	2280	
49	Pitkyaranta	Galena	" "	14.26	14.77	33.23	2440	2430	[8]
50	Pitkyaranta region	Granite gneiss from Archean cupolas	Granite gneisses form the base of the Ladoga (Sortavali) series and outcrop as cupolas bordered by amphibolites and carbonate rocks of the Sortvali series	26.40	17.40	46.90	(modern)		[19]

Table 3 (Continued)

Sample No.	Locality	Sample[1]	Description of deposit and country rock	Isotopic composition of lead			Absolute age in 10^6 years according to the graph		Reference
				$\frac{Pb^{206}}{Pb^{204}}$	$\frac{Pb^{207}}{Pb^{204}}$	$\frac{Pb^{208}}{Pb^{204}}$	207/206	208/206	
51	Pitkyaranta region	Rapakivi granite	Rapakivi granites are the latest Precambrian acid rocks (age – 1650 million yrs.)	17.58	15.44	37.29	(modern)		[20]
52	"	"	" "	17.55	15.64	37.00	(modern)		[20]
			3. Other deposits						
54	Faddein-Kel'ya	Galena	Polymetallic mineralization in Archean granite gneisses side by side with Tulomozero iron ore deposits lying in the Karelian schists	14.90	14.92	33.71	2110	2100	
55	"	"		14.79	14.99	33.76	2230	2190	
53	Velimyaki	Pyrrhotite	Basic rocks with titanmagnetite ores. The pyrrhotite is evidently from the veinlets cutting these ores	18.02	15.32	37.70	310	440[4]	

[1] Samples Nos. 27 and 53 were obtained from the A. E. Fersman Mineralogical Museum, Academy of Sciences USSR; Nos. 34, 36, 37 and 40 were received from G. O. Glebova-Kul'bakh (LAGED); Nos. 35, 38, 39, 54 and 55 were obtained from Yu. V. Bogdanov (VSEGEI); Nos. 41, 42, 43, 44, 45, 46, 47 and 48, from N. N. Pertsev (IGEM).

[2] On the basis of $\Delta Pb^{206}/\Delta Pb^{207}$ ratio.

[3] The high age value given by the graph is discussed in the text.

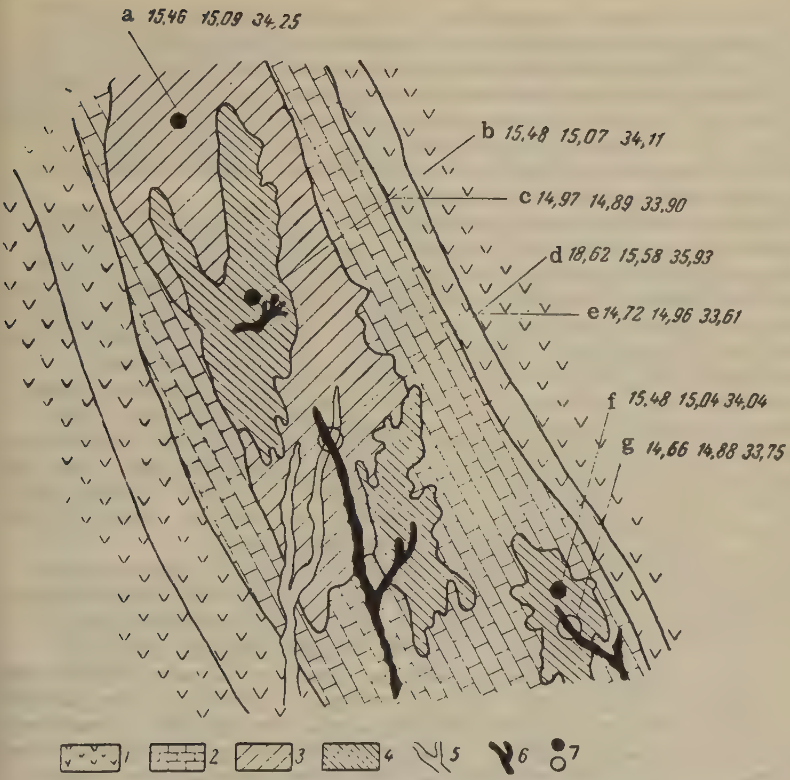

Fig. 4. Sketch map showing the geological location of the samples from Pitkyaranta

a) molybdenite (early skarns), No. 41; b) magnetite ore in skarn, No. 42; c) later sphalerite from this ore, No. 43; d) magnetite ore in skarn, No. 46; e) galena from a carbonate veinlet in this ore, No. 47; f) chalcopyrite in skarn, No. 44; g) galena in the chalcopyrite (younger than chalcopyrite), No. 45.

1 - Hornblende schists and amphibolites; 2 - limestone; 3 - skarns; 4 - magnetite ores in skarns; 5 - nests and veinlets of chalcopyrite; 6 - nests and carbonate veinlets with galena and sphalerite; 7 - samples.

The figures represent the isotopic composition of lead: Pb^{206}/Pb^{204}, Pb^{207}/Pb^{204} and Pb^{208}/Pb^{204}.

omposition as the magnetites. As shown by preliminary calculations, the ge of lead of the first type may well be 1800 million years, i.e., the same s the probable age of the principal ores of Pitkyaranta, formed nearly ontemporaneously with the intrusion of the post-Ladoga granites and pegatites and the accompanying granitization and migmatization. The second ype of lead must be older than 2000 million years. One of the galenas

(No. 49) has a still older composition. It is noteworthy that chalcopyrite No. 44 containing lead of anomalous composition is intermediate in the sequence of ore deposition between magnetite ores and the later sulfide veinlets, or at least is contemporaneous with the latter, for galena from these veinlets (No. 45) occurs as segregations in chalcopyrite and is undoubtedly later than it. It is difficult to say whether these two minerals were deposited a long time apart or whether the hydrothermal galena lagged only slightly behind other sulfides in the usual way.

The Yalonvara sulfide deposit located not far from Pitkyaranta essentially repeats the same pattern of isotopic compositions, the first type of lead occurs in pyrrhotite and pyrite (No. 34, 35) from the pyrite ore; the lead from the quartz of the later molybdenite-bearing quartz veins is anomalous and corresponds, as it were, to the lead from Pitkyaranta chalcopyrite (No. 44). The still later veins with galena (No. 38, 39) contain lead of the second type, like that from the late Pitkyaranta sulfides but with a somewhat higher Pb^{208} content. It is interesting that the lead from molybdenite (No. 40) of the "Seraya Gorka" pegmatite (Impilakhti), one of the second group of post-Ladoga pegmatites, is also anomalous in composition. It differs from the lead from the Pitkyaranta chalcopyrite and the quartz of molybdenite-bearing veins of Yalonvara in its Pb^{206} and Pb^{207} content, but is practically identical with them in its Pb^{208} content (35.74, 35.93, 35.61, respectively, for Impilakhti, Pitkyaranta and Yalonvara).

In the more westerly area of the Karelides, in Finland, almost on the boundary with the Svecofennian region, the same regularities are found but there are additional interesting details. The western-most lead points, Panjavara (No. 25) and Keiasiioki (No. 26), contain galenas (Table 3) whose lead has identical composition with the leads of the main Svecofennian group of deposits. This may be the only example of identity in composition of lead from the Karelian and Svecofennian zones. No analysis of lead from Outokumpu is at present available. The galenas from the chalcopyrite veins cutting these ores (No. 28, 29), like the Pitkyaranta galenas have a much older composition. Galena from occasional pyrrhotite veins is strongly anomalous (No. 31). If it is assumed that uranium was present in the galena itself and that no uranium has been lost since the formation of galena, then the age of the mineral, according to the Pb^{207}/Pb^{206} ratio, is 1930 million years, assuming that the initial composition of lead was the same as in sample No. 28. If it is assumed that the anomalous lead accumulated in some source with the above initial composition of lead and was separated t_m years afterwards, then the age of the galena may be anywhere from 0 (modern) to 1100 million years (it cannot be older under the given conditions). All Outokumpu leads have a relatively high Pb^{208} content and are similar in this to the Svecofennian leads. The same high Pb^{208} content (in relation to Pb^{204}) is found in the Nunnanlakhti galena (No. 31), whose composition is unusually old, although its geological setting is equivalent to that of the Outokumpu ores.

Unfortunately, we know neither the geological characteristics nor the exact location of the Kinon-Koznal deposit (Nos. 33, 34, Table 3).

The sulfide deposits of Southern and Eastern Karelia are very interesting so far as the isotopic composition of their leads (Table 4) is concerned. The pyrite ores of the Ulyalegi and Parandovo deposits contain lead of very old composition comparable only to the composition of lead from the Pitkyaranta deposit (No. 49) and occupying, evidently, the lowermost position in the early Karelian section (Nos. 57, 64, 65).

The pyrite ores of Khautovara (Nos. 59. 119), a deposit located in the

Table 4

Isotopic Composition of leads from the Ores of Central and Eastern Karelia

Sample No.	Locality	Sample[1]	Description of deposit and country rock	Isotopic composition of lead			Absolute age in 10^6 years according to the graph	
				$\frac{Pb^{206}}{Pb^{204}}$	$\frac{Pb^{207}}{Pb^{204}}$	$\frac{Pb^{208}}{Pb^{204}}$	207/206	208/206
			4. Central Karelian zone					
56	Gimoli	Ferruginous schists	Ferruginous schists and leptites of the Gimoli series	18.15	15.70	36.58	430 (anomalous)	140
57	Ulyalegi	Pyrite and pyrrhotite-pyrite ores	Sulfide lenses in strongly metamorphosed effusive-sedimentary rocks (hornblende schist) evidently analogues of the Parandovo series	14.07	14.59	33.08	2480	2530
58	Nyalmozero	Polymetallic lead ore	Effusive-sedimentary rocks, evidently analogues of the Parandovo series	14.80	14.98	33.57	2210	2130
59	Khautovara	Pyrite from pyrite-pyrrhotite ore	Sulfide deposits in strongly metamorphosed effusive-sedimentary rocks of the Parandovo series	15.02	15.14	34.01	2150	2080
60	"	Pyrrhotite from the same sample (No. 59)	" "	15.38	15.08	34.12	1900	1840
115	"	Massive fine-grained pyrite ores	" "	15.04	15.07	34.10	2100	2080
61	"	Coarsely crystalline sphalerite	Veins with coarsely crystalline sphalerite cutting main sulfide ores	25.45	16.36	38.55	(anomalous)	

Table 4 (Continued)

Sample No.	Locality	Sample[1]	Description of deposit and country rock	Isotopic composition of lead			Absolute age in 10^6 years according to the graph	
				$\frac{Pb^{206}}{Pb^{204}}$	$\frac{Pb^{207}}{Pb^{204}}$	$\frac{Pb^{208}}{Pb^{204}}$	207/206	208/206
118	Voronov Bor	Chalcopyrite in quartz vein	Quartz veins in Middle Proterozoic (?) rocks	20.53	15.67	41.08	(anomalous)	
62	Sondala (Mt. Lebedev region)	Chalcopyrite	Quartz-chalcopyrite veins in Lower Proterozoic basalts.	15.82	15.10	35.62	1630 (anomalous) (?)	1830
63	"	Galena	" "	14.88	14.91	33.31	2120	2030
			5. East Karelian zone					
64	Parandovo	Massive pyrite ore	Sulfide lenses in strongly metamorphosed effusive-sedimentary rocks of the Parandovo series	14.27	14.91	33.75	2510	2550
65	"	Pyrite ore	" "	14.39	14.89	33.88	2420	2500
66	"	Pyrrhotite ore	" "	18.32	15.36	37.64	130	180
67	Nadvoitsy	Chalcopyrite	Quartz-chalcopyrite gold-bearing veins in the Tunguda series which is younger than the Parandovo series	21.74	15.73	37.90	(anomalous)	
117	Voitskoe	Chalcopyrite	" "	23.98	16.19	40.41	(anomalous)	
114	Shuezero	Chalcopyrite	Quartz veins with chalcopyrite and molybdenite in Tunguda and a younger series (upper Lower Proterozoic)	15.41	15.14	34.23	1910	1840

[1] Samples Nos. 56, 61 – from I. V. Barkanov (SZGU); Nos. 57, 58, from S. E. Bresler (SZGU); Nos. 59, 60, 115, 118, 67 and 114, from the TsNIGR Museum (VSEGEI); Nos. 62, 63 and 117, from the A. E. Fersman Mineralogical Museum; Nos. 64, 65, 66, from G. O. Glebova-Kul'bakh (LAGED).

higher horizons of the Parandovo series, have admixed lead of a somewhat younger composition, but pyrrhotite No. 60 (Table 4) from the same sample as pyrite No. 59 has composition similar to that of the main magnetite ores of Pitkyaranta and the sulfide ores of Yalonvara. This agrees very well with the idea that in a number of pyrite deposits pyrrhotite formed later as a result of metamorphism of pyrite ore [21]. It indicates also that not all sulfide deposits were formed at the same time and by the same process. Evidently the vein of the Shuezerskoe deposit (No. 114) was formed contemporaneously with the Khautovara pyrrhotite and Pitkyaranta magnetite. The lead from the chalcopyrite in quartz veins was found to be anomalous (Nos. 62, 67, 117, 118, Table 4).

The analyses of galenas from the lead deposits of southern and southwestern Karelia (Nos. 54, 55, 58, Table 4) have the same composition as the leads of the second type from Pitkyaranta; i.e., they are old. Perhaps the Faddein-Kel'ya deposit is old, since it lies in the granite gneisses of the pre-Karelian basement; but more likely it was formed by the same process as the older Pitkyaranta sulfides.

The lead ores of Pechenga are very much alike and are near in type to the leads of the main ores of Pitkyaranta but have a somewhat lower Pb^{206} and Pb^{207} content and higher Pb^{208} content (in relation to Pb^{204}) (Nos. 87, 88, 89, Table 5).

The syngenetic porphyry ores of the Monchegora mineralized area [22] (Nittis-Kumuzh'e) and the ore shoots (Mt. Nyud), which are considered as having been redeposited almost in situ (Nos. 90, 91, 92, Table 5), contain lead corresponding in its isotopic composition to the late Precambrian age of the enclosing ultrabasic rocks (Fig. 5). The vein leads (Nos. 94-101,

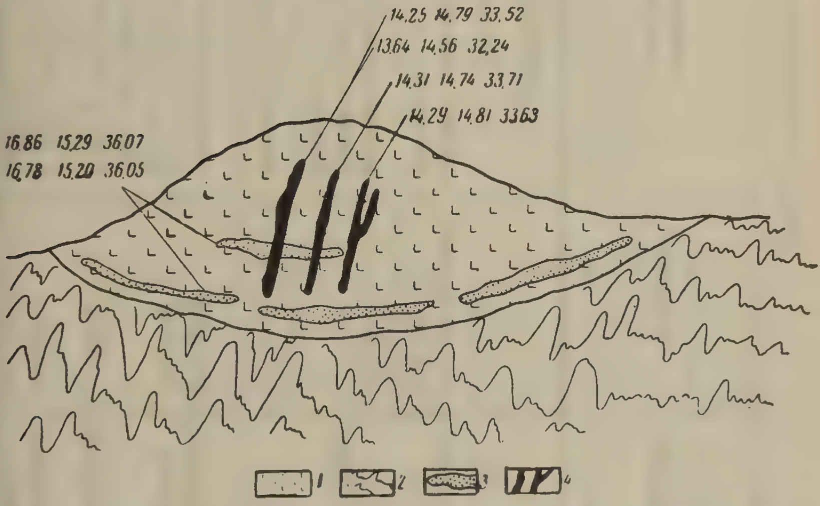

Fig. 5. Diagrammatic section of the Nittis-Kumuzh'e deposit (Monchetundra)

1 - pyroxenites and peridotites; 2 - Archean gneisses; 3 - syngenetic sulfide porphyry ores; 4 - epigenetic massive sulfide veins.

Table 5

Isotopic Composition of the Kola Peninsula Leads

Sample No.	Locality	Sample[1]	Description of deposit and country rock	Isotopic composition of lead			Absolute age in 10^6 years according to the graph	
				$\frac{Pb^{206}}{Pb^{204}}$	$\frac{Pb^{207}}{Pb^{204}}$	$\frac{Pb^{208}}{Pb^{204}}$	207/206	208/206
			7. Kola-Northern Norway Zone					
			a) Southern part					
81	Medvezhii Island	Coarse-grained galena	Quartz-carbonate veins in Archean gneisses	14.04	14.65	32.87	2520	2510
82	"	Galena	" "	16.13	15.19	35.83	1490	1630
83	Malaya Pir'ya Bay	Galena	Quartz-carbonate veins in migmatized granites near a porphyritic granite massif	16.09	15.18	36.03	1500	1700
			b) Central, northern and northwestern parts					
84	Bjornevann, Kirkenes	Magnetite schists	Ferruginous schists of Varanger fiord (analogues of the ferruginous schists of the Archean series on Kola Peninsula)	21.65	15.71	43.55	(anomalous)	
85	Olenogorsk	Hematite ore	Ferruginous schists in the Archean gneiss series of Kola Peninsula	-	-	-	-	-
86	Serpovidny Range	Galena	In amazonite pegmatites of alkalic granites of Proterozoic age (1670 million years)	-	-	-	-	-

Table 5 (Continued)

Sample No.	Locality	Sample[1]	Description of deposit and country rock	Isotopic composition of lead			Absolute age in 10^6 years according to the graph	
				$\frac{Pb^{206}}{Pb^{204}}$	$\frac{Pb^{207}}{Pb^{204}}$	$\frac{Pb^{208}}{Pb^{204}}$	207/206	208/206
87	Pechenga, Kaula	Massive pyrrhotite ore from the main ore body	Massive sulfide deposits in serpentinite of the Pechenga series and at contacts between serpentinites and schists of the same series	15.27	14.89	34.38	1860	1960
89	Pechenga, Kaula	Pyrrhotite-pentlandite ore from a separate orebody parallel to the main one	" "	15.17	14.79	34.57	1880	2090
88	Pechenga	Pyrrhotite	" "	15.22	14.85	34.50	1870	2040
			Monchegora mineralized area					
90	Nyud Mountain	Massive pyrrhotite ore from Sul'fidnoe oreshhot in audit 2	Syngenetic oreshoots and disseminated ores in the ultrabasic rocks of the Proterozoic (Pt_{1-2}) Monchegora intrusion	16.84	15.40	35.80	1130	1070
91	Nittis-Kumuzh'e	Pyrrhotite with small segregations of pentlandite	" "	16.78	15.20	36.05	1060	1160

Table 5 (Continued)

Sample No.	Locality	Sample[1]	Description of deposit and country rock	Isotopic composition of lead			Absolute age in 10^6 years according to the graph	
				$\frac{Pb^{206}}{Pb^{204}}$	$\frac{Pb^{207}}{Pb^{204}}$	$\frac{Pb^{208}}{Pb^{204}}$	207/206	208/206
92	Nittis-Kumuzh'e	Chalcopyrite with pyrrhotite and pentlandite. Segregations in disseminated ores	Syngenetic oreshoots and disseminated ores in the ultrabasic rocks of the Proterozoic (Pt_{1-2}) Monchegora intrusion	16.86	15.29	36.07	1050	1100
93	Nittis-Kumuzh'e level 255	Massive magnetite ore	A series of massive sulfide ores cutting the differentiated Monchegora intrusive. Veins dip to the south and along the strike merge gradually into gabbro pegmatites. Massive sulfide veins are later than the disseminated ores and segregations	13.64	14.56	32.24	2740	2620
94	Nittis-Kumuzh'e level 255	Chalcopyrite with segregations of pentlandite	Vein 26	14.25	14.79	33.52	2460	2510
95	Nittis-Kumuzh'e level 142	Pentlandite ore		14.23	14.75	33.65	2450	2450

Sample No.	Locality	Sample[1]	Description of deposit and country rock	Isotopic composition of lead			Absolute age in 10^6 years according to the graph	
				$\frac{Pb^{206}}{Pb^{204}}$	$\frac{Pb^{207}}{Pb^{204}}$	$\frac{Pb^{208}}{Pb^{204}}$	207/206	208/206
96	Nittis-Kumuzh'e audit 2	Pyrrhotite with inclusions of pentlandite	Vein 18 A series of massive sulfide ores cutting the differentiated Monchegora intrusive. Veins dip to the south and along the strike merge gradually into gabbro pegmatites. Massive sulfide veins are later than the disseminated ores and segregations	14. 29	14. 73	33. 60	2390	2500
97[2]	"			14. 31	14. 74	33. 71	2400	2500
98	"	Pyrrhotite with inclusions of pentlandite		14. 39	14. 74	33. 69	2340	2450
99	Nittis-Kumuzh'e level 222	Chalcopyrite-pyrrhotite ore with pentlandite and occasional euhedral grains of magnetite		14. 28	14. 71	33. 54	2390	2500
100	Nittis-Kumuzh'e	Massive chalcopyrite ore with small segregations of pyrrhotite	Vein 16 " "	14. 29	14. 81	33. 63	2440	2500
101	Nittis-Kumuzh'e audit 2	Fine-grained chalcopyrite-pyrrhotite ore with pentlandite and sparse segregations of magnetite	" "	14. 35	14. 84	33. 66	2420	2470

Table 5 (Continued)

Sample No.	Locality	Sample[1]	Description of deposit and country rock	Isotopic composition of lead			Absolute age in 10^6 years according to the graph	
				$\frac{Pb^{206}}{Pb^{204}}$	$\frac{Pb^{207}}{Pb^{204}}$	$\frac{Pb^{208}}{Pb^{204}}$	207/206	208/206
			Murmansk coast					
102	Bazarnaya Bay	Galena	All veins on the coast are localized in the migmatized garnet-biotite Archean gneisses	16.81	15.05	35.24	960	990
103	Dolgaya Bay	Galena from "Anna" vein	" "	16.84	15.07	35.32	950	980
104	Dolgaya Bay	Galena from "Victoria" vein	" "	16.89	15.10	35.26	940	930
105	Chernaya ludka	Coarsely crystallized galena	" "	16.75	15.03	35.17	990	1020
106	Vaida Bay (Rybachii Peninsula)	Galena	Veins in the sandstone-shale strata of the upper part of the Hyperborean (Sparagmite) formation referred to the Eocambrian	16.84	15.07	35.24	950	960
107	Kil'din Island	Galena pebbles 2 x 4 cm	Kil'din Island is also composed of Eocambrian rocks	18.21	15.37	37.60	220[3]	270[3]
			Paleozoic alkalic intrusives					
108	Lovozero, Mt. Punkaruaiv	Galena	Galena in ussingite pegmatites	17.92	15.66	38.32	360[4]	250[4]

Table 5 (Continued)

Sample No.	Locality	Sample[1]	Description of deposit and country rock	Isotopic composition of lead			Absolute age in 10^6 years according to the graph	
				$\frac{Pb^{206}}{Pb^{204}}$	$\frac{Pb^{207}}{Pb^{204}}$	$\frac{Pb^{208}}{Pb^{204}}$	207/206	208/206
109	Khibiny, Mt. N'yuoryabrpakh	Galena from albitized pegmatite sahlband	Albitized pegmatites in foyaites	17.97	15.81	38.23	470	220
110	Khibiny, Mt. Kukisvumchorr	Galena from pegmatite	Natrolitized pegmatites in pyroxene rischorrites	17.86	15.68	38.54	400	460
111	Khibiny, Mt. Yukspor	Galena from the "Polymineral'naya vein	Pegmatite vein – "Polymineral'naya" in nepheline syenite massif (later than khibinites but earlier than foyaites)	18.15	15.82	38.28	290	140
112	"	"	Galena in veinlets in the body of the vein	18.23	15.82	38.25	240	50
113	Sebl'-yavr	Galena in small pods	Galena from carbonatite veinlets in pyroxenites of the Sebl'-yavr intrusive	18.66	15.62	38.28	30	+30

[1] Samples Nos. 81, 84, 88, 91, 92, 96, 97, 105, 106 and 107 received from the A. E. Fersman Mineralogical Museum, Acad. Sci. USSR; Nos. 82 and 83, from Yu. V. Bogdanov (VSEGEI); No. 86, from E. I. Semenov (IMGRE); Nos. 87, 89, 90, 102, 103 and 104, from O. E. Yushko-Zakharova (IMGRE); Nos. 93, 94, 98, 100 and 101, from A.E. Genkin (IGEM); No. 95, from the TsNIGR Museum (VSEGEI); No. 108, from A. I. Polyakov (GEOKhI); Nos. 109 and 110, from I. P. Tikhonenkov (IMGRE); No. 113, from A. G. Bulakh (VSEGEI).

[2] Sample from the same bulk sample as No. 96.

[3] Age from the same Precambrian graph.

[4] The ages of galenas from Paleozoic alkalic intrusives were determined from the Paleozoic graph.

Table 5) from the Nittis-Kumuzh'e deposit are still older in composition than the leads of the Pitkyaranta galenas and are similar only to the lead from the Parandovo pyrite ores and from one Pitkyaranta galena (Nos. 64, 65, 49, Table 4). The samples of the Nittis-Kumuzh'e ores collected from three veins gave the same result. Only one sample (No. 94), the lead from magnetite of vein 26, gave an older composition than that of the lead from pentlandite and chalcopyrite from the same vein. Mineralogically, this magnetite must be referred to the magnetites of the later generation replacing pyrrhotite and forming sahlbands or occurring in the thin vein terminations mainly in the upper parts of the deposit [22]. The isotopic composition of lead from this magnetite suggests that such magnetites must have had a slightly different source than the sulfides of the veins. On the whole, the vein matter had nothing in common at the time of formation with the enclosing basic and ultrabasic rocks.

Rather near in composition to the leads of syngenetic type of ores of Monche-Tundra are the leads of the galenas on the Murmansk coast (Nos. 102-106, Table 5). The leads from similar veins of the Kandalaksha region (Nos. 82, 83, Table 5), related to the porphyritic (rapakivi-like) granites, are very similar in composition to some of the leads of southern Finland, which may be genetically related to postorogenic intrusions or to the first rapakivi phases (Nos. 13, 17, Table 2).

Our attempt to determine the primary composition of lead from the iron deposits of Karelia and Kola Peninsula similar to the deposits of Utö in Sweden (No. 1, Table) did not succeed, because the leads separated from the magnetite ore of the Gimoli deposit (Nos. 56, Table 4) and of the Varanger Fiord region (No. 84, Table 5) turned out to be anomalous, with compositions approaching modern.

Among the leads from galenas and other minerals of the White Sea region pegmatites (Table 6) related to granitization and migmatization, there are old (Nos. 68, 69, 70) and anomalous leads. We shall discuss them in detail in the last section. There, also, we shall consider the leads of the Paleozoic Khibina and Lovozero alkalic intrusions (Table 5).

2. DETERMINATION OF THE AGE OF LEAD BY ITS ISOTOPIC COMPOSITION

If the leads of a given region separated at different times from rocks which had undergone various changes during the course of time, except loss or addition of uranium, thorium and lead, then on the 207/206 graph the points representing isotopic compositions of all leads of the region would fall on a theoretical "time -- isotopic composition" curve, or, in the case of variation in the uranium-lead ratio, they would be distributed among the corresponding isochronal curves of the graph. Usually one or the other of these methods of dating lead by its isotopic composition has been used, for example by Patterson [26], Vinogradov [3, 8], Kulp [9], Houtermans [27], Gerling [2] and others. However, our experience in generalizing the isotopic data for the Baltic shield and also for the leads of Africa, the U. S. A. and other regions shows that the isotopic abundance points do not fall either on the theoretical "time-isotopic composition" curves or on the usual isochronals. This means that leads of the same age but separated from the rocks with disturbed U/Pb and Th/Pb ratios do not fall on a unique evolutionary curve but on two or more depending on the number of differentiations

Table 6

Isotopic Composition of Leads of the White Sea Region

Sample No.	Locality	Sample	Description of deposit and country rock	Isotopic composition of lead			Absolute age in 10^6 years according to the graph		Reference
				$\frac{Pb^{206}}{Pb^{204}}$	$\frac{Pb^{207}}{Pb^{204}}$	$\frac{Pb^{208}}{Pb^{204}}$	207/206	208/206	
			6. White Sea Region (Belomor'e)						
68	Severnaya varaka	Galena	Pegmatites in Archean gneisses (above the middle part of the Belomor'e series)	14.58	14.80	35.20	2260	2680	[24]
69	"	Galena	" "	14.97	15.13	35.00	2180	2340	[19]
70	Tedino Lake	Galena	Pegmatites from the upper part of the Belomor'e gneiss sequence	14.67	14.85	35.17	2230	2610	[25]
71	"8-e marta"	Galena	Pegmatite veins in the Archean Belomor'e gneisses	18.02	15.42	37.91	370	480	[25]
72	Alakurtti	Galena	" "	18.27	15.18	37.56	(anomalous)		[25]
73	Postel'noe Lake	Galena	" "	20.38	15.68	38.70	(anomalous)		[24]
74	Kamennaya Taibola	Galena	" "	20.40	15.93	39.90	(anomalous)		[24]
75	"	Galena	" "	20.40	15.62	39.00	(anomalous)		[24]
76	"	Galena	" "	21.16	16.10	40.30	(anomalous)		[23]

Table 6 (Continued)

Sample No.	Locality	Sample	Description of deposit and country rock	Isotopic composition of lead $\frac{Pb^{206}}{Pb^{204}}$	$\frac{Pb^{207}}{Pb^{204}}$	$\frac{Pb^{208}}{Pb^{204}}$	Absolute age in 10^6 years according to the graph 207/206 208/206	Reference
77	Bol'shoi Olenchik	Galena	Pegmatite veins in the Archean Belomor'e gneisses	22.15	16.35	39.03	(anomalous)	[24]
78	Kheto-Lambina	Oxidized copper minerals	" "	39.56	16.92	38.22	(anomalous)	[24]
79	Alakurtti	Oxidized copper minerals	" "	25.60	16.49	37.59	(anomalous)	[25]
80	Kemi	Galena	There is no description of the deposit. Most likely galena is from pegmatites related to granites of the "Poduzhemskii" type which are younger than the Belomor'e granites. They are known as granites of Group III	15.43	14.87	34.50	1760/1880	[8]

undergone by the parent rocks which were responsible for the disturbance of the ratios.

According to the general formulas for the increment of lead, the composition of lead t_n years after time t_0 (using the ratios of Pb^{206}, Pb^{207}, Pb^{208}, U^{238}, U^{235} and Th^{232} to Pb^{204}) will be:

$$\frac{Pb_n^{206}}{Pb^{204}} - \frac{Pb_0^{206}}{Pb^{204}} = \frac{U_0^{238}}{Pb^{204}}\left(1 - e^{-\lambda^{238} t_n}\right) \qquad (1)$$

$$\frac{Pb_n^{207}}{Pb^{204}} - \frac{Pb_0^{207}}{Pb^{204}} = \frac{U_0^{235}}{Pb^{204}}\left(1 - e^{-\lambda^{235} t_n}\right) \qquad (2)$$

$$\frac{Pb_n^{208}}{Pb^{204}} - \frac{Pb_0^{208}}{Pb^{204}} = \frac{Th_0^{232}}{Pb^{204}}\left(1 - e^{-\lambda^{232} t_n}\right) \qquad (3)$$

$$\frac{Pb_n^{207} - Pb_0^{207}}{Pb_n^{206} - Pb_0^{206}} = \nu_0 \frac{\left(1 - e^{-\lambda^{235} t_n}\right)}{\left(1 - e^{-\lambda^{238} t_n}\right)}, \qquad (4)$$

where $\nu_0 = \frac{U_0^{235}}{U_0^{238}}$

$$\frac{b_n^{208} - Pb_0^{208}}{Pb_n^{206} - Pb_0^{206}} = q_0 \chi_0 \frac{\left(1 - e^{-\lambda^{232} t_n}\right)}{\left(1 - e^{-\lambda^{238} t_n}\right)}, \qquad (5)$$

where $\chi_0 = \frac{Th_0^{232}}{U_0^{238}}$,

Here, Pb_n^{206}, Pb_n^{207}, Pb_n^{208}, etc., are amounts of a given isotope at time t_n; v_o is derived from the modern value of $v = 1/138$ and the constant for the given t_o; q_o is a coefficient defining the variation in the Th/U ratio at time t_o; $\lambda^{238} = 1.541 \cdot 10^{-10}$ years, $\lambda^{235} = 9.722 \cdot 10^{-10}$ years, $\lambda^{232} = 4.987 \cdot 10^{-11}$ years are the decay constants of U^{238}, U^{235} and Th^{232}.

Formulas (1, 2, 3) show that the absolute value of radiogenic increment of each of the isotopes, Pb^{206}, Pb^{207}, Pb^{208}, depends on the change in the U_o^{238}/Pb^{204}, U_o^{235}/Pb^{204} and Th_o^{232}/Pb^{204} ratios, respectively, or actually on the U/Pb and Th/Pb ratios, while the increment of Pb^{208} depends also on the value of X = Th/U. In practice this means that, if a certain value of U_o^{238}/Pb^{204} is taken as the basis, then all its variations and the variations in the increment ΔPb^{204} may be described by coefficient k. If $k > 1$, ΔPb^{206} will increase and if $k < 1$, ΔPb^{206} will decrease. The same holds for Pb^{207} and Pb^{208}. In the last case, a basic value of X may be taken and

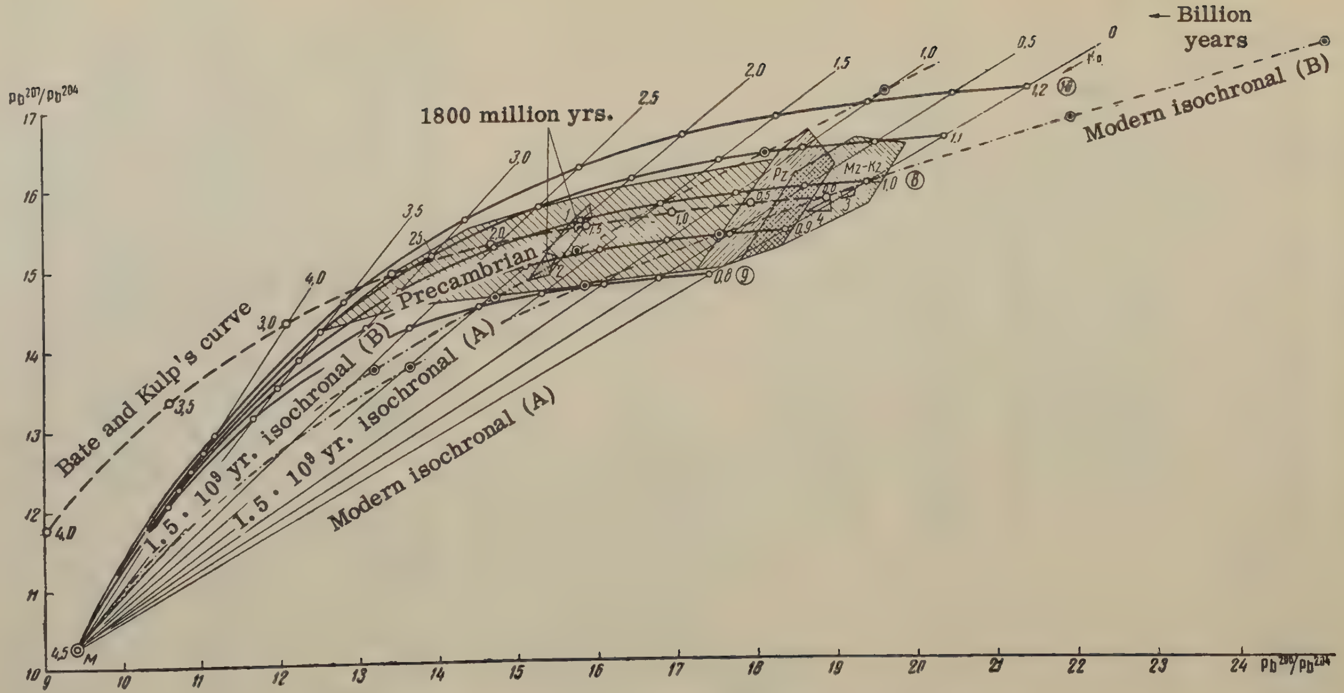

Fig. 6. Variation curves for the isotopic composition of lead.

1 - leads from Svecofennian areas of Sweden and Finland (~ 1800 mill. yrs.); 2 - leads of the Karelides (1800 mill. yrs.); 3 - leads of Vesuvius (modern); 4 - leads from oceanic bottom muds (modern).

its variations will then be reflected in the coefficient q (formula 5). In the calculations which follow, the initial isotopic composition of terrestrial lead is taken as that of the lead from the Cañon Diablo iron meteorite: $Pb^{206}_o = 9.41$, $Pb^{207}_o = 10.27$, $Pb^{208}_o = 29.16$ (with $Pb^{204} = 1$); the initial time t_o as 4.5 billion years and the U^{238}_o/Pb^{204} ratio as 20.

Let us examine Fig. 6. Here, the curves of evolution of the isotopic composition of lead in the troilite of the Cañon Diablo iron meteorite (point M) beginning 4.5 billion years ago are shown on the 207/206 graph. Curve 8 represents the assumed average value of $U^{238}_o/Pb^{204} = 20$ in the primeval lead. Curves 10 and 9 represent changes in this ratio amounting to 1.2 and 0.8 of the initial value (coefficient $k_o = 1.2$ and 0.8); i.e. they correspond to a certain differentiation of the primeval lead ending 4.5 billion years ago.

The intermediate curves correspond to the values of $k_o = 1.1$ and 0.9. The points representing change in the isotopic composition are plotted on each curve at intervals of 500 million years and isochronal curves are drawn through synchronous points. It can be seen that theoretically it is possible to have contemporaneous leads with very different composition (for example the modern compositions of curves 9 and 10).

The cross hatched contour in Fig. 5 encloses the points representing the isotopic composition of natural leads of the world (based on the data of about 1000 analyses) omitting the anomalous leads. It is evident at first glance that this contour agrees well with the curves of the diagram; it is practically coincident with the $k_o = 0.8$ curve below, the $k_o = 1.1$ curve at the top and with the modern isochronal curve. But if the world contour is disregarded and contours bounding the areas of distribution of contemporaneous leads of different regions are considered, a very different picture is obtained. Thus, the generalized contour of Paleozoic and Mesozoic-Cenozoic leads does not coincide with the slope of the isochronal curves of 500 million and 0 years, to which it should be very near if the method of isochronal curves is correct. The slope of these contours is incomparably steeper, so that they cut the isochronal curves. If the extreme points of the Paleozoic contour are taken, it turns out that, according to the system of isochronal curves, these points correspond to 1200 and 500 million years (i.e. they are pre-Paleozoic!) and along the lower boundary, to 300 and +200 million years (i.e., they lie in the future). In the same way the Mesozoic and Cenozoic contour includes ages from 700 to 150 million years and from 0 to +150 million years, respectively, as indicated by the overlapping of the Paleozoic and Mesozoic contours.

Without going into a detailed discussion of isotopic contours, it may be said that each of them encloses a relatively narrow zone along the abscissas, and a wider one along the ordinates (i.e. along Pb^{207}) while the slopes of the contours vary within narrow limits, remaining near the slopes of the general Paleozoic and general Mesozoic contours.

Examples of such regional isotope contours are the contours of leads from Altai, Kazakhstan, Middle Asia, Caucasus and Transbaikalia in the USSR, Western Canada and U.S.A. and the Appalachians in North America, the Andes in South America, Western Europe, etc. In the Precambrian, similar contours may be found in Africa, Canada, Australia and the Baltic shield. An example of the latter is the contour for the leads of the Svecofennian and Karelian zones of the Baltic shield plotted in Fig. 7, which corresponds to 1800 - 1850 million years (or, according to the isochronal curves, to 1650 - 2100 million years!).

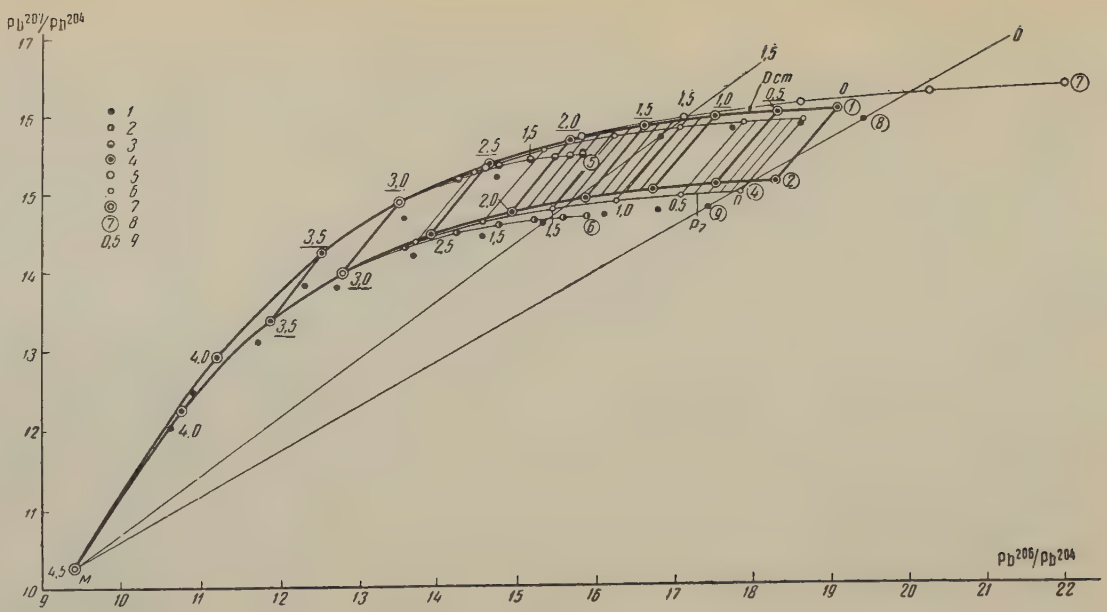

Fig. 7. Construction of graphs for determination of lead ages by their isotopic composition (for the Baltic shield).

1 - points on "undifferentiated" curves; 2 - points on curve No. 6 of the lower family with coefficient 0. 9; 3 - points on curve No. 5 of the upper family with coefficient 0. 8; 4 - points on the Precambrian computation graph; 5 - points on the anomalous curve; 6 - points on the Paleozoic computation graph; 7 - point of 3 billion years' differentiation; 8 - numbers of curves; 9 - age in billions of years (ages on the Precambrian graph are underlined).

In other words, it may be asserted that on the 207/206 graph the contemporaneous leads of a given region from all continents and of all epochs characteristically fall within contours with much greater slope than that of the corresponding isochronal curves and at the same time very similar for the different regions. Comparison shows that such slopes occur only among the isochronal curves for the interval of 4.5 – 3.5 billion years. Thus, these contours and their slopes can not be explained on the basis of a single differentiation assumed in constructing isochronal diagrams.

It may be supposed that instead of a single differentiation occurring 4.5 billion years ago, a continuous differentiation has taken place with constant coefficient k, and this would explain the origin of the contours and their slopes. It is not intended to present detailed calculations here, but a number of points representing modern compositions of leads and their compositions 1.5 billion years ago, computed on the assumption of multiphase differentiation, are plotted in Fig. 6. Every 500 million years, the U^{238}/Pb^{204} ratio is assumed to change by the value of coefficient k, and this corresponds rather closely to continuous differentiation. As was to be expected, with $k > 1$ this ratio becomes anomalously high, and with $k < 1$, anomalously low. In this case, approaching that of continuous differentiation, straight isochronal curves become curved. Two of them are drawn in Fig. 6 through calculated points. It will be seen that the average slope of these curves (isochronals) is gentler than of the isochronals on the previously examined graph, and therefore the observed variation in leads cannot be explained by this process. Evidently, in the case of really continuous differentiation, the isochronal curve would be even more convex in the $k > 1$ region and still flatter in the $k < 1$ region, and this would lead to still greater anomalies and still lower slope of the segment of the curve which interests us.

We are led to the conclusion that in determining the age of leads it is impossible to use either isochronal curves or curves of continuous differentiation (i.e. with k = constant) or differentiation of a similar kind or any average curve like that of Kulp and Bate (Fig. 6). At the same time, our analysis shows that there are definite regularities in the scatter of the isotopic compositions of lead which, it seems to us, could be used as the basis for a method of solving this problem, as described below.

In most cases, the isotope contours on the 207/206 graph have very similar slopes, whatever the time of formation of the leads or the geographic position of the mineralized region from which they were taken. This indicates that the slope of the isotope contours is determined by a process common to the earth's crust as a whole.

The large scatter of the Pb^{207} vales argues against the assumption that there exists a single evolutionary curve for lead. There must exist either two curves bounding the contours at top and bottom (the leads within these curves being mixtures of the two boundary types), or a large number of curves.

As can be seen from Fig. 6, curves with very different k_0 (U/Pb ratio) have very different intervals between like ages, and this causes spreading of the isochronal curves. The similarity in the slope of the contours, i.e., the parallelism of the boundary curves, indicates that both the upper and curves (or all evolutionary curves) have very similar intervals, i.e., very similar values of U/Pb.

The appearance of the upper and lower curves could have been caused by the change in k only at a very ancient time, because curves for the time later than 3 billion years ago have very gentle slopes. According to

Table 7

Calculated Values of Isotopic Composition of Lead for Evolution Curves*

Curve	Time, 10^9 yrs. / isotope	4,5	4,0	3,5	3,0	2,5	2,0	1,5	1,0	0,5	0,0	Character of curve
			$K_1=1,0$					Coefficient $K_{2-9}=1,0$				
10	206 207 208		→	12,84 14,56 —	14,37 15,55 —	15,78 16,19 —	17,09 16,57 —	18,30 16,80 —	19,42 16,94 —	20,46 17,03 —	21,42 17,09 —	Upper boundary curve
					$K_3=1,2$			Coefficient $K_{4-9}=1,2$				
7	206 207 208				→	14,58 15,35 —	15,78 15,71 —	17,11 15,96 —	18,60 16,15 —	20,25 16,29 —	22,00 16,40 —	An example of anomalous curve
					$K_3=1,237$			Coefficient $K_{4-9}=1,0$				
1	206 207 208				→	14,61 15,37 34,63	15,64 15,67 35,87	16,60 15,85 37,08	17,49 15,97 38,27	18,31 16,04 39,42	19,07 16,08 40,55	Upper computation curve for the Precambrian
		$K_0=1,2$	$K_1=0,8$	$K_2=0,8$	$K_3=1,04$			Coefficient $K_{4-9}=1,04$				
3	206 207 208	→ $q=1,3$	11,19 12,03 30,94	12,51 14,24 32,29	13,49 14,88 33,35	14,43 15,29 34,42	15,33 15,55 35,51	16,21 15,72 36,62	17,05 15,83 37,74	17,86 15,90 38,88	18,64 15,94 40,03	Upper computation curve for the Paleozoic
					$K_3=0,9$			Coefficient $K_{4-9}=0,9$				
12	206 207 208				→	14,30 15,23 34,28	14,97 15,43 35,09	15,54 15,54 35,81	16,02 15,60 36,44	16,41 15,63 36,97	16,74 15,65 37,47	Possible curves for the deep parts of the Svecofennian areas assuming "continuous" differentiation (K<1)
					$K_3=0,8$			Coefficient $K_{4-9}=0,8$				
5	206 207 208				→	14,21 15,19 34,17	14,74 15,35 34,82	15,14 15,43 35,32	15,44 15,46 35,71	15,65 15,48 36,02	15,82 15,49 36,26	"Undifferentiated" curves
		$K_0=1,0$					Coefficient $K_{1-9}=1,0$					
8	206 207 208	9,41 10,27 29,16	10,89 12,49 30,30	12,28 13,85 31,41	13,54 14,69 32,40	14,71 15,20 33,54	15,80 15,52 34,57	16,81 15,71 35,58	17,75 15,83 36,56	18,61 15,91 37,51	19,41 15,95 38,45	Lower computation curve for the Precambrian
					$K_3=1,2758$			Coefficient $K_{4-9}=1,0$				
2	206 207 208				→	13,88 14,46 32,43	14,90 14,75 33,28	15,84 14,93 34,10	16,70 15,04 34,92	17,51 15,11 35,70	18,25 15,15 36,46	Lower computation curve for the Paleozoic
					$K_3=1,05$			Coefficient $K_{4-9}=1,05$				
4	206 207 208				→	13,69 14,37 32,28	14,56 14,63 33,01	15,42 14,79 33,75	16,24 14,89 34,52	17,05 14,96 35,30	17,83 15.01 36,10	
		$K_0=0,9$						Coefficient $K_{1-9}=0,9$				
6	206 207 208	→ $q=0,9$	10,75 12,26 30,08	11,86 13,37 30,87	12,78 13,98 31,57	13,56 14,32 32,18	14,20 14,50 32,72	14,74 14,59 33,19	15,19 14,65 33,60	15,56 14,68 33,96	15,86 14,70 34,28	Possible curves for the deep parts of the Karelides and the inner parts of the mantle on the assumption of "continuous" differentiation (K<1)
					$K_3=0,8$			Coefficient $K_{4-9}=0,8$				
11	206 207 208				→	13,47 14,28 32,11	13,98 14,42 32,53	14,36 14,50 32,86	14,64 14,53 33,12	14,84 14,55 33,32	15,00 14,56 33,48	
		$K_0=0,8$	$K_1=1,0$					Coefficient $K_{2-9}=10$				
9	206 207 208	→	10,60 12,04 —	11,70 13,13 —	12,71 13,30 —	13,66 14,21 —	14,53 14,47 —	15,34 14,62 —	16,08 14,72 —	16,77 14,78 —	17,42 14,81 —	Lower boundary curve

* Thick arrows for K >1, thin arrows, for K <1.

Note. Coefficient K in the Table corresponds to k in the text.
Comma represents decimal point.

calculations they could have appeared only in the interval between 4.5 and 4.0 billion years ago.

It has been established that on the 208/206 graph all common lead points are practically enclosed within the curves representing the Th_0^{232}/U_0^{238} rations from 40 to 70, i.e. the ratios of 4.5 billion years ago.

Using all these data, we attempted to calculate standard curves and to construct a graph for dating the leads of the Baltic shield. The basis for the calculations was the concept of differentiation of matter in the earth's crust and the upper part of the mantle, proceeding towards an increase in the U/Pb and Th/Pb ratios ($k < 1$) in the acid differentiates and towards decrease in these ratios in the basic remainder ($k < 1$). To simplify calculations, a differentiation scheme with 500 million interval was adopted. Selected standard curves and the differentiation schemes are shown in Fig. 7 and Table 7.

On the 208/206 graph, the curves with different k's but the same value of q_o (see formula 5, p. 15) lie very close together. To simplify calculations, q was assigned two values, $q = 0.9$ and $q = 1.3$, with the average $X_o = Th^{232}/U^{238} = 46.2$ corresponding to 4.5 billion years ago, and subsequent changes in the value of q were not considered.

The calculations showed the impossibility of constructing graphs at the same time for both Paleozoic and Precambrian leads. For this reason, a pair of curves was calculated for each of these groups of lead (upper and lower curves). The Svecofennian leads (1800 million years) served as the starting point for the upper Precambrian curves, and the Karelian leads (also 1800 million years old, see section 1), for the lower. The starting point for the Paleozoic curves was the left boundary of the Paleozoic contour shown in Fig. 6, which was assigned the age of 450 - 500 million years. This, of course, is arbitrary, and the graph for Paleozoic leads is therefore less reliable than that for the Precambrian. The point of initial differentiation is 4.5 billion years, and the point of main differentiation on each curve (upper and lower) is 3 billion years. When k remains constant over a large period of time, we shall speak of "continuous" differentiation. The data for calculating these curves and the values of coefficient k are presented in Table 7. The procedure consisted in selecting a pair of curves with slopes near those of the curves based on experimental data. As a result of calculations, a pair of curves was obtained for Precambrian leads (1 and 3) and a pair of curves for Paleozoic leads (2 and 4) (Fig. 7).

In constructing the graph (Fig. 8), the points of the same age on the paired curves (1 and 3, 2 and 4) were joined by straight lines or "isochronals" after the points for intermediate ages had been plotted. The ages of leads are determined by superimposing the 207/208 and 208/206 graphs (Fig. 8) on the corresponding graph of the isotopic composition of common lead (Fig. 2) and reading the age directly by the position of lead points in relation to the "isochronals" on the calculated graph.

Besides the standard curves 1 and 3 and 2 and 4, the graph of Fig. 8 has also curves 12 and 5 and 6 and 11. These are curves of "continuous" differentiation with coefficient k being constant and less than unity. Evidently, if, during differentiation, material is formed (a portion of the crust) with coefficient $k > 1$, then in the adjoining part of the crust (mantle) affected by the same process, a corresponding diminution of U/Pb and Th/Pb ratios must occur; i.e. k must be less than unity.

When the value of q changes, for example when the removal of uranium exceeds the removal of thorium and lead, k diminishes and q increases, and this causes displacement of points along curves of types 5 and 12 or 6 and 9 (Fig. 8) on the 207/206 graph, and on graph 208/206 to a sharp upward bending of these curves as they pass to the family of curves with a different q. Thus, the points of isotopic composition of these leads being displaced on graph 208/206 upwards with respect to the Karelian curves, and therefore to the left of their "isochronals," must be of anomalously great age. We believe that this may explain the anomalous ages given by 208/206 graph

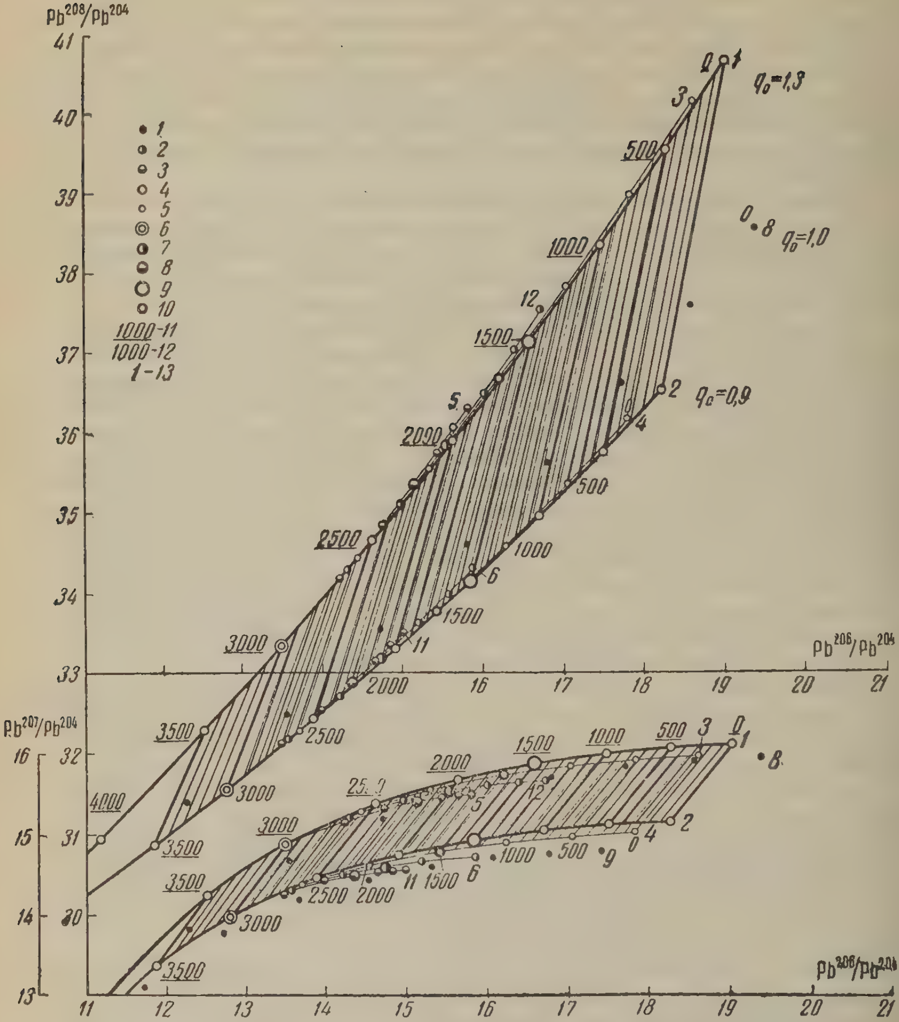

Fig. 8. Graph for determination of absolute age of leads of the Baltic shield by their isotopic composition.

1 - points on "undifferentiated" curves; 2 - points on curves 6 and 12 with coefficient 0.9; 3 - points of curves 5 and 11 with coefficient 0.8; 4 - points on curves of the Precambrian computation graph; 5 - points on curves of the Paleozoic computation graph; 6 - points for differentiation of 3 billion years; 7, 8, 9, 10 - the same points as 2, 3, 4, 5 but for 1.5 bill. years; 11 - age in 10^6 years for Precambrian curves; 12 - age in 10^6 years for Paleozoic curves, 13 - number of curve.

for some of the leads of the Baltic shield related, for example, to the ultrabasic rocks.

Graphs 2 and 8 show that the nominal error of mass spectrometric determinations, ± 1%, corresponds to the interval of 150 to 200 million years on the age graph; i.e., the error of the proposed method for a given point of isotopic composition of lead may be taken as ± 100 million years. As a rule, we are concerned with dating a group of geologically contemporaneous points, and this allows determination of average age and increases the accuracy of the method to ± 30 - 50 million years.

It should be stated in conclusion that the proposed graph evidently is applicable to Precambrian leads of Africa and the Canadian shield but not at all to the Precambrian of the North American Cordillera. For accurate results, it is necessary to construct special regional graphs, especially for the Paleozoic.

The graphs given here are a first attempt at a new approach to the solution of the problem of determination of the age of common leads from their isotopic composition by using not one but two curves of evolution of the isotopic composition calculated on the basis of all available analytical data on the isotopic composition of the leads of the world. Undoubtedly these curves are not the only ones possible. They may be regarded as the first approximation to the solution of the problem. For example, a more accurate estimate of the time of main differentiation, taken by us as 3 billion years, would refine the computed curves. This will change the ages in one direction or another but apparently not to any great extent.

3. DISCUSSION AND SUMMARY

The two main types of leads on the Baltic shield. It has already been mentioned that the isotopic composition of the Baltic shield leads can be rather clearly related to their regional geological setting (see 207/206 and 208/206 graphs, Fig. 2). There are the leads falling on the upper evolutionary curve of the isotope contour of the Baltic shield: these are the Svecofennian leads of Sweden and Finland and the pre-Karelian leads of the White Sea region including the Kandalaksha coast; and there are the leads of the lower evolutionary curve belonging to the Karelide zone. It is remarkable that in the border regions the leads of one zone penetrate into the other, the foreign zone:

a) The Outokumpu galenas of the Karelian zone contain lead of Svecofennian composition.

b) Lead from the oldest galena of Medvezhii Island (No. 87) (Marealbian or Belomor'e zone) has Karelian composition, while the younger leads of this region have the 208/206 ratio of the Karelian leads.

c) All galenas of the Bazarnaya Bay region, lying in the zone of ancient gneisses of the Murmansk block, have lead of typically Karelian composition. They are intimately related to basic dikes and contain secondary cobalt and nickel minerals suggesting a relationship with copper-nickel deposits.

d) The pegmatites of the alkalic intrusives of Kola Peninsula are located in the former Karelian zone but contain galenas whose lead definitely continues the evolutionary line of the Svecofennides.

It is not difficult to see that the Karelian type of lead characterizes the very mobile zones of the second half of the Precambrian which were developing throughout that time. The Svecofennian leads belong to zones already largely stabilized at the beginning of the accumulation of Svecofennian supracrustal rocks. The mobile areas remaining in these zones did not have clearly expressed geosynclinal character.

The Svecofennian type of lead is evidently related to the areas which had reached a higher degree of differentiation, at least in their upper parts, and had undergone rather intensive differentiation even in the early stages of their development (compare curves 1 and 2, Fig. 7, and the data of Table 7, using coefficient k). This differentiation tended to increase the U/Pb and Th/Pb ratios, while in the Karelian zones, during the early stages, it tended to decrease these ratios, and hence the difference between the leads. Evidently the material of the Karelian zones represents the more deep-seated and less differentiated parts of the crust and the mantle.

Thus the isotopic composition of Svecofennian and Karelian leads reveals clearly enough the definite geochemical character of differentiation of the mantle material and the difference in its composition in the two regions of the Baltic shield.

The border zones were influenced by both types of material and hence contain both Karelian and Svecofennian leads. It is precisely on the borders between different regional geologic structures that there are numerous ultrabasic intrusives emplaced over a long period of time (1.5 – 2.0 billion years, as in the Pechenga-Varzuga zone and the adjoining Marealbian and northern Kol'skian zones). The very presence of these large masses of ultrabasic rocks points to the great depth of the boundary seam. So far, it is here only that the leads with the oldest isotopic composition have been found, in the Nittis-Kumuzh'e magnetite (No. 93) and the Nunnanlakhti galena (No. 31).

A comparison of the main geological characteristics of the three types of areas of the Baltic shield (for the Karelian and Svecofennian stages) is given in a generalized and sometimes rather schematic form in Table 8.

Lead age groups. According to their isotopic composition, the leads of the Baltic shield may be divided into eight age groups (Table 9). Both 207/206 and 208/206 graphs were used in the calculations (Fig. 8). The age groups according to Gerling and Polkanov [2] and the data on the age of igneous rocks and the metamorphism of supracrustal deposits are given for comparison. The computed ages give the time of the first separation of lead from its source (magma, rock).

There are cases when the computed age is considerably greater than the actual geological age. In Table 9 all such negatively anomalous leads are placed in the general list of leads according to their computed ages, but are distinguished by heavy type. The arrows in the last column of the table point to the actual age of the ores containing these leads.

Redeposited leads. The presence among primary ores, with the isotopic composition of lead indicating an age of 1800-1850 million years of veinlets and veins of younger ores containing lead with considerably older isotopic composition (Pitkyaranta, Monche-tundra, etc.), up to 2500 million years, points definitely to redeposition of the older leads. For one reason or another, these leads have preserved their isotopic composition unchanged or almost unchanged during many hundred millions of years.

According to the time of redeposition, these leads may be divided into three groups:

1. The leads of the White Sea region pegmatites. The difference in time between their initial separation and the formation of galena during the post-pegmatitic stage is from 100-150 million years. They were redeposited 1950 million years ago.

Table 8

Comparison of the fundamental geological characteristics of the Kareli-Fennoscandian development of various parts of the Baltic Shield and those indicating their particular isotopic lead content

Types of areas	Fennoscandian and older	Transitional zones	Karelian zones
1. Names of zones	Swedish and Central Finnish, Marealbian, Murmansk block. Large blocks of pre-Karelian rocks within the boundaries of Karelian and transitional zones.	West Karelian, Central Kol'skian (western part)	Central and Eastern Karelian, Central Kol'skian (eastern part)
2. Type of development	Uncompleted geosynclinal	Completed geosynclinal	Completed geosynclinal
3. Sediment types of the lower part of Karelian and Fennoscandian sections	Iron-bearing sequences, schists, dominantly acid extrusives and their tuffs (absent in the White Sea region)	Predominantly basic effusives, thick schistose flysch deposits	Very thick spilite-keratophyre effusive-sedimentary sequences
4. Intrusives a) acid	Granites exposed over very large areas; very intensive granitization and migmatization; palingenesis	Local regional granitization and migmatization. Granites widely distributed	Granites occur locally and granitization and migmatization are manifested near them only
b) basic and ultrabasic	Basic intrusives predominate. Ultrabasic, subordinate	Basic intrusives and a very characteristic development of ultrabasic intrusives of the ophiolitic and interformational type	Mainly basic intrusives

Table 8 (Continued)

Types of areas	Fennoscandian and older	Transitional zones	Karelian zones
5. Basement	Either unknown or is composed of repeatedly metamorphosed and ultrametamorphosed gneisses and granite gneisses	Ultrametamorphosed gneisses and granite gneisses	Ultrametamorphosed gneisses and granite gneisses
6. Types of ore deposits	Sedimentary, metamorphic, skarn and magmatic iron ores. Polymetallic skarn ores. Different pegmatites	Skarn iron ores. Sulfide ores. Copper ores with nickel and cobalt Lead veins. Pegmatites rare	Sulfide ores. Copper veins. Molybdenum veins. Lead veins
7. Characteristics of the isotopic composition of lead	Lead composition very uniform in the investigated deposits. The evolution of leads is essentially along the upper evolutionary curve	Great variety among leads. Redeposition of lead from the deeper levels. Redeposition of the older leads is characteristic (?). This is observed in the areas with ultrabasic intrusives. The leads fall both on the upper and lower evolutionary curve	Great variety of leads, repeated introduction of leads with a different composition. Redeposition of old leads from the basement into the higher levels is characacteristic. Development of leads along the lower evolutionary curve

Table 9

Leads of the Baltic Shield Grouped According to Their Computed Absolute Ages

Age group	Geologic time and age limits according to the isotopic composition of leads, 10^6 yrs.	Group in Fig. 8	Locality	Sample No. [1]	Corresponding K/A, Rb/Sr, Pb/U ages [2, 7]		Age of leads from the graph, 10^6 years		Isotopic composition			Time and place of redeposition of leads, 10^6 years of redeposition of leads, 10^6 years
					Gerling and Polkanov's time scale	Actual age, 10^6, years[2]	207/206	208/206 [3]	$\frac{Pb^{206}}{Pb^{204}}$	$\frac{Pb^{207}}{Pb^{204}}$	$\frac{Pb^{208}}{Pb^{204}}$	
				PALEOZOIC								
VIII	Middle Paleozoic		Yukspor (late Khibina leads)	111 *, 112 *		Khibina feldspars	240—290	50—140	18,15	15,82	38,28	
	Lower Paleozoic	F	Early Khibina and Lovozero leads	208 *, 109 *, 110 *		300	360—470	250—460	17,92	15,66	38,32	
				PRECAMBRIAN								
VII	Eocambrian		Galenas of Murmansk coast	102—105 *		Glauconites from enclosing rocks	940—990	930—1020	16,89	15,10	35,26	
		E	Vaida Bay	106 *		920-1010	950	960	16,84	15,07	35,24	
	950—1100		Monchetundra	91, 92		720-1030	1050—1060	1100—1160	16,78	15,20	36,05	
			(syngenetic ores)	90		Sericite 1010	1130	1070	16,84	15,40	35,80	X ~ 1100 ↑
VI	Hoglandian-Jotnian		Rapakivi (feldspar)	18		Rapakivi 1640	> 1480	> 1560	16,39	15,52	36,42	│
	~ 1500 (post-rapakivi)		Orijärvi	14 *		Post-orogenic granites 1540-1670	1500	1530	16,50	15,70	36,80	│
			Kandalaksha	82 *, 83 *			1490—1500	1630—1700	16,13	15,19	35,83	│
V	Hoglandian-Jotnian ~ 1700 (post-orogenic intrusives)		Orijärvi	13 *		Rapakivi 1640 Post-orogenic granites 1540-1670 Lemi rapakivi 1650 Lemi granite 1630-1690	1690—1700	1730—1750	16,09	15,56	36,17	│
			Lemi	17 *					16,13	15,60	36,42	│

Table 9 (Continued)

IV	Late Baltic time 1800—1900 (Orogeny, migmatization granitization)	C	Swedish ore deposits	1,2*, 7*, 116*	Karelo-Sveco-fennides [2]	Pegmatites 1790-1810 1730	1800—1850	1800—1820	15,89 15,61 35,86
			Southern Finland	8*, 9*, 10*, 12*	»	Syn and post orogenic intrusives 1760-1860 1770	1790—1860	1830—1900	15,80 15,46 35,88
			Finnish Karelides	15*, 16*	»	Pegmatites 1845	1850—1860	1840—1980	15,73 15,36 35,30
		C-D	Orijarvi	11*	»	see above	1840	1850	15,74 15,46 34,08
			Sala	4*			1810	1990	15,40 14,95 34,90
			Falun	6*			1870	1800	15,34 14,99 33,84
		D	Kemi	80*	Karelo-Sveco-fennides [2]	Granites 1860 Syn and post orogenic granites and pegmatites 1780-1860 1600-1850 1720-1780	1760	1880	15,43 14,87 34,50
			Shuezero	114			1910	1840	15,41 15,14 34,23
			Khautovara	60			1900	1840	15,38 15,08 34,12
			Yalonvara	34,35			1840—1850	1800—1830	15,48 15,11 34,29
			Pitkyaranta	41, 42, 46			1810—1840	1750—1800	15,46 15,09 34,25
			Pechenga	89, 88, 87			1860—1870	1960—2090	15,17 14,79 34,57
III	Middle Baltic time 2100—2300	B	Faddein-Kel'ya	54*	Belomerides (1900—2100)	Actually all galenas are younger than 1850 million years. Khautovara pyrites have computed age 2100-2150	2110	2100	14,90 14,92 33,71
			Sondala Khautovara	63*			2120	2030	14,88 14,91 33,31
			Pitkyaranta	59,115			2100—2150	2080	15,02 15,14 34,01
				43			2060	2100	14,97 14,89 33,90
			Pitkyaranta	47*, 48*			2250—2280	2280	14,60 14,86 33,54
			Yalonvara	38*, 39*			2150—2160	2200—2210	14,95 15,04 34,35
			Nyalmozero	58*			2210	2130	14,80 14,98 34,57
			Faddein-Kel'ya	55*			2230	2190	14,79 14,99 33,76
			Kinon-Koz-nala	32*			2190	2300	14,85 14,99 34.44

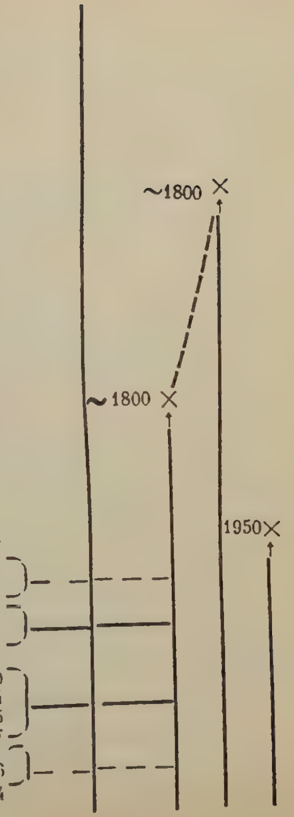

Table 9 (Continued)

		B'	Outokumpu	28 *, 29 *	Correspond to the interval between Belomorides and Upper Saamides (2100-2300)	About 1840 (pegmatites)	2270—2310	**2440—2520**	14,84	15,21	35,29
			Belomor'e	68 *, 69 *, 70 *		Rocks enclosing pegmatites 1900-1950	2180—2260	**2340—2680**	14,67	14,85	35,17
II	Early Baltic time 2350—2500	A	Monche-tundra (ore veins) Pitkyaranta	94—101 49 *	Upper Saamides	Actually: < 1100 < 1800 computed age probably correct	2340—2460	**2450—2510**	14,29	14,73	33,60
			Kinin-Koznala	33 *			2440	2430	14,26	14,77	33,23
			Medvezhii Island (Kandalaksha)	81 *			2370	2370	14,27	14,64	32,96
							2520	2510	14,04	14,65	32,87
			Parandovo	64,65	(2300—2450)	2420-2520	2420—2510	**2500—2550**	14,39	14,89	33,88
			Ulyalegi	57			2480	2530	14,07	14,59	33,08
I	Murmanides (Saamides) 2700—2800		Monche-tundra (magnetite from ore veins)	93	Corresponds to the Lower Saamide-Catarchean interval	Actually: < 1100	2740	2620	13,64	14,56	32,24
			Nunnalakhti	31 *	(2600-2820)	about 1850	2870	3200	13,64	14,81	34,14
—	Catarchean		—	—	Catarchean (2800-3480)	—	—	—	—	—	—
	The oldest isotopic composition of lead on Earth		Rosetta Mine, Africa	R. M.	—	—	3320—3370	**3600—3670**	12,58	14,11	32,77

---

[1] Asterisk marks galenas.
[2] Ages of igneous rocks are printed in ordinary type; age of metamorphism of the enclosing supracrustal rocks, in italics.
[3] Heavy type indicates anomalously high ages given by the 208/206 graph as compared with ages given by the 207/206 graph.
Note: Comma represents decimal point.

Table 10

Types of Redeposited Leads

Age group	Time of redeposition (millions of years ago)												Primary prototype
	1100				1800				1950				
		Pb^{206}	Pb^{207}	Pb^{208}		Pb^{206}	Pb^{207}	Pb^{208}		Pb^{206}	Pb^{207}	Pb^{208}	
B					Pitkyaranta	14.60	14.86	33.54					
III					Sondala	14.88	14.91	33.71					
					Nyalmozero	14.80	14.98	33.57					
					Yalonvara	14.95	15.04	34.35					
B'					Outokumpu	14.84	15.21	35.29	White Sea region	14.67	14.85	35.17	
II A	Monche-tundra	14.29	14.73	33.60	Pitkyaranta	14.26	14.77	33.23					Parandovo 14.39 14.89 33.88
I	Monche-tundra	13.64	14.56	32.24	Nunnanlakhti	13.64	14.81	34.15					?

2. The leads of the late galenas (and sphalerite) of Pitkyaranta, Yalonvara, Faddein-Kel'ya, Nyalmozero, Sondala and Outokumpu. For all of these leads the difference in time between the initial separation and redeposition is from 250 to 500 million years. For one Pitkyaranta galena (No. 49), it is about 640 million years, and for one Nunnalakhti galena (No. 31), 1000 million years. The time of redeposition is about 1800 million years ago.

3. The leads of the massive sulfides from the Monchegora mineralized area. Here the time interval is 1300 million years for lead from the sulfides and 1640 million years for lead from magnetites. The time of redeposition is about 1100 million years ago.

Among the oldest leads (group II) are the leads from the pyrite deposits of Ulyalegi and Parandovo. There is no reason to believe that the lead from these deposits, and hence the ores themselves, have been redeposited. These are metasomatic deposits and the metasomatism, if it occurred not at the time indicated by the isotopic composition of lead (2400-2500 million years ago) but much later, would have inevitably resulted in mixing of the leads introduced by the ore solutions from the depths and the leads of the metasomatized rocks.

What are the characteristics of the redeposited leads?

a) First of all, they are limited exclusively to the Karelide zones.

b) The first two groups coincide in age with the time of very intensive ultrametamorphism in the areas of their occurrence (migmatization and regional granitization).

c) In spite of the geographical separation and difference in time of redeposition of these leads (1950, 1800, 1100 million years ago) the isotopic composition of many of them is similar (Table 10).

For example, the leads of the White Sea region (age 1950 million years) are similar to the leads from the Outokumpu galenas (age 1800 million years). The two types of lead of Monche-tundra (1100 million years old) from the sulfides and magnetite are similar to the leads of the Pitkyaranta and Nunnalakhti galenas, respectively (1800 million years), (assuming the existence of Svecofennian and Karelian types of lead here assumed to be the same).

d) The redeposited leads with the age of 1800 million years have been found, so far, in galenas only (and in one sphalerite).

e) A single deposit may contain redeposited leads of different ages (Pitkyaranta, Nittis-Kumuzh'e, and the Outokumpu and Nunnalakhti deposits located near each other) introduced at about the same time. In the case of Monche-tundra magnetite, the older lead was introduced later. This suggests that the process of extraction of the old leads affected rocks of different ages and extended to a considerable depth.

If it is assumed that the older the isotopic composition of lead, the deeper the horizon where it was originally deposited, and if it is considered that the Parandovo and Ulyalegi ores date back to the early stages of the Karelian geosyncline, and the Khautovara ores (Nos. 59, 115), to the somewhat later stages, then the following assertions can be made. The source of lead for the redeposited leads of groups III and II may have been he oldest Karelian beds and, possibly, the pyrite ores enclosed in them (Perhaps disseminated mineralization of the fahlband type) which formed n the interval of time between the formation of the Ulyalegi ores and the arly Khautovara ores. Another source of lead might have been the pre-Karelian gneisses and granite gneisses, possibly containing deposits synhronous with the above, which were later redeposited. The feldspars of the pre-Karelian gneisses and granite gneisses may also have served as a source. The source of the lead of the Unnalakhti type must have been in considerably older rocks.

Similarly, the source of lead of the Monchegora sulfide veins must have been either in the analogues of the basal part of the Parandovo series if they are present in the region or in the ancient subvolcanic or interformational ultrabasic intrusives containing sulfide inclusions (they must have been early Karelian in age). The lead from magnetite is undoubtedly older and was extracted from the pre-Karelian gneiss complex. That the leads of group II existed in their primary form is shown by the presence of such lead in galena No. 81, whose calculated age may be regarded as correct.

In the White Sea region the leads were fedeposited locally during the formation of pegmatites. Evidently they were derived from the eutectic quartz-feldspar fraction melted out of the oldest gneisses during granitization and migmatization.

In all the numerous cases of redeposition there are only three groups of isotopic composition of lead (if the equivalent Svecofennian and Karelian leads are regarded as one). The composition of each group is amazingly uniform, and this indicates: 1) the regional nature of redeposition, 2) the correctness of the idea that there is a close correspondence between the majority of leads and geological time (taking the evolution along two or more similar curves into consideration), the isolation of redeposited leads from the moment of their separation from the effects of radiogenic additions of uranium and thorium leads and 4) the selective character of their secondary extraction and the absence of foreign leads from the transportation solutions or melts.

It may be assumed that a large role in the process of secondary extraction was played by selective melting of sulfide or silicate components during granitization and migmatization.

Anomalous ages given by the 208/206 graph. In most cases, the ages computed by the 207/206 and 208/206 graphs agree within ± 50 - 60 million years, and often coincide exactly. Sometimes, however, the age given by the 208/206 graph differs from that given by the 207/206 graph by more than ± 70 - 100 million years, i. e., by considerably more than the possible discrepancy due to the error of mass spectrometric determinations. Especially interesting is the case of greater 208/206 ages (printed in heavy type in Table 9). They are given by the leads from: a) the syngenetic and vein ores of Moncha-tundra, the Nunnalakhti galena, the Outokumpu galenas and the Pechenga ores; b) the galenas from the pegmatites of the White Sea region; and c) the galenas of the Kandalaksha coast. This anomaly may be ascribed to an increase in the Th/U ratio during the evolution of the isotopic composition of lead resulting in a shift of its points to the older "isochronals" of the 208/206 graph. The increase in the Th/U ratio is especially common in ultrabasic rocks (it may become several times as high as in granites and basic rocks).

Primary, redeposited and anomalous leads. Let us return to the age groups of leads. Most of the leads older than 1900 million years are redeposited leads. This includes the entire group I and almost all leads of groups II and III. In group IV and in the younger groups, no redeposition has been proved so far; i. e., only the old leads were redeposited.

The oldest primary leads of the Baltic shield are the leads from the pyrite ores of Parandovo and Ulyalegi, and from the galenas of Medvezhii Island (?) (group II). Slightly younger are the leads of the primary pyrite ores of Khautovara (Nos. 59, 115) (group III). Group IV consists of primary leads only, and its age, like that of the leads of groups V and VI, is not in question. Very interesting are the galenas of the Murmansk coast and of Vaida Bay on Rybachii Peninsula. They are identical in the isotopic composition of their lead and in geological characteristics, and must be of the same age. The galena-bearing veins in the region of Vaida Bay are the upper part of the sedimentary section which was at one time referred to the Hyperborean (late Precambrian) formation, and in reference [28], to the Cambrian. The isotopic composition of the leads definitely indicates late Precambrian age of these strata and the impossibility of assigning the entire sequence of beds on Srednii and Rybachii peninsulas to the Cambrian.

New in group IV is the subdivision of the Khibina leads into younger and older subgroups. Evidently the leads of Yukspor are related to the late metasomatic processes and belong to the Middle Paleozoic, while the formation of the older subgroup may be referred to the end of the Caledonian and beginning of the Hercynian time.

The data on the ages of the leads of the Baltic shield indicate contemporaneity of formation of the main ores of Pitkyaranta and Yalonvara, the metamorphism of the Khautovara ores and the formation of the Pechenga ores (referred to lower Karelian!) and of some other deposits.

The isotopic composition of lead and the Precambrian history of the Baltic shield. In determining the time of formation of the Karelian geosyncline, both the geological evidence and the absolute age and isotopic composition of common lead from the ores must be considered. The geological evidence shows that the basal Karelian strata are the Gimoli and Parandovo series resting on ultrametamorphic gneisses and granite gneisses, whose age is about 2500 million years. The metamorphism of the rocks of these series and of the overlying upper Karelian beds occurred between 1850 and 1700 million years ago, for the ages of pegmatite and granites cutting these rocks are within this interval. All this indicates that the deposition of the supracrustal rocks occurred between 2500 and 1900 million years ago. Inasmuch as the pegmatites of the White Sea region were formed 1950-2000 million years ago, and until lately were regarded as older than the Karelian supracrustal deposits, the age of the latter was believed to be between 1900 and 1800 million years, which allowed only 100 million years for their deposition. This interval of time was supposed to cover the entire cycle of development of the Karelian geosyncline: Its inception, subsidence, filling with many kilometers of sedimentary and volcanic rocks, folding, emplacement of the early intrusives, metamorphism, granitization and migmatization on a regional scale, and also more or less prolonged interruptions in sedimentation occurring at least twice in the Karelian section. It is difficult to imagine that only 100 million years were required for all this. Even in the Paleozoic a complete cycle like that occupied from 200 to 300 million years. Very likely the development of the Karelian geosyncline also lasted not less than 200-300 million years. All the absolute ages for the geosyncline were determined on rocks from the final stages in its development ormed by regional metamorphism, intrusion of large granitic masses, ltrametamorphism and granitization. There are no data for the sedimentation cycle and the associated processes.

The isotopic composition of lead from the pyrite deposits of Karelia provides this missing information.

It was mentioned earlier that it cannot be assumed that the leads of the Parandovo, Ulyalegi and Khautovara pyrite ores are redeposited. Therefore the isotopic composition of these leads indicates not only the time of their separation from the source but also the time of separation of the pyrite ore which evidently had the same origin. The ages of these leads are from 2500 to 2200 million years and correspond to the different stages in the development of the geosyncline, as shown by the stratigraphic position of individual deposits (see section 1). The age data obtained from the leads of the ores are in very good agreement with stratigraphy. The later intrusion of granites caused metamorphism of the previously formed pyrite ores and introduced large quantities of iron liberated at considerable depth by regional granitization, which formed magnetite ores in the skarns of the Pitkyaranta type or new pyrite ores of the Yalonvara type.

The genesis of the pyrite ores of the early stages (Parandovo, Ulyalegi, the early ores of Khautovara) may be credited either to subvolcanic and interformational hypabyssal bodies or to accumulations of iron sulfide during subaqueous eruptions.

All this makes it very probable that the Karelian geosyncline had its inception in the granite gneiss basement about 2500 million years ago (at least in eastern and southern Karelia and especially in the more westerly Karelo-Finnish zone; the Karelides of the Kola Peninsula, particularly the Imandra-Varzug and Pechenga formations may be somewhat younger). The geosynclinal stage, i. e., the period of maximum subsidence and the early stages of the orogenic cycle evidently continued until 2000-2200 million years ago. The beginning of orogeny coincided with the development of migmatization, granitization and the formation of pegmatites of the White Sea region. For this reason, it seems to us more correct to consider the Belomorides not an independent orogenic complex, as has been customary until now, but to regard the migmatites and pegmatites of this age (1950-2000 million years) in the White Sea region as the products of the Karelian stage formed under special conditions. The rocks now exposed represent the roots of the core structure of the Karelian zone which, after having undergone the preliminary geosynclinal processes in pre-Karelian time (the thickness of the supracrustal gneisses is up to 15000 m) was plunged to a very great depth. At the time of maximum subsidence of some areas of the Karelian geosyncline, these roots reached the region of migmatization and granitization. Thus the accumulation of the early Karelian supracrustal rocks and the formation of migmatites and pegmatites of the White Sea region were essentially contemporaneous processes but occurred at different depths.

If this is so, then the considerable time interval between the culmination of pre-Karelian folding in Karelia and eastern Finland (2400-2500 million years ago) and the time of emplacement of the first Karelian intrusions and the formation of migmatites (1850 million years ago) becomes understandable. This time interval was occupied by deposition of supracrustal rocks and the formation of pyrite deposits, the earlier ones at Ulyalegi and Parandovo (age--2500 million years) and the later ones, of the Khautovara type (age--2100-2200 million years).

The early Karelian intrusions, granitization and migmatization produced a new series of ore deposits--the skarns of Pitkyaranta, the pyrite ores of Yalonvara, some of the molybdenum-copper quartz veins of the Shuezero type and metamorphosis of the Khautovara ores (pyrrhotite from samples Nos. 59-60). Finally, the deep-seated processes of migmatization and granitization, whose products are now clearly exhibited only in the southwest, in the Ladoga region [29], the feldspathic fraction and, in part, the fahlbands of the early Karelian strata released lead with a "frozen" isotopic composition corresponding to the age of 2100-2300 million years, less commonly, to 2400 million years, which was deposited in veinlets cutting previously deposited ores. It is noteworthy that the older leads such as occur in the Nunnalakhti ores and in Nittis-Kumuzh'e magnetite have been found, so far, only in the regions where ultrabasic intrusions play an important role, i.e., in those regions where materials had been introduced from very great depths. Evidently the numerous quartz veins with chalcopyrite or molybdenite of the Yalonvara, Voitskoe and Sondala types either antedate these leads or are practically contemporaneous with them (in the Ladoga region and Karelia).

The contemporaneity of the Svecofennides and Karelides discussed earlier does not mean that only the intrusion, granitization and migmatization occurred synchronously. The events of the entire geological history of the Svecofennides and Karelides, beginning with the accumulation of sedimentary iron ores and pyrite-bearing spilite-keratophyres, must be considered as synchronous.

For this reason, the earlier age division into Karelides and Svecofennides loses its original meaning (the Karelides were regarded as younger than the Svecofennides) but retains a regional-structural significance, for it indicates that the development in one area occurred according to the Karelide type and in the other, according to the Svecofennide type. The division into Archean and Proterozoic, however, loses all meaning, for it is evident that, under the circumstances, the boundary must lie at the base of the Karelides and Svecofennides, and its age of about 2500 million years places it in the oldest Archean as it is understood now. Consequently we have abandoned the use of these terms (Archean and Proterozoic).

Inasmuch as, according to the point of view here presented, the Karelides must include a part of the upper Saamides (of Gerling and A. A. Polkanov), the Belomorides, as well as the Karelides, and in the west the entire supracrustal section of both the Svecofennides and Karelides (as understood by Swedish geologists), we propose to call the entire complex of these supracrustal rocks the Baltic supracrustal complex. In the Karelian series (Lower and Middle Proterozoic of K. O. Krats [14]), and in the Svecofennian areas, into corresponding Svecofennian series. The age boundaries of the Baltic time are from 2500 to 1700 million years, i.e., from the time of deposition of the basal sediments to the beginning of Hogland-Jotnian sedimentation and intrusion of postorogenic rapakivi granites. The latter initiate the platform cycle. An outline of this subdivision is presented in Table 9.

These ideas provide one possible geological explanation of the isotopic composition of the pyrite ores of Parandovo and Ulyalegi. If it is shown by later investigations that these leads are not primary, as we believe, then the beginnings of the Baltic (Karelian) geosyncline must be shifted to 2100-2200 million years ago, i.e., to the time of formation of the primary pyrite ores of Khautovara. This will not introduce any basic modifications into he age scheme proposed here but only certain corrections. It will be necessary: 1) to regard the Gimoli series as either older than the Parandovo series and contemporaneous with the iron-bearing series of Kola Peninsula, or younger than the Kola iron-bearing series; 2) to give up the idea that the Parandovo and Ulyalegi pyrite ores are related to granites of group III and he spilite-keratophyres and to seek their source at a great depth (?); 3) to consider the ores of these deposits as magmatic or of a very similar type and therefore to provide a new interpretation of their origin; and 4) to consider that 300 million years elapsed (the period between 2500 and 2100-2200 million years) between the culmination of pre-Baltic orogeny and the accumulation of the Baltic supracrustal complex.

In propsoing our scheme, we fully realize that it may not be entirely satisfactory to geologists so far as its agreement with the existing geological evidence, or rather with its interpretation, is concerned. We tried to keep the geological evidence in mind so far as its unfortunately still rather numerous contradictions permitted. It is precisely because of these contradictions that we decided to present the sequence of geological events as suggested to us by the isotopic composition of lead. Whether this was the correct course to take will be shown by future investigations.

A practical project of immediate importance is the study of the isotopic composition of leads from a series of ores.

1. The economically most important type of ore in the Monchegora region is massive sulfide veins. The isotopic composition of their lead differs sharply from that in the syngenetic, mainly poor disseminated ores. Therefore, admixed lead found at a new prospect or in the drill core of sulfide ores with the composition similar to that of the lead from the massive sulfides: 14.29, 14.73, 33.60, will definitely indicate the presence of rich ore in the form of massive veins or other bodies or in the form of brecciated ore. The prospecting value of the isotopic composition of lead in magnetite: 13.64, 14.56, 32.24, is not clear. At present it may be regarded as an indicator of ancient magnetite mineralization. Evidently the veins with chromite found in the Monchegora mineralized area will have the same, or even older, composition of lead.

2. In the same way, lead with the isotopic composition characteristic of the Pechenga type of copper-nickel ores: 15.17, 14.79, 34.57, would indicate the presence of promising ore.

To check and refine these suggestions, it is necessary to sample the copper-nickel mineralization recently found on the Kola Peninsula at many points and to investigate also the isotopic composition of lead in other deposits of the Pechenga region.

3. Lead with the isotopic composition of the type: 14.07–14.29, 14.59–14.89, 33.08–33.88, found in Parandovo-Ulyalegi pyrites, characterizes old, dominantly pyritic ores, and may serve as a criterion for distinguishing them from the younger pyrite-pyrrhotite ores formed by later metamorphism and poorer in sulfur. Rich pyrite ores are of considerable interest to industry, especially in Karelia.

4. It is possible that further investigation will show that the isotopic composition of admixed lead of the type: 15.41, 15.14, 34.23 (Shuezero) is characteristic of molybdenum-bearing quartz veins.

In these studies it is necessary to consider not only the data of analyses but also the position of points of the leads under investigation on the 207/206 and 208/206 graphs. The use of lead isotope indicators in prospecting will permit, if what has been said is confirmed, a much more rapid evaluation of deposits.

The brief discussion of the material presented here* may be summarized as follows:

1. The actual variations in the isotopic composition of lead in the ores of the Baltic shield can be explained only by the existence of two or more evolutionary curves of lead. On the basis of empirical assumptions, two reference curves were computed for the Precambrian (and Paleozoic) leads of the Baltic shield. These curves were used to construct a graph which

---

*A more detailed work will be published.

permits dating of nonanomalous leads by the 207/206 ratio. The 208/206 graph serves the same purpose and in some cases provides information on the geochemical and geological conditions under which a given lead was formed, partly by the difference in the age obtained for it from the 207/206 and 208/206 graphs. The upper evolutionary curve corresponds to the Svecofennian type of development of lead on the Baltic shield, the lower, to the Karelian type.

2. Altogether, eight age groups of leads have been established, of which the first three include redeposited leads carried up from deep and ancient levels. The redeposited leads have been found in the Karelides only, but distributed over a large territory. At present only two episodes of redeposition are known, one that occurred 1800 million years ago in the south and another 1100 million years ago in the north. In spite of geographical separation and difference in age, only three types of redeposited leads have been found.

3. The leads of some of the pyrite deposits date the time of accumulation of supracrustal beds, and this is very important. In Karelia, in particular, the information about the ages of the Ulyalegi, Parandovo and Khautovara ores fills the time interval between 2500 and 2000 million years ago, for which absolute ages were lacking until now.

4. The isotopic composition of the leads from the ores indicates Precambrian age of the Pechenga series and of the formations of the Rybachii and Srednii peninsulas, and the absence of genetic relationship between rapakivi granites and the Ulyalegi and Pitkyaranta ores (it is possible that ores related to these granites will be found in the Khopunvaara and/or Lyupikko areas).

5. The isotopic composition of common leads suggests contemporaneity of accumulation of supracrustal Karelian beds and of granitization and migmatization in the White Sea region. These processes must have gone on at the same time but at different levels.

6. Only the use of the isotopic composition of admixed lead (and not lead from galenas only) from different types of ore gives a complete geological history of shields and other areas, in combination, of course, with geological and age data.

In conclusion, the authors express their thanks to Yu. V. Bogdanov, I. V. Barkanov, S. E. Bresler, A. G. Bulakh, A. D. Genkin, G. O. Glebova-Kul'bakh, N. N. Pertsev, A. I. Polyakov, E. I. Semenov, I. P. Tikhonenkov, L. L. Shilin and O. E. Yushko-Zakharova for providing specimens from their own collections, to N. A. Kruglova, Associate of the A. E. Fersman Mineralogical Museum, Academy of Sciences USSR, N. V. Nikiforova, Associate of the TsNIGR Museum of VCEGEI, for their help in selecting specimens from the collections of these museums, and to L. D. Ivannikova, who took part in calculating and drafting the graphs.

The authors are especially grateful to E. B. Evdokimova, who did all of the chemical preparation of the samples.

REFERENCES

1. Vinogradov, A. P., S. I. Zykov and L. S. Tarasov (1958). Geokhimiya, No. 6.
2. Gerling, E. K., and A. A. Polkanov (1957). Geokhimiya, No. 8.

3. Vinogradov, A. P. (1955). Izotopy Svintsa i Ikh Geokhimicheskoe Znachenie. Sessiya AN SSSR po Mirnomu Ispol'zovaniyu Atomnoi Energii 1-5 Iyula 1955 g. Zasednaie Otd. Khimich. Nauk (Lead isotopes and their geochemical significance. Academy of Sciences conference on the peaceful uses of atomic energy, June 1-5, 1955. Meeting of the Division of Chemical Sciences). Izd. Akad. Nauk SSSR.
4. Vinogradov, A. P., L. S. Tarasov and S. I. Zykov (1957). Geokhimiya, No. 1.
5. Simonen, A. (1953). Bull. Comm. Geol. Finl., N 160
6. Gavelin, S. (1955). Econ. Geol. 50, No. 8.
7. Kouvo, O. (1958). Bull. Comm. Geol. Finl. N 182.
8. Vinogradov, A. P., I. K. Zadorozhnyi and S. I. Zykov (1954). Tr. I Sessii Komisii po Opredeleniyu Abs. Vozr. Geol. Form (Transactions of the First Conference of the Committee for Determination of Absolute Ages of Geological Formations). Izd. Akad. Nauk SSSR.
9. Bate, G. L. and J. L. Kulp (1955). Variations in the isotopic composition of common lead and the history of the crust of the earth. Lamont Geol. Observ. Tech. Rep. Contract AT (30-1), 1114.
10. Nier, A. O., R. W. Thompson and B. F. Murphy (1954). Sb. Izotopy i Geologiya (Collection: Isotopes and Geology). Izd. inostr. lit.
11. Avdzeiko, G. V. and G. R. Rik (1953). Doklady, 90, No. 5, Izd. Akad. Nauk SSSR.
12. Velikoslavonskii, D. A. (1953). Tr. LAGED, vyp. 3.
13. Krats, K. O. and V. N. Numerova (1957). Materilay po Geologgi i Poleznym Iskopaemym S. Z. SSSR (Materials on geology and ore deposits of Southwestern USSR), vyp. 1.
14. Krats, K. O. (1958). Izv. Kar. i Kol'sk filialov AN SSSR, No. 2.
15. Perevozchikova, V. A. (1957). Materilay po Geologii i Poleznym Iskpaemym S. Z. SSSR (Materials on geology and ore deposits of Southwestern USSR), vyp. 1.
16. Shurkin, K. A. (1958). Geologicheskii Ocherk Pitkyaranskogo Polya Keramicheskikh Pegmatitov (Geological description of the Pitkyaranta field of ceramic pegmatites). Izd. Akad. Nauk SSSR.
17. Trüstedt, O. (1907). Bull. Comm. Geol. Finl., N 19.
18. Saksela, M. (1952). Bull. Comm. Geol. Finl., N 154.
19. Vinogradov, A. P. and S. I. Zykov (1955). Doklady, 105, No. 1, Izd. Akad. Nauk SSSR.
20. Starik, I. E. et al. (1958). Tr. V Sessii Komissii po Opredeleniyu Absolyutnogo Vozrasta Geologicheskikh Formatsii (Trans. of the Fifths session of the Committee on Determination of Absolute Age of Geological Formations). Izd. Akad. Nauk SSSR.
21. Bogdanov, Yu. V. (1957). Mater. VSEGEI, n.-s. v. 21. Petrograpficheskii Sbornik, No. 2 (Tr. of the All-Union Geological Research Institute, n. s., vyp. 21: Petrographic essays, No. 2).
22. Eliseev, N. A. et al. (1956). Máter. lab. geolog. dokembr., v. 3. Izd. Akad. Nauk SSSR.
23. Starik, I. E., F. E. Starik, G. V. Avdzeiko, A. Ya. Krylov et al. (1957). Trudy IV Sessii Komissii po Opredeleniyu Absolyutnogo Vozrasta Geologicheskikh Formatsii (Trans. of the Fourth session of the Committee for Determination of Absolute Ages of Geological Formations). Izd. Akad. Nauk SSSR.

24. Zhirov, K. K. and S. I. Zykov (1957). Trudy IV Sessii Komissii po Opredeleniyu Absolyutnogo Vozrasya Geologicheskikh Formatsii (Trans. of the Fourth session of the Committee for Determination of Absolute Ages of Geological Formations). Izd. Akad. Nauk SSSR.
25. Zhirov, K. K., S. I. Zykov and N. I. Stupnikova (1958). Geokhimiya, No. 3.
26. Patterson, C. (1955). Geochim. et Cosmochim. Acta, 10, 4.
27. Houtermans, F. G. (1947). Z. Naturforsch., 2a, 322.
28. (1958). Geologiya SSSR, t. XXVII, Murmanskaya obl., ch. 1 (Geology of the USSR, v. XXVII, Murmansk district, pt. 1). Gosgeoltekhizdat.
29. Sudovikov, S. G. (1954). Tr. LAGED, vyp. 4.

Received for publication
August 14, 1959

ACCUMULATION OF A^{38} IN URANIUM MINERALS

E. K. GERLING and YU. A. SHUKOLYUKOV
Laboratory of Precambrian Geology,
Academy of Sciences, USSR, Leningrad

(ABSTRACT)

The A^{38} content has been investigated in 17 uranium minerals ranging in age from $2 \cdot 10^8$ to $2 \cdot 10^9$ years. The content of U, Pb, rare earths, He, Xe, Cl has been determined in the samples. Corrections for the A^{38} loss have been made according to the data on the He and Xe losses. The calculated excessive quantity of A^{38} in minerals of the same age decreased with the increase of the Cl content which may be explained by the reaction Cl^{35} $(n\gamma)$ $Cl^{36} \xrightarrow{\beta} A^{36}$.

Corrections have been made for A^{38} according to the quantities of radiogenic A^{36}. The earlier proposed nuclear reactions cannot explain the experimental data. There is a proportionality between the U content and the A^{38} content. Between the quantities of A^{38} and xenon of neutron fission (Xe_n) a dependence of the type $A^{38} = aXe_n + b$ has been determined. Samples have been found which at a complete absence of Xe_n contain noticeable quantities of A^{38} ($A^{38} = b$). The possibility of A^{38} formation by the spontaneous fission of U^{238} and the neutron fission of U^{235} has been assumed. The A^{38} formation goes through the hypothetical radioactive isotope with $T_n = (690 \pm 230) \cdot 10^6$ years. The yield of the latter by U fission must be 3 per cent.

Fleming and Thode [1] discovered a shift in the isotopic composition of argon in pitchblende samples of different age. They found that the amount of A^{38} was three times as high as in the atmospheric argon. Wetherill [2] measured the excess of this isotope in pitchblende, monazite and euxenite. The following nuclear reactions have been suggested to explain the production of A^{38} in uranium minerals:

1. $Cl^{35}(\alpha, \underline{n})\,K^{38} \xrightarrow{\beta^+} A^{38}$
2. $Cl^{35}(\alpha, \underline{p})\,A^{38}$
3. $Cl^{37}(\underline{n}, \gamma)\,Cl^{38} \xrightarrow{\beta^-} A^{38}$
4. $K^{41}(\underline{n}, \alpha)\,A^{38}$

We present here the results of our determinations of the content and isotopic composition of argon in 17 uranium minerals of known age.

The method of liberation of argon and its preparation for mass-spectrometric analysis was the same as for xenon and was described by us earlier [3, 4]. Mass spectrometer MS-2M was used.

The amount of excess A^{38} was computed by the formula

$$\underline{V}^{38}_{\text{comp}} = \left[\frac{A^{38}_o/A^{36}_o}{A^{40}_o/A^{36}_o} - \frac{A^{36}_o/A^{40}_o}{A^{36}_A/A^{38}_A}\right]\underline{V}^A \qquad (1)$$

Here $\underline{V}^{38}_{\text{comp}}$ and $\underline{V}^A$ are the volume of excess A^{38} and the total volume of argon. The latter was usually 10^{-4} cm.^{3} and was measured in a McLeod gauge. The condition $V^A \gg V^{38}_{\text{comp}}$ was observed. The expressions in parentheses are the ratios of the isotopes in the sample $\left(\frac{A^{38}_o}{A^{36}_o}, \frac{A^{40}_o}{A^{36}_o}\right)$ and in atmospheric argon (A^{36}_A/A^{38}_A). As a rule the measured A^{36}_A/A^{38}_A ratios in atmospheric argon agreed well with the standard and ranged from 5.2 to 5.5. With poor adjustment of the mass spectrometer, an increase in peak height at mass 39 was observed, which made it difficult to separate peak 38. Careful adjustment removed the effect of peak 39.

In spite of the use of traps with liquid air a "background" always appeared near masses 36 and 38. But the peaks of the "background" were always lower than the peaks being measured and introduced no serious distortions. This was checked by measurements of the isotopic composition of atmospheric argon taken in approximately the same amounts as were liberated from the minerals. The value obtained for atmospheric A^{40}_A/A^{36}_A ratio was always near the standard value.

The A^{36}_o/A^{38}_o ratio in old minerals was usually 0.2–0.7, but in the younger minerals it was higher, 1.0–5.2 The A^{40}_o/A^{36}_o ratio was usually higher than in atmospheric argon (296). This indicates an admixture of potassium in uranium minerals: $K^{40} \xrightarrow{\text{K capture}} A^{40}_p$.

It was shown by us earlier that besides losing much of their helium (92–99%), the minerals under investigation lost also a considerable part of radiogenic xenon (20–70%). Evidently these minerals also lose a certain portion of A^{38}. The A^{38} loss was computed by two methods. In the first, it was assumed that the loss of He, A^{38} and Xe from the uranium minerals is inversely proportional to the square root of mass, i.e., that the following relation obtains:

$$\frac{P_1}{P_2} = \sqrt{\frac{A_1}{A_2}} \qquad (2)$$

where P is the loss of a given gas from the mineral and A is its atomic weight.

In the second method, it was assumed that only helium atoms can escape from the lattices of uranium minerals by diffusion. The heat of diffusion of these minerals is ~ 100,000 kcal./g. atom [5]. The heats of diffusion of A^{38} and Xe in uranium minerals, calculated with the aid of Barrer's data [6] on diffusion of He and A in silica are >100,000 kcal./g. atom. This excludes the possibility of loss of A^{38} and Xe. However, the experimental data show that Xe is lost from the minerals. We assumed that the gases are lost as a result of radiation damage to the crystal lattices of radioactive minerals and metamorphism. In this loss mechanism atomic weight does not play a significant role. In the first approximation, therefore, the loss of A^{38} may be equated with the loss of Xe. The loss of He must obviously be greater, because of the additional escape by diffusion.

In the general case, in uranium minerals, the loss of Xe and A^{38} must occur by both mechanisms, i.e., as a result of damage to the crystal lattice and as a result of diffusion through the somewhat damaged lattice.

Column 6 of Table 1 gives the data on the A^{38} content in the investigated minerals and column 7, the content corrected for loss. The averages of the results obtained by both methods were taken as the most reliable. However, the use of the data obtained by either method does not significantly affect the final results.

Knowing the corrected A^{38} content in the minerals, the discovery of its source may be attempted. The A^{38} content was compared with the amount of chlorine in each mineral in order to check the possibility of the reactions listed above (1). Table 1 shows that the hypothesis of the production of A^{38} in uranium minerals by a reaction with chlorine nuclei must be abandoned. A perfectly clear reverse relationship was found in samples Nos. 11-17 which are all of the same age: the higher the chlorine content, the lower the A^{38} content (content of U in the sample being taken into account) (Fig. 1).

This may be explained as follows: the neutron radiation in uranium min-

$Cl^{35}(n, \gamma)Cl^{36} \xrightarrow[T\,=\,3.1\,\cdot\,10^{-5}\text{ years}]{\beta^-} A^{36}$. The cross section for this reaction is 40b, and for Cl^{37} it is only 0.56b [7].

The presence of radiogenic A^{36} must affect the value of A^{36}_{0} in formula (1) and hence the amount of A^{38} determined in the mineral. It is necessary, therefore, to find a method of calculating the content of isotope A^{36} produced by neutron radiation in uranium minerals.

As shown by the results of earlier investigations [3, 8, 9] a significant role in uranium minerals, besides the spontaneous U^{238} fission, is played by neutron-induced fission of U^{235}. The amount of xenon formed by it varies from sample to sample, depending on the content of neutron-absorbing rare earth elements.

First, the case of accumulation of fissiogenic Xe in the minerals, $[Xe_n]$, was examined.

Let us denote the amount of fissiogenic xenon by n. Then $n = Xe^{sp}_{n} / Xe^{sp}_{n} + Xe^{sp}_{S}$, where Xe^{sp} is the xenon found in the sample and the subscript S indicates spontaneous fission. Previous investigations show that uranium minerals lose a considerable part of xenon [3, 10]. Symbols Xe_n

Table 1

Sample	t·10⁶ years	U, %	Cl, %	Amount of gas in cm.³/g. U · 10⁻⁸							
				Xe_n	V^{38}	V^{38}_{C}	V^{36}_{Cl}	V^{38}_{Cl}	V^{38}	V^{38}_{S}	V^{38}_{n}
Pitchblende, Ukraine	2100	29,4	0,024	355	28,0	142	24	5	147	62	85
Uraninite, Ch. Salma	1950	55,5	0,152	177	20.0	97	43	8	105	55	50
" Chupa No. 1	1950	59,7	0,220	480	21,0	125	160	30	155	55	100
" Chupa No. 2	1950	62,7	0,175	353	16,0	90	94	18	108	55	53
" Chkalov Mine No. 1	1950	64,5	0,350	415	13,0	91	208	39	130	55	75
" Ch. Mine No. 2	1950	56,5	0,200	49	16.0	66	16	3	69	55	14
" B. Lapot'	1950	59.0	0,198	193	11,0	85	31	6	91	55	36
Mendeleyvite	~500	15,1	≤0,03	42	1,40	4,6	≤20	≤4	6,6	3,4	3,2
Samarskite, Ilmne' Mountains	264	6,7	—	0	1,50	1,5	0	0	1,5	1,5	0
Pitchblende G1	230	67,8	0.058	8	0.40	0,9	2,20	0,40	1,3	1,1	0,2
" G2	230	52,0	0.005	20	0,80	2,1	0,80	0,20	2,3	1,1	1,2
" G3	230	69,0	0,001	12	1,00	1,7	0.05	0,01	1,7	1,1	0,6
" G4	230	18,8	0.032	11	0,50	1,1	6,40	1,20	2,3	1,1	1,2
" N230	230	70,5	0,052	8,5	0.85	1,2	2,00	0,40	1,6	1,1	0,5
" Vp	~200	70,5	0 120	9	0,50	0,6	5,00	0,90	1,5	1,1	0,4
" Jachymov	~200	53,8	0.062	10	0,02	0,7	3,90	0,70	1,4	1,1	0,3
" Neugeboren	~200	45,4	0,042	0	0,03	1,1	0	0	1,1	1,1	0

Note: Comma represents decimal point.

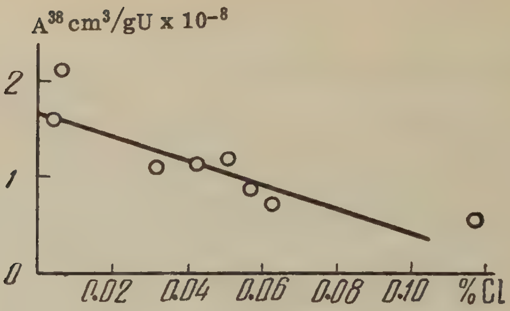

Fig. 1. Dependence between content of A^{38} and Cl in uranium minerals

and Xe_S will be used for the total amount of xenon formed during the life of a mineral. For the ages $t < 2 \cdot 10^8$ years there is a proportionality between the loss of xenon produced by neutron-induced and spontaneous fission. Hence the following expressions are justified:

$$Xe_n \approx \frac{n}{1-n} Xe_S , \qquad (3)$$

$$\frac{dXe_n}{dt} \approx \frac{Xe_n}{t} \approx \frac{n}{1-n} \frac{Xe_S}{t} \qquad (4)$$

In the general case ($t > 2 \cdot 10^8$ years), however, the proportionality between the loss of Xe_n and Xe_S does not exist, because of the difference in the decay rates of U^{238} and U^{235}.

The samples investigated by us were of approximately cubic shape and from 0.2 to 3 cm. on the edge.

A system consisting of "blocks" of uranium minerals more or less uniformly distributed through a very large mass of the enclosing rock may be regarded as a heterogeneous "nuclear reactor." Each crystal is a source of neutrons formed by fission of U and by (α, n) reactions [11]. Calculations taking in consideration the average chemical composition of the radioactive minerals [12] and the enclosing rock [13] show that after a certain delay the radioactive mineral emits ~ 0.5 m.e.v. neutrons. Within a narrow zone, 30-35 cm. from the source, the neutrons are slowed down to the level of resonance energies (200-7 e.v.). At 45 cm. from the source the neutrons become thermal. The average distance within which the neutrons are absorbed is several meters. It follows that, the distance between the "blocks" of uranium minerals being considerable, they are subjected mainly to the action of thermal neutrons.

This model of a natural "nuclear reactor" enabled us to make an approximate calculation of the amount of Xe_n and, further, of neutron-induced

A^{36}*. For the sake of simplicity we assumed: 1) that the coefficient of neutron yield was << 1; 2) that the investigated samples were subjected to approximately the same thermal neutron flux; and 3) that the old minerals had lost most of their radiogenic xenon.

The rate of production of neutron-induced xenon may be represented as:

$$\frac{dXe_n}{dt} \approx \Phi_M \cdot y_{Xe} \cdot \sigma_{235} \cdot H^{N_{235}} \cdot e^{\lambda_{235} t} e^{\lambda_{238} t}. \quad (5)$$

where y_{Xe} is the yield of Xe isotopes from fission, $H^{N_{235}}$, the number of atoms at present and σ_{235}, the cross section of U^{235} fission. The last factor takes into account the variation in flux with time, and Φ_M is the effective neutron flux. In the general case, the value of Φ_M is less than that of the actual flux Φ_0, which a mineral is subjected to because a portion of the neutrons is absorbed by the rare earths almost always present in uranium minerals. The numerical value of flux Φ may be found by measuring the isotopic composition of Xe. In samples with the minimum content of RE (and maximum value of n), the flux determined by formula (5) practically coincides with the actual flux Φ_0. The flux $\Phi_M \approx \Phi_0$ was calculated for three minerals which had maximum Xe_n content: G2, H230 and Katanga pitchblende (42), and satisfied condition (4),

$$\Phi_0 \approx (2.0 + 0.2) \cdot 10^7 \frac{\text{neutrons}^{**}}{g \cdot \text{year}}.$$

The variation in the initial flux due to the absorption of neutrons in the mineral may be related to the Xe_n/Xe_s ratio. Setting $t = 0$ and using expressions (4) and (5), we have:

$$\frac{n}{1-n} \cdot \frac{Xe_S^{\text{Theor}}}{t} = \frac{\Phi_M}{\Phi_0} \cdot 2 \cdot 10^7 \cdot \sigma_{235} \cdot H^{N_{235}}; \Phi_M/\Phi_0 \approx 1.4 \frac{n}{1-n}.$$

The Φ_M/Φ_0 ratio may be interpreted as the "coefficient of transmission" for a uranium mineral. The case when Φ_M/Φ_0 becomes greater than unity ($n > 0.45$) may be interpreted either as the result of multiplication of neutrons in the natural "nuclear reactor" or as the result of good preservation of radiogenic Xe in the mineral. Substitution of Φ_0 and Φ_M/Φ_0 in (5) gives the following formula for the rate of accumulation of Xe:

---

*Yu. G. Pliner derived appropriate formulas based on the theory of the heterogeneous nuclear reactor. But the use of these exact formulas requires the knowledge of many parameters and very complicated calculations. We adopted Pliner's model of a natural "nuclear reactor" but used a simpler method of calculation.

**The determined value of neutron flux may explain the enrichment of uranium minerals in Pu^{239}, an isotope produced by the action of neutrons on U [14, 15].

$$\frac{dXe_n}{dt} \approx 4.6 \cdot 10^4 \frac{n}{1-n} \cdot U \cdot e^{1.12 \cdot 10^{-9}t} \frac{\text{atoms}}{\text{g} \cdot \text{year}} \tag{6}$$

Integration of this expression gives the formula for the amount of xenon produced in a uranium mineral in t years as the result of neutron fission of U^{235}.

$$Xe_n = 15 \cdot 10^{-7} \frac{n}{1-n} (e^{1.12 \cdot 10^{-9}t} - 1) \text{ cm.}^3/\text{g. U} \tag{7}$$

The rate of production of A^{36} is given by the formula similar to (6)

$$\frac{dA^{36}}{dt} = 1.5 \cdot 10^7 \frac{n}{1-n} e^{0.154 \cdot 10^{-9}t} \text{ Cl atoms/g} \cdot \text{year} \tag{8}$$

where Cl is given in g./g.

Kuroda and his associates [16] have measured the activity of Cl^{36} separated from Great Bear Lake pitchblende. The activity $(\frac{dA^{36}}{dt})$ determined experimentally amounted to $(4 \pm 1) \frac{\text{fissions}}{\text{g. Cl} \cdot \text{min.}}$. Calculations by formula (8) gave $(5 \pm 1.5) \frac{\text{fissions}}{\text{g. Cl} \cdot \text{min.}}$.

Integration of (8) after development into Taylor's series gives an equation describing the accumulation of radiogenic isotope A^{36} in uranium minerals:

$$A^{36}_{Cl} = 5.5 \cdot 10^{-13} \frac{n}{1-n} Cl \cdot t \text{ cm.}^3/\text{g} . \tag{9}$$

The amounts of the radiogenic isotope A^{36} determined by equation (9) are listed in column 8, Table 1. But in the derivation of formula (1) all A^{36}_0 was considered atmospheric. It is necessary, therefore, to introduce a correction for the additional amount of A^{38}, also taken as atmospheric in the initial calculations. If V^{38} is the true excess of isotope A^{38} in the mineral, V^{38}_c, the amount found after correction for loss and V^{36}_{Cl}, the amount of radiogenic argon A^{36}, then:

$$V^{38} = V^{38}_c + \frac{V^{36}_{Cl}}{5.35} . \tag{10}$$

Column 9 gives the corrections $V^{36}_{Cl}/5.35$ and column 10, the corrected amounts of argon 38.

An examination of the magnitude of the corrections makes it clear why the relationship shown in Fig. 1 holds for the relatively young minerals, but not for the older ones ($t \sim 2 \cdot 10^9$ years). In the latter case the correction is larger. Its relative magnitude, however, is about 5 times less than for minerals ∼ 2 · 10^8 years old. In the older samples the effect of other processes discussed below become more significant.

To evaluate the possibility of reaction with potassium nuclei $K^{41}(\underline{n}, \alpha) Cl^{38} \xrightarrow{\beta^-} A^{38}$, the content of excess A^{38} in the investigated minerals was compared with the amounts of radiogenic A_r^{40} found in them. In minerals of the same age the A_r^{40}/A^{38} ratio varies without the slightest regularity. This is due, evidently, to the variation in the K content. Considering also that the cross section of this reaction is only 0.03b [7], it must be concluded that it is impossible to explain the accumulation of A^{38} in uranium minerals by the reaction of neutrons with the K^{41} nuclei.

We know of no other nuclear processes which could cause the production of A^{38} in uranium minerals either by alpha activity or neutron-induced fission. Therefore, it may be assumed that A^{38} is produced in uranium minerals either quite independently of neutron or alpha-particle emission, merely from the decay of some unknown admixtures, or owes its existence to uranium alone.

Fig. 2 a represents the relation between A^{38} and U content. With an increase in the latter, the content of A^{38} also increases. In Fig. 2 b the same amounts of A^{38} are plotted on the axis of the ordinates but are referred to one gram of U. Although there is a tenfold increase in the content of uranium in the samples, the amount of argon in cm.^{3}/g. of U remains almost constant. This indicates the impossibility of formation of A^{38} from an admixed substance. We must assume, then, that the accumulation of A^{38} is related to the decay of uranium isotopes.

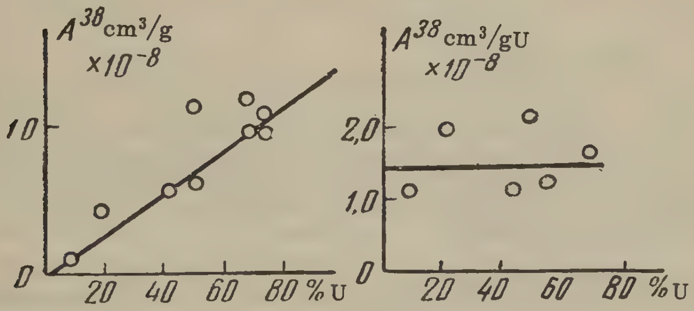

a

b

Fig. 2. Dependence between content of A^{38} and U in uranium minerals

A comparison of the amounts of A^{38} and Xe produced in neutron fission of U^{235} was made. Formula (7) was used to calculate the content of Xe_n. It follows from Fig. 3 that there are two sources of A^{38} in uranium minerals. Part of it is produced together with Xe_n, for the content of A^{38} increases in proportion to the increase in Xe_n. For samples of the same age, $\underline{t}$, the Xe_n/A^{38} ratio remains constant. Inasmuch as $Xe_{\underline{n}}$ is produced as a

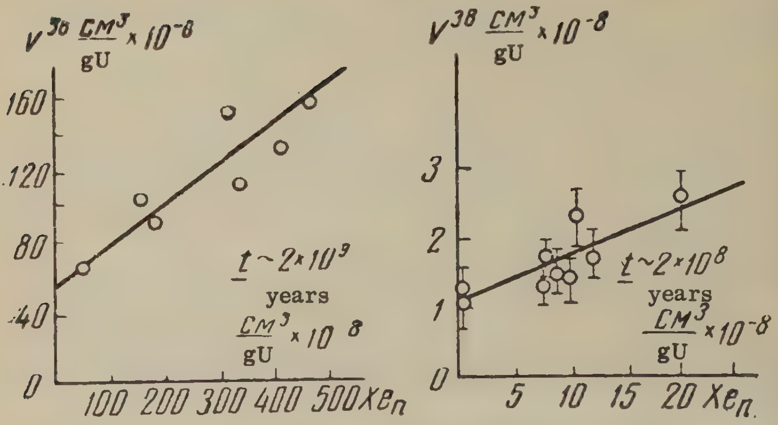

Fig. 3. Dependence between content of A^{38} and $Xe_{\underline{n}}$ in uranium minerals

result of decay of U^{235} nuclei, it may be supposed that A^{38} also is produced by neutron fission of this uranium isotope. The symbol $A^{38}_{\underline{n}}$ will be used to designate A^{38} from this source.

The rest of A^{38} is evidently of a different origin, for in some of the samples practically no neutron fission of U^{235} occurred and yet A^{38} accumulated in notable amounts (samarskite, uraninite from Chkalov Mine No. 2, Neugeborn). This is illustrated by Fig. 3 where the intercepts on the axis of the ordinates represent amounts of A^{38} not produced by neutron fission. It may be assumed that a part of A^{38} was formed by spontaneous U^{238} fission. This part will be designated $A^{38}_{\underline{S}}$.

However, these assumptions meet with difficulties in the analysis of variations in the $Xe_{\underline{n}}/A^{38}_{\underline{n}}$ and $Xe_{\underline{S}}/A^{38}_{\underline{S}}$ ratios. In the case of contemporaneous samples these ratios do remain constant. But both ratios vary considerably in samples of different ages. They increase several times from samples with the ages of $\underline{t} \sim 2 \cdot 10^9$ years to the younger ones with $\underline{t} \approx 2 \cdot 10^8$ years.

This difficulty could be removed by assuming that A^{38} forms in the fission of uranium isotopes, not directly, but through an intermediate radioactive substance with a longer half life. This substance will be designated M (mother substance).

The rate of accumulation of the hypothetical substance M in spontaneous U fission equals:

$$\frac{d_S N_M}{dt} = {}_{\underline{S}}y_M \cdot \frac{\lambda_S}{\lambda_{238}} (\lambda_s + \lambda_{238}) N_{238} - \lambda_M N_M. \qquad (11)$$

Here λ_S and λ_{238} represent the rate of spontaneous fission and alpha decay of U^{238}, respectively; λ_M is the rate of decay of M; $\underline{N}$, the number of atoms; and ${}_{S}y_{M}$, the yield of M in spontaneous fission of U^{238}. The first term on the right side of equation (11) is the rate of formation of the hypothetical substance M; the second is the rate of its decay.

Solving the differential equation (11), we have:

$$ {}_{S}N_{M} = {}_{H}N_{238} \cdot \frac{{}_{S}y_{M}\lambda_{S}}{\lambda_{M}} [e^{\lambda_{238}t} - e^{(\lambda_{238} - \lambda_{M})t}] \qquad (12) $$

where ${}_{H}N_{238}$ is the number of atoms at present. Equation (12) determines the amount of substance M in a mineral of any age t.

The amount of A^{38}_{S} is given by the expression:

$$ A^{38}_{S} = \int_{0}^{t} -\left(\frac{d\,{}_{s}N_{M}}{dt}\right)_{fiss} dt = \int_{0}^{t} \lambda_{M} \cdot {}_{S}N_{M}dt = \qquad (13) $$

$$ = {}_{H}N_{238} \cdot {}_{S}y_{M} \cdot \lambda_{S} \left\{ \frac{1}{\lambda_{238}} (e^{\lambda_{238}t} - 1) - \frac{1}{\lambda_{238} - \lambda_{M}} [e^{(\lambda_{238} - \lambda_{M})t} - 1] \right\} $$

For two minerals of ages t_1 and t_2 the following expression holds: (14)

$$ \frac{(V^{38}_{S})_1}{(V^{38}_{S})_2} = \frac{6.5(e^{0.154 \cdot 10^{-9}t_1} - 1) \cdot 10^9 - \frac{1}{0.154 \cdot 10^{-9} - \lambda_M} \cdot [e^{(0.154 \cdot 10^{-9} - \lambda_M)t_1} - 1]}{6.5(e^{0.154 \cdot 10^{-9}t_2} - 1) \cdot 10^9 - \frac{1}{0.154 \cdot 10^{-9} - \lambda_M} \cdot [e^{(0.154 \cdot 10^{-9} - \lambda_M)t_2} - 1]} $$

Substituting different values of λ_M in (14) it is possible to find a value for which the right side of the equation becomes equal to the experimentally determined left side. Table 2 presents the values of λ_M found for a group of minerals of different ages.

Thus the hypothetical substance forming from spontaneous decay of U^{238} and transmuting into A^{238}_{S} must have half life of (690-200) · 10^6 years.

Table 2

Determination of the Value of λM

t_1, years	$(V^{38}_{S})_1$, cm.³/g. U	t_2, years	$(V^{38}_{S})_2$, cm.³/g.	U λ_M, year^{-1}
$1.95 \cdot 10^9$	$55 \cdot 10^{-8}$	$0.23 \cdot 10^9$	$1.1 \cdot 10^{-8}$	$1.4 \cdot 10^{-9}$
$1.95 \cdot 10^9$	$55 \cdot 10^{-8}$	$0.264 \cdot 10^9$	$1.5 \cdot 10^{-8}$	$0.8 \cdot 10^{-9}$
$0.264 \cdot 10^9$	$1.5 \cdot 10^{-8}$	$0.23 \cdot 10^9$	$1.1 \cdot 10^{-8}$	$0.7 \cdot 10^{-9}$

Average $(1.0 \pm 0.3) \cdot 10^{-9}$

Using formula (13) and experimental data, it is possible to determine the yield of substance M in spontaneous fission of U^{239} (Table 3).

Table 3

Yield of the Hypothetical Substance M in Spontaneous Fission U^{238}

$\underline{t}$, years	$1.95 \cdot 10^{9}$	$0.264 \cdot 10^{9}$	$0.230 \cdot 10^{9}$
${}_{S}Y_{M}$	3.8	4.0	3.2

Average ${}_{S}Y_{M}$ = (3.7 ± 0.3)%

The rate of accumulation of the hypothetical substance M in neutron fission of U^{235} is expressed by the equation:

$$\frac{d\,{}_{n}N_{M}}{dt} = \Phi_{M} \cdot {}_{n}y_{M} \cdot \sigma_{235} \cdot N_{235} - \lambda_{M} \cdot {}_{n}N_{M} \cdot \qquad (15)$$

The solution of this differential equation gives an approximate expression for the content of M in a mineral at any moment of time $\underline{t}$:

$${}_{n}N_{M} = \frac{\Phi_{M} \cdot {}_{n}y_{M} \cdot \sigma_{235}}{\lambda_{M} - \Phi_{M} \cdot {}_{n}y_{M} \cdot \sigma_{235}} \cdot {}_{H}N_{235} \cdot e^{1.12 \cdot 10^{-9}t} \cdot (e^{-\Phi_{M} \cdot {}_{n}y_{M} \cdot \sigma_{235}t} - e^{-nMt}). \qquad (16)$$

For changing to $A_{\underline{n}}^{38}$ we use the condition:

$$\frac{dA_{n}^{38}}{dt} = \lambda_{M} \cdot {}_{n}N_{M} \cdot \qquad (17)$$

Substituting expression (16) in (17) and simplifying, we obtain, after integration:

$$V_{n}^{38} = 1.3 \cdot 10^{-5} \cdot \frac{n}{1-n} \cdot {}_{n}y_{M} \cdot (e^{1.12 \cdot 10^{-9}t} - 6.5 \cdot e^{0.12 \cdot 10^{-9}t} + 5.5) \frac{\text{cm.}^{3}}{\text{g} \cdot \text{U year}} \cdot \qquad (18)$$

Formula (18) gives the amount of A^{38} formed by neutron-induced fission of U^{235}. Inasmuch as $\underline{V}^{38}$ is determined experimentally as the difference between V^{38} and $V_{\underline{S}}^{38}$, expression (18) may be used to find ${}_{\underline{n}}y_{M}$, the yield of A^{38} in U^{235} fission.

Table 4

Yield of the Hypothetical Substance M in neutron-Induced Fission of U^{235}

Sample	$\underline{t} \cdot 10^6$ years	$\underline{n}$	$V_n^{38} \cdot 10^{-8}$ cm.^{3}/g. U	$_{\underline{n}}y_M$%
Pitchblende, Saksagan'	2100	0.20	85	2
Uraninite, Ch. Salma	1950	0.13	50	5
" Chupa No. 1	1950	0.29	100	3
" Chupa No. 2	1950	0.24	53	2
" Chkalov Mine No. 1	1950	0.26	75	3
" Chkalov Mine No. 2	1950	0.04	16	5
" B. Lapot'	1950	0.08	36	6
Mendelevite	500	0.27	3.2	3
Pitchblende G1	230	0.17	0.2	1
" G2	230	0.34	1.2	2
" G3	230	0.24	0.6	4
" G4	230	0.22	1.2	5
" H230	230	0.18	0.5	3
" Vp	200	0.19	0.4	2
" Jachymov	200	0.21	0.3	1

The calculated values are given in Table 4.

Table 4 shows that in spite of the tenfold change in $\underline{t}$, eightfold change in $\underline{n}$ and variation in the value of $V_{\underline{n}}^{38} \sim 500$, the yield of substance M remains practically constant within the limits of error of determination: $_{\underline{n}}y_M$ = (3 ± 1)%.

It follows from equations (16) and (18) that the following relation holds for two minerals of different ages:

$$\frac{\left(V_n^{38}\right)_1}{\left(V_n^{38}\right)_2} = \frac{\left(\frac{n}{1-n}\right)_1 \left\{\frac{1}{\lambda_{235}+0,154\cdot 10^{-9}}\left[e^{(\lambda_{235}+0,154\cdot 10^{-9})\cdot t_1}-1\right] - \frac{1}{\lambda_{235}+0,85\cdot 10^{-9}}\left[e^{\lambda_{235}-0,85\cdot 10^{-9})\cdot t_1}-1\right]\right\}}{\left(\frac{n}{1-n}\right)_2 \left\{\frac{1}{\lambda_{235}-0,154\cdot 10^{-9}}\left[e^{(\lambda_{235}+0,154\cdot 10^{-9})\cdot t_2}-1\right] - \frac{1}{\lambda_{235}-0,85\cdot 10^{-9}}\left[e^{(\lambda_{235}-0,85\cdot 10^{-9})\cdot t_2}-1\right]\right\}} \qquad (19)$$

Here $0.154 \cdot 10^{-9} = \lambda_{238}$, $0.85 \cdot 10^{-9} = \lambda_M - \lambda_{238}$. It is possible by using the graphic method to select a value for the rate of alpha decay of U^{235} which would make the right and left sides of the above expression equal. If all the above calculations and the hypothesis of formation of A^{38} and substance M from fission of uranium are correct, a standard value of λ_{235} should be obtained. The calculations gave the following results:

$$\lambda_{235} = (1.0 \pm 0.3) \cdot 10^{-9} \text{ year}^{-1} \text{ and } \underline{T}_{235} = (690 \pm 200) \cdot 10^{6} \text{ years.}$$

The values accepted at present [17] are:

$$\lambda_{235} = 0.97 \cdot 10^{-9} \text{ years}^{-1} \text{ and } \underline{T}_{235} = 710 \cdot 10^{6} \text{ years.}$$

Thus the obtained value for the rate of alpha decay of U^{235} agrees with the standard value, the error of determination being taken into account. This is one of the confirmations of the correctness of the hypothesis that A^{38} accumulates as a result of fission of uranium nuclei.

The question of the mechanism of the formation of argon nuclei in the process of fission now arises.

The simplest explanation would be the formation of substance M and then of A^{38} by the division of the U^{238} and U^{235} nuclei into three fragments of commensurable mass. Energetically, this process may even be more advantageous than the usual splitting into two fragments [18, 19]. However, according to the data of the photographic [20] and ionization [20, 21] methods, the probability of fission into three commensurable masses is less by 2 or 3 orders of magnitude than the yield of y_M.

It has been shown by the radiochemical method that the yield of Cl in fission amounts to several percent [22] (the data of this work have not been checked), and this points to the possibility of considerable yield in the region of mass ~ 40.

It may be supposed that in addition to splitting into fragments whose masses are in the ratio 2 to 3, there occurs also a more asymmetrical fission with the mass ratio 1:5. This could result in the formation of nuclei of the hypothetical substance M with mass ~ 40. This contradicts the data of radiochemical investigations [23]. While some results of ionization measurements show that the yield in the neighborhood of mass 40 approaches 1% [24], the data of other authors are in agreement with the results of radiochemical work [25].

The formation of A^{38} from the highly excited fission fragments has little probability. The passage of a nucleus with mass 40 through a potential barrier requires energy in excess of 50 m.e.v. The actual excitation energy of the fragments is much smaller.

The formation of A^{38} as a result of collision of fission fragments having considerable kinetic energy with the nuclei of the atoms in the mineral is also improbable. This might result in a reaction similar to that which occurs when accelerated heavy ions (C^{12}, O^{16}, N^{14}) act on the nuclei of heavy elements [26]. However, the cross section of such a process is negligibly small.

The available experimental data, as well as the theory of nuclear fission in its present form, can neither confirm nor disprove our hypotheses. Further investigations are needed for a final solution of the problem.

Summary

1. The A^{38} content has been determined in 17 uranium minerals. It depends on the age of the mineral, the content of U and also on the value of $Xe_{\underline{n}}/Xe_{\underline{n}} + Xe_{\underline{S}}$. The nuclear reactions with K and Cl proposed earlier cannot explain the experimental data.

2. Considerable amounts of A^{36} are formed in uranium minerals by the reaction: $Cl^{35} + \underline{n} \rightarrow Cl^{36} \xrightarrow{\beta-} A^{36}$. This must be taken into account in measuring A^{38} in minerals.

3. A relationship of the $A^{38} = aXe_{\underline{n}} + \underline{b}$ type has been found between the content of A^{38} and $Xe_{\underline{n}}$. Considerable amounts of A^{38} have been found in the samples, although xenon derived from neutron fission of U^{235} is completely absent; i.e. $A^{38} : Xe_{\underline{n}} = 0$, $A^{38} = \underline{b} > 0$. The production of a part of the A^{38} is not due to neutron activity.

4. It is concluded that A^{38} may be produced both in spontaneous fission of U^{238} nuclei ($A^{38}_{\underline{S}}$) and in neutron-induced fission of U^{235} ($A^{38}_{\underline{n}}$).

5. The variation of the $A^{38}_{\underline{n}}/Xe_{\underline{n}}$ and $A^{38}_{\underline{S}}/Xe_{\underline{S}}$ ratios with time indicates that A^{38} is formed, not directly, but through an intermediate unknown radioactive mother substance (M). The half life of this substance $T_M = (690-200) \cdot 10^6$ years; its yield in spontaneous fission, ${}_{\underline{s}}y_M = (3.7 - 0.3)\%$, and in neutron induced fission, ${}_{\underline{n}}y_M = (3 - 1)\%$.

REFERENCES

1. Fleming, W., and H. Thode. Phys. Rev., Vol. 90 (1953).
2. Wetherill, G. Phys. Rev., Vol. 96 (1954).
3. Gerling, E. K., and Yu. A. Shukolyukov. Radiokhimiya, vyp. 2 (1959).
4. Shukolyukov, Yu. A. Tr. V Sessii Komissii po Opredeleniyu Absolyutnogo Vozrasta Geologicheskikh Formatsii (Trans. of the Fifth Session of the Committee for Determination of Absolute Ages of Geological Formations), p. 289. Moscow (1958).
5. Gerling, E. K. Tr. Radievogo in-ta Akad. Nauk SSSR, VI (1957).
6. Barrer, R. M. Diffuziya v Tverdykh Telakh (Diffusion in and through solids). Izd. inostr. lit., Moscow (1958).
7. Boyd, A., F. Brown and H. Lounsbery. Canadian J. Phys., Vol. 33, No. 2 (1955).
8. Macnamara, J. and H. Thode. Phys. Rev., 80, No. 3 (1950).
9. Fleming, W. and H. Thode. Phys. Rev., Vol. 92, No. 2 (1958).
10. Wetherill, G. Phys. Rev., Vol. 92, No. 4 (1958).
11. Kashkarov, L. K. and V. V. Cherdyuntsev. Geokhimiya, No. 7 (1958).
12. Soboleva, M. V. and I. L. Pudovkina. Mineraly Urana (Uranium minerals). Gosgeoltekhizdat, Moscow (1957).

13. Labuntsov, A. N. Pegmatity Severnoi Karelii Pegmatity SSSR i Ikh Mineraly (Pegmatites of Northern Karelia and their minerals. Pegmatites of the USSR). Izd. Akad. Nauk SSSR, Moscow (1939).
14. Levine, Ch. and G. Seaborg. J. Amer. Chem. Soc., Vol. 73 (1951).
15. Starik, I. E., A. P. Ratner, M. A. Pasvik and F. L. Ginzburg. Geokhimiya, No. 2 (1957).
16. Kuroda, P., R. Edwards, B. Robinson, J. Jonte and G. Goolsby. Geochim. et Cosmochim. Acta, Vol. 11 (1957).
17. Seaborg, G. T., I. Perlman and J. Hollander. Tablitsa Isotopov (Table of isotopes). Izd. inostr. lit. (1956).
18. Present, R. Phys. Rev., Vol. 59 (1941).
19. Perfilov, N. A. Fizika Deleniya Atomnykh Yader. Prilozhenie No. 1 k zh. Atomnaya Energiya (Physics of nuclear fission. Supplement No. 1, J. of Atomic Energy (1957).)
20. Dutta, S. Indian J. Phys., Vol. 27, No. 11 (1953).
21. Rosen, L. and A. Hudson. Phys. Rev. Vol. 78 (1950).
22. Radiochemical Studies. The fission products. v. 1 (1951).
23. Prawitz, J. and J. Rydberg. Acta Ch. Sc., Vol. 12 (1958).
24. Kovrigin, B. S., and K. A. Petrzhak. Atomnaya Energiya, 4, vyp. 6 (1958).
25. Milton, J. S. D. Proc. of the symposium on the physics of fission held at Chalk River, Ontario (1956).
26. Polikanov, S. M. Author's abstract of dissertation in physics and mathematics. Dubna (1958).

Received for publication
May 21, 1959

RADIOACTIVITY OF THE WATERS OF THE INDIAN OCEAN

V. I. BARANOV and L. A. KHRISTIANOVA
V. I. Vernadskii Institute of Geochemistry
and Analytical Chemistry
Academy of Sciences USSR, Moscow

(ABSTRACT)

A direct determination of uranium content in some tens of water samples of the Indian Ocean has been carried out. It is found that the uranium content in the central areas of the ocean averages $1.8 \cdot 10^{-6}$ g/l.

In the south-western part the content is somewhat higher ($1.0 \cdot 10^{-8}$ g/l). By calculation the concentrations of thorium ($1.0 \cdot 10^{-8}$ g/l) and of ionium ($6 \cdot 10^{-13}$ g/l) have been estimated for water in the central part of of the ocean where a distinct disturbance of the radioactive equilibrium is established in the uranium family towards a considerable ionium deficiency compared to uranium.

In 1956 the authors began a systematic radiochemical investigation of the bottom muds of the Indian Ocean. This investigation revealed general regularities in the distribution of radioelements in bottom sediments of different lithological types and the rates of sedimentation in different parts of the ocean [1]. A natural extension of this work was a study of radioactivity of the waters of the Indian Ocean. This is important not only for the correct understanding of the regularities of deposition of radioactive elements on the ocean bottom but may also be useful in the solution of some oceanographic problems, for example in the determination of the rate of circulation of oceanic waters [2].

At our request, during the second cruise of the Second Complex Antarctic Expedition, V. M. Kutyurin collected samples of sea water at different points in the ocean. The temperature, salinity and other properties of the samples were determined on board ship and their uranium content was concentrated with the organic precipitant methyl violet by the method of V. I. Kuznetsov and T. G. Akimova [3]. The dry uranium-bearing residues were delivered to us for luminescence analysis.

The samples of water were collected along two oceanic sections from the southern tip of Africa to Antarctica and along a meridian from Antarctica to the Bay of Bengal. The samples were taken from the surface and from different depths.

The results of analyses and coordinates of the sampling points are presented in the table.

Uranium Content in the Surface Waters of the Indian Ocean
(samples collected February 22 - May 14, 1956)

Coordinates of sampling points	Concentr. of U, γ/1	Salinity, %	pH	Temperature of water, °C	No. of station
40°04′S 20°01′E	3,0	34,99	8,15	21,40	no No.
30°10′S 25°35′E	3,3	35,37	8,15	19,73	266
40°37′S 27°13′E	2,3	35,33	8,15	21,40	267
40°37′S 27°13′E	2,7	33,93	—	15,30	no No.
42°41′S 32°06′E	3,1	34,75	8,17	13,03	268
42°41′S 32°06′E	2,9	34,09	—	10,00	no No.
45°05′S 34°59′E	2,3	33,93	8,07	7,95	269
45°05′S 34°59′E	1,7	33,81	—	5,70	no No.
49°49′S 41°21′E	3,3	33,85	8,09	4,87	271
52°18′S 53°31′E	3,4	33,87	8,03	3,80	273
52°32′S 57°42′E	2,2	33,88	8,05	3,29	274
53°07′S 71°48′E	1,9	33,82	8,12	3,10	276
60°04′S 77°34′E	1,8	33,90	8,03	0,54	280
62°27′S 97°35′E	1,9	34,03	8,05	—0,05	281
60°51′S 97°38′E	2,2	34,06	8,04	0,45	284
55°54′S 96°58′E	1,8	33,92	8,08	1,57	287
51°36′S 97°02′E	1,9	33,86	8,04	4,04	289
42°29′S 97°05′E	2,1	34,58	8,16	11,80	295
36°05′S 97°02′E	2,1	35,40	8,15	16,36	299
29°13′S 97°01′E	1,4	35,83	8,14	21,07	303
21°26′S 97°04′E	2,2	34,60	8,17	25,18	307
16°48′S 96°54′E	1,6	34,57	8,16	26,32	309
7°48′S 90°48′E	2,0	34,19	8,13	29,00	214
00°02′N 88°32′E	1,4	34,52	8,13	29,40	318
07°56′N 80°03′E	1,8	32,99	8,15	30,90	322
19°04′N 88°06′E from 25 m depth	1,4	33,40	8,11	29,90	325
20°01′N 88°0′ E	1,5	33,21	8,12	29,00	328
20°55′N 88°01′E	1,8	34,21	8,14	28,40	329

Note: Comma represents decimal point.

The table shows that the uranium content in the surface samples along the Africa-Antarctica section averages $2.7 \cdot 10^{-6}$ g/l with slight variations in both directions. The salinity and acidity of the water are practically constant, and the temperature decreases regularly from 21.4°C in the region of Africa to 4.1°C in the region of Antarctica.

Along the Antarctica-Bay of Bengal section, the uranium content falls to $2 \cdot 10^{-6}$ g/l and apart from slight variations remains practically constant.

Thus, the waters of the southwestern part of the Indian Ocean contain $2.7 \cdot 10^{-6}\%$ uranium and its southern, northern and central parts, $1.8 \cdot 10^{-6}\%$. This is an average between the concentration of uranium in the Pacific Ocean, $1.3 \cdot 10^{-6}\%$ for normal salinity of $35°/_{00}$ and its concentration in the Atlantic Ocean, where it reaches $3.3 \cdot 10^{-6}\%$ [4].

At most stations deep samples were taken which gave uranium concentrations at different depths in the ocean.

The results are shown on the graph, with the depths plotted on the axis of the abscissas and the uranium content, on the axis of the ordinates (Figs. 1 and 2). Most stations show high uranium content at the depth of 100 m (stations 269, 264, 291, 299, 303 and 322) and at 1000 m (stations 266, 269, 303 and 322). Low concentrations of uranium were found at 400 m (269, 274, 281, 280). The samples collected from the depth of several thousand meters (3000-5000 m) contain, as a rule, the same amount of uranium as the upper levels, about $2 \cdot 10^{-6}$ g/l U (stations 318, 322, 303, 299, 314, 289, 274). At stations 266, 269 and 318 the highest uranium content was found at 2000 m. In a number of cases, high uranium content was found also at 700 m. On the whole, the range of content is not great and lies between $2 \cdot 10^{-6}$ and $3 \cdot 10^{-6}$ g/l U.

Koczy [5] found a similar distribution of uranium with depth in the waters of the Pacific and Atlantic oceans, but there the absolute values were even lower, between $1 \cdot 10^{-6}$ g/l and $1.5 \cdot 10^{-6}$ g/l. The causes of variation in uranium content with depth are not clear at present. Possibly the determination of CO_2 in water would throw light on this problem. The investigations of I. E. Starik [6] show that, depending on the content of the carbonate ion, uranium may be present in sea water either as $[UO_2(CO_3)_3]^{4-}$ complex (carbonate ion content $> \underline{n} \cdot 10^{-6}\underline{N}$) or as the products of hydrolysis adsorbed on the silica-bearing colloidal particles (Carbonate ion content $< \underline{n} \cdot 10^{-6}\underline{N}$). In the last case, uranium settles to the ocean bottom. It is possible that at the depth of 1000-2000 m the concentration of the carbonate ion is relatively low and this causes a certain concentration of uranium. This hypothesis requires special verification.

No direct determination was made of the thorium and ionium content in the Indian Ocean waters. However, the content of these elements may be estimated by a calculation based on their content in the bottom sediments. Throium isotopes are carried to the ocean bottom by the sesquioxides. "Their chemical properties are such that they are easily precipitated from solutions by iron hydroxide at certain pH values. This is the process used in analysis. The same process occurs in the ocean, where colloidal iron, manganese, aluminum and other hydroxides precipitate and concentrate thorium isotopes in the red clay" (A. P. Vinogradov [7]).

This concept is confirmed by several cores from stations 97, 103, 107, 119, 116 and 136, in which there is a clearly defined proportionality between the content of thorium isotopes and the content of iron and manganese [1]. It may be assumed, then, that the Fe/Th and Fe/Io ratios in the bottom deposits are the same as in sea water.

This makes it possible to calculate thorium and ionium concentration in sea water from their ratio to iron in the sediments and the content of iron in sea water.

We found ater performing appropriate calculations that the Indian Ocean waters contain $1.0 \cdot 10^{-8}$ g/l Th and $11.0 \cdot 10^{-13}$ g/l Io. These values are in good agreement with those of E. Picciotto et al. [8], who by the use of the nuclear emulsion technique obtained $2 \cdot 10^{-8}$ g/l for thorium and $6 \cdot 10^{-13}$ g/l for ionium content in the waters of the Atlantic Ocean.

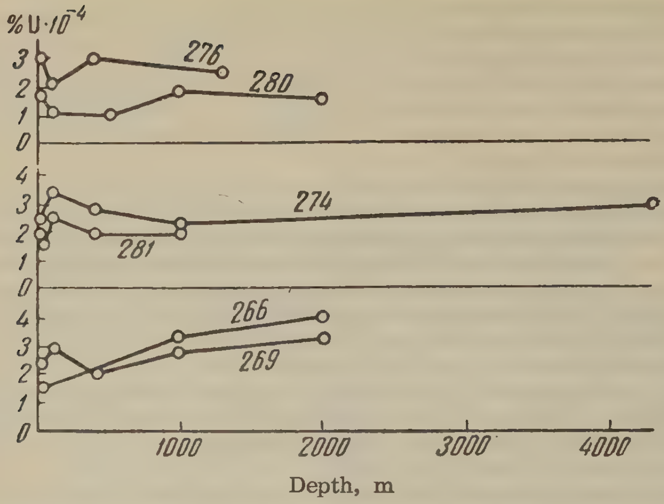

Fig. 1. Uranium content in the Indian Ocean water along a vertical section at six stations (southern tip of Africa–Antarctica)

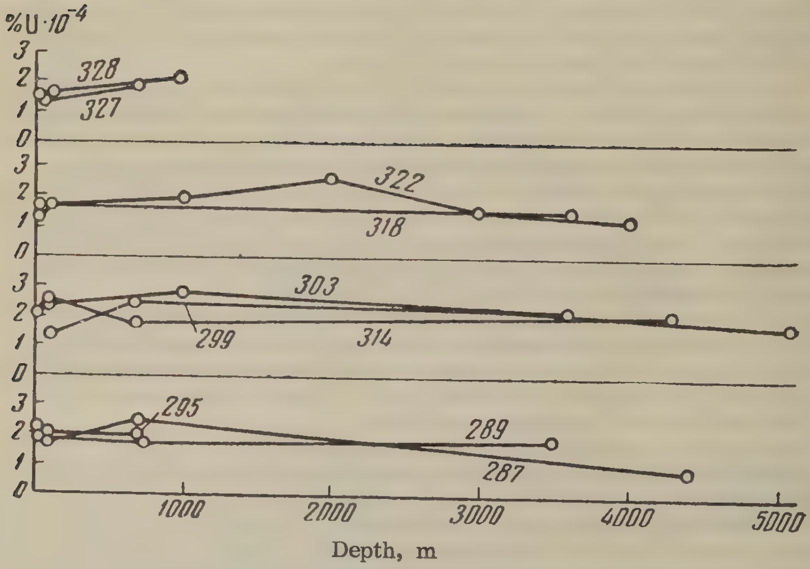

Fig. 2. Uranium content in the Indian Ocean water along a vertical section at ten stations (Antarctica– Bay of Bengal)

The waters of the Indian Ocean contain:

Uranium -- $1.8 \cdot 10^{-6}$ g/l
Thorium -- $1.0 \cdot 10^{-8}$ g/l
Ionium -- $11 \cdot 10^{-13}$ g/l or $0.06 \cdot 10^{-6}$ g/e U
Radium -- $255 \cdot 10^{-13}$ g/ or 75^{-6} g/e U

(According to Joly [9]).

The concentration of ionium expressed in terms of equivalent uranium constitutes only 5% of the amount which would be in radioactive equilibrium with uranium. The concentration of radium, on the other hand, exceeds this amount several times.

Summary

1. Uranium content in the Indian Ocean waters has been determined. The waters of the central regions of the ocean contain $1.8 \cdot 10^{-6}$ g/l uranium, on the average. The highest concentration was found at the depth of 1000-2000 m, and the lowest, at 400 m.

2. The concentrations of thorium and ionium were calculated to be $1.0 \cdot 10^{-8}$ g/l and $11.0 \cdot 10^{-13}$ g/l, respectively.

3. There is a definite disturbance of radioactive equilibrium towards a deficiency of ionium in the water as compared with uranium, indicating that ionium is actively accumulated on the ocean bottom.

REFERENCES

1. Baranov, V.I. and L.A. Kuz'mina (1958). Geokhimiya, No. 2.
2. Goldberg, E.D., C. Patterson and T. Chow (1957). Second International Conference on the Peaceful Uses of Atomic Energy, Geneva, Report 1980.
3. Kuznetsov, V.I. and T.G. Akimova (1958). Zh. analit. khimii, No. 1.
4. Rona, E., G.O. Gilpatric and G. Jeffrey (1956). Trans. Amer. Geophys. Union, 37, No. 6.
5. Koczy, F.F. (1956). Yadernaya Geologiya (Nuclear geology). Izd. inostr. lit.
6. Starik, E.E. and L.B. Kolyadin (1957). Geokhimiya, No. 3.
7. Vinogradov, A.P. (1944). Uspekhi Khimii, XIII, No. 1.
8. Koczy, F.F., E. Picciotto, G. Poulaert and S. Wilcain (1957). Geochim. et Cosmochim. Acta, 11.
9. Joly, J.J. (1909). Radioactivity and Geology.

Received for publication
March 11, 1959

ON THE DISTRIBUTION OF SCANDIUM IN IGNEOUS ROCKS ON THE EXAMPLE OF SOME MASSIFS OF THE SOVIET UNION

L. F. BORISENKO
Institute of Mineralogy, Geochemistry,
and Crystal Chemistry of the Rare Elements,
Academy of Sciences, U. S. S. R., Moscow.

(ABSTRACT)

The results of an investigation of scandium distribution in a number of intrusive massives of the Soviet Union have shown that: 1. Higher scandium contents are typical for ultrabasic and basic rocks (~ 0.003% of Sc_2O_3) and lower contents for intermediate (~ 0.0005 of Sc_2O_3) and acid rocks (~ 0.0002% of Sc_2O_3). 2. The character of FeO, MgO and Sc_2O_3 distribution in rocks of the ultrabasic type bears witness of a more probable geochemical bond of scandium and divalent iron. Pyroxenites are characterized by the highest Sc_2O_3 content (up to 0.017%).

G. Eberhard, first qualitatively [1], and later Goldschmidt quantitatively [2] carried out a large series of analyses of magmatic rocks with the aim of establishing the presence of scandium in them. He first noted the general tendency of scandium to decrease in content from basic rocks to acid rocks. Later this regularity was confirmed as the result of the studies of Tongeren [3], Kvalheim [4], Sahama [5], and others (Table 1).

The results of our studies (Table 2) also confirm this regularity of the distribution of scandium in igneous rocks. In all there were studied about 50 samples of different rocks, selected from a series of intrusive massifs of the Soviet Union. Part of the samples were kindly submitted to the author by fellow-workers D. A. Rodionov and A. A. Sitnim of the Institute of Mineralogy, Geochemistry, and Crystal Chemistry of Rare Elements, Academy of Sciences, U. S. S. R.

The determination of the content of scandium in the rocks was carried out by the spectrochemical method. Preliminary enrichment of the samples was by the chemical method by the use of extraction of scandium with

Table 1

Contents of scandium oxide in the principal types of igneous rocks

Ultrabasic rocks		Basic rocks		Intermediate rocks		Acid rocks		Literature reference
Number analyzed	Content	Number analyzed	Content	Number analyzed	Content	Number analyzed	Content	
–	–	11	0. 002	–	–	14	0. 00013	[6]
3	0. 001	29	0. 0005	65	0. 0002	46	0. 0002	[3]
20	0. 0065	–	–	–	–	–	–	[4]
–	–	2	0. 0035	–	–	–	–	[7]
–	–	4	0. 0013	–	–	–	–	[8]
2	0. 003	6	0. 002	14	0. 0006	–	–	[9]
–	–	7	0. 0032	16	0. 0007	–	–	[10]
–	–	14	0. 002	–	–	–	–	[11]
–	0. 00065	–	0. 002	–	0. 0002	–	0. 00006	[12]
–	–	–	–	3	0. 00033	–	–	[13]
–	–	1	0. 002	–	–	–	–	[14]
–	–	3	0. 001	–	–	–	–	[15]
–	–	5	0. 004	–	–	–	–	[16]
13	0. 0009	–	–	–	–	–	–	[17]
–	–	57	0. 0037	–	–	–	–	[18]
–	0. 0046	–	0. 0013	–	0. 00046	–	0. 00013	[19]
–	–	–	0. 0025	–	–	–	–	[20]
–	–	–	0. 003	–	–	–	–	[21]
–	–	11	0. 0022	–	–	–	–	[22]

Table 2

Contents of Sc_2O_3 in magmatic rocks of the U. S. S. R.

Name of Rock	Locality collected	No. of Samples	Range of content of Sc_2O_3, %	Average Content
Pyroxenite	Arbarastakh, Yakutia	3	0. 015–0. 017	0. 016
Pyroxenite	Rai-Iz, Polar Urals	2	0. 004–0. 005	0. 0045
Pyroxenite	Near Katunregion, Altai	1	–	0. 005
Pyroxenite	Vuoriyanvi, Karelia	1	–	0. 01
Peridotite	Rai-iz, Polar Urals	2	0. 0008	0. 0008
Dunite	Rai-iz, Polar Urals	2	0. 0005	0. 0005
Gabbro	Patyn, Kuznetsk Alatau	1	–	0. 003
Gabbro	Western Transbaikal	1	–	0. 003
Gabbro	Southern Urals	1	–	0. 002
Gabbro	Rai-iz, Polar Urals	2	0. 003–0. 004	0. 0035
Gabbro-pegmatite	Pai-er, Polar Urals	2	0. 005–0. 006	0. 0055
Gabbro-pegmatite	Rai-iz, Polar Urals	2	0. 004–0. 006	0. 005
Gabbro-pegmatite	Gold rock, northern Urals	1	–	0. 008
Gabbro-diabase	Cape Kerson, Lake Onezhsk	1	–	0. 003
Diorite	Rai-Iz, Polar Urals	1	–	0. 00045
Granodiorite	Bukuka, eastern Transbaikal	3	0. 0003–0. 0007	0. 0005
Granodiorite	Belukha, eastern Transbaikal	2	0. 0003–0. 0004	0. 00035
Porphyritic biotite Hornblende granite	Belukha, eastern Transbaikal	1	–	0. 00003
Granite, greisenized	Belukha, eastern Transbaikal	1	–	0. 0003
Granite, greisenized	Kukal bei, eastern Transbaikal	1	–	0. 00036
Granite porphyry	Sherlova Mt., eastern Transbaikal	3	0. 0001–0. 0002	0. 00015
Granite	Duralguevsk massif, eastern Transbaikal	2	0. 00016–0. 00018	0. 00017
Amazonite granite	Etykinsk massif, eastern Transbaikal	1	–	0. 00004

Table 2 (Continued)

Name of Rock	Locality collected	No. of Samples	Range of content of Sc_2O_3, %	Average Content
Granite with average grained biotite	Ubino-Belorechensk massif, Altau	1	-	0.0001
Biotized granite	Omchikandinsk massif, Yakutia	3	0.0001-0.00013	0.00011
Granite	Kzul-Tass massif, central Kazakhstan	6	0.0002-0.0006	0.0004

tributyl phosphate, carried out by L. T. Zhuravlev, and the further determination of scandium by the spectral method by L. I. Sosnovska. The sensitivity of the determination of scandium in the original material was 1×10^{-6}. The average error in the spectrochemical method of determination of scandium in the rocks is ± 10%.

The results obtained showed the presence of scandium in all analyzed samples of igneous rocks (Table 2). The highest content attained 0.017% Sc_2O_3, found for pyroxenites. Samples were analyzed of pyroxenites from four ultrabasic massifs of the Soviet Union (Polar Urals, Yakutia, Altai, Karelia). For all these there was shown the characteristic content of scandium, exceeding its clarke* (from 0.004 to 0.017% Sc_2O_3). The average content of scandium in the pyroxenites of the studied massifs is ~ 0.008%. The content of scandium in peridotites (~ 0.0008% Sc_2O_3) and dunites (~ 0.0005% Sc_2O_3) are approximately an order of magnitude lower than in the pyroxenites. The content of scandium determined in gabbro, as well as in pyroxenites and peridotites, is higher than its clarke. Analysis of samples of gabbro from four intrusive massifs of the Soviet Union (Ural, Kuznets Alatau, near-Baikal) showed contents of scandium from 0.002 to 0.004% Sc_2O_3. The average content of Sc_2O_3 in the gabbros studied is ~ 0.003%. It was also established that the content of scandium in gabbro-pegmatites (from 0.004 to 0.008% Sc_2O_3) is higher than in the parent gabbro. The contents of scandium in samples of diorites, granodiorites, and granites, selected from ten different massifs of the Soviet Union (Ural, Altai, central Kazakhstan, eastern Transbaikal, and Yakutia) were mostly lower than the clarke.

In Table 3 are given the average contents of Sc_2O_3 in various magmatic rocks, calculated from data in the literature and also obtained by the

Table 3

Average contents of Sc_2O_3 in various magmatic rocks (in %)

Type of rock	Average content of Sc_2O_3, according to the literature*	Average content of Sc_2O_3 for intrusive rocks of some massifs of the Soviet Union**
Ultrabasic rocks	0.0042	0.003
Basic rocks	0.0035	0.004
Intermediate rocks	0.0006	0.0004
Acid rocks	0.0002	0.0002

*According to data of V. M. Goldschmidt [2], D. Tongeren [3], and others.

**According to the author's data.

---

*The clarke of scandium for the rocks of the Earth's crust is 6 p.p.m., according to I. and W. Noddack.

authors. The results given show excellent convergence. (The contents of Sc_2O_3 in magmatic rocks were calculated as arithmetic average).

The contents of scandium obtained in the different types of igneous rocks of the Soviet Union permit one to speak of higher average contents of it in basic and ultrabasic rocks than in intermediate and acid rocks (Table 3).

As is known, most of the scandium occurring in igneous rocks is contained in the ferromagnesium minerals: pyroxenes, amphiboles, and biotites [19, 23]. Scandium is practically absent in feldspar, quartz, and nepheline. The similar character of the distribution of scandium in the rock-forming minerals is explained in the first place by the closeness of the sizes of the ionic radii of scandium and the common rock-forming elements iron and magnesium. The most probable form of entry of scandium into the ferromagnesium minerals of magmatic rocks is the heterovalent isomorphous replacement of divalent iron or magnesium. Compensation of valence may be accomplished at the expense of aluminum according to the scheme $Sc^{+3} + Al^{+3} = Fe^{+2} + Si^{+4}$. Thereby in minerals of more complex composition, heterovalent isomorphous replacement, apparently, is accomplished more easily than in minerals of simpler composition. For example, pyroxenes, as a rule, are characterized by higher contents of scandium than olivines. According to the data of V. M. Goldschmidt [19], the content of Sc_2O_3 in pyroxene is 0.01% and in olivine 0.0007%. Dunites, composed sometimes almost wholly of olivine, and peridotites, containing about 50% olivine, are poorer in scandium than pyroxenites, in the composition of which olivine plays a subordinate role.

Scandium, the ionic radius of which equals 0.83A., may replace in ferromagnesian minerals both divalent iron (r = 0.80A.) and also magnesium (r = 0.74A.). However, the magnitudes of the electronegativities are much closer for scandium and divalent iron, which suggests a greater probability of association of scandium in minerals of magmatic rocks with divalent iron, and not with magnesium. This was first stated by Ringwood [24].

Tables 4 and 5 give the average contents of Sc_2O_3, FeO, MgO, and the atomic ratios Fe/Sc and Mg/Sc in magmatic rocks. From Table 4, it follows that in the main types of magmatic rocks (pyroxenite, gabbro, diorite, granite), the variations in average contents of Sc_2O_3, FeO, and MgO have approximately the same character – in the direction from pyroxenite to

Table 4

Average contents of FeO, MgO, and Sc_2O_3 in magmatic rocks

	Content in %			Ratios	
Rocks	FeO*	MgO*	Sc_2O_3	Fe/Sc	Mg/Sc
Pyroxenite	10.85	12.13	0.008	1630 : 1	1400 : 1
Gabbro	5.95	7.51	0.003	2450 : 1	2370 : 1
Diorite	3.77	2.80	0.0005	9700 : 1	5100 : 1
Granite	1.67	1.15	0.0002	10,100 : 1	5300 : 1

*Contents of FeO and MgO after R. Daly [25].

Table 5

Average contents of FeO, MgO, and Sc_2O_3, in ultrabasic rocks

	Content in %			Ratios	
Rocks	FeO*	MgO*	Sc_2O_3	Fe/Sc	Mg/Sc
Pyroxenite	10.85	12.13	0.008	1630 : 1	1400 : 1
Peridotite	7.97	30.92	0.0008	12,800 : 1	36,000 : 1
Dunite	5.54	46.32	0.0005	12,900 : 1	84,000 : 1

*Contents of FeO and MgO after R. Daly [25].

granite, there are lower contents of Sc_2O_3, FeO, and MgO. Thus, on the basis of this example, it is difficult to speak of the preferential geochemical association of scandium with divalent iron or with magnesium. Also in the rocks of the ultra-basic complex (pyroxenite, dunite, peridotite), diminishing average contents of FeO are correlated with diminishing average contents of Sc_2O_3 and are accompanied by increasing average contents of MgO (Table 5). In fact, pyroxenites, characterized by maximum contents of FeO (~ 11%) and minimum MgO (~10%), contain the largest amount of Sc_2O_3 (0.008%) and, on the contrary, dunites, having the maximum content of MgO (55%) and minimum content of FeO (5%) contain the least amount of Sc_2O_3 (~0.0005%). This gives us some basis for stating that there is probably a predominant geochemical association of scandium with divalent iron and not wigh magnesium.

The same conclusion was reached by S. R. Nockolds and R. Allen [27], who, for the examples of the Caledonian rocks of Scotland, the Southern California batholith, and some others, established that "scandium behaves similarly to iron, in the sense that it is somewhat higher in the least magnesian parental magmas."

Conclusions

1. For the example of the principal types of magmatic rocks of some massifs of the Soviet Union, it was shown that higher contents of scandium are characteristic for ultrabasic and basic rocks (~ 0.003%) - 0.004% Sc_2O_3), and lower for intermediate (~ 0.0004% Sc_2O_3) and acid rocks (~ 0.0002% Sc_2O_3).
2. The character of the distribution of the contents of Sc_2O_3, FeO, and MgO in rocks of ultrabasic complexes confirms the conclusion of Nockolds of the more porbable association of scandium with divalent iron. Pyroxenites, having among the ultrabasic rocks the maximum content of FeO, are characterized by the highest contents of Sc_2O_3 (up to 0.017%).

REFERENCES

1. Eberhard, G. Uber die weite Verbreitung des Scandiums auf der Erde I - II, 1908-1910.
2. Goldschmidt, V. and Cl. Peters. Zur Geochemie des Geochemie des Scandiums. Math-Phys. Kl., Gottingen, 1931.
3. Tongeren, W. On the occurrence of rarer elements in the Netherlands East Indies. Amsterdam, 1938.
4. Kvalheim, A. and L. W. Strock. Spectrochim. acta 1 (1939).
5. Sahama, Th. Bull. comm. geol. Finlande No. 135 (145).
6. Noll, W. Chem. Erde 8 (1934).
7. MacGregor, A. G., Phil. Trans. Roy Soc. London B, 229, 1 (1938).
8. Wager, L. R. and R. L. Mitchell, Min. Mag., 26, N 180 (1943).
9. Nockolds, S. R. and R. L. Mitchell, Trans Roy Soc. Edinburgh 61, 1944-1948.
10. Larsen, E. S. J. Geol. 46 (1948).
11. Macdonald, G. A. U. S. Geol. Survey, Prof. Paper 214-D (1949).
12. Rankama K. and Th. Sahama, Geochemistry, Chicago (1950).
13. Mackenzie, G. and K. Murata, Econ. Geol. 47, No. 2 (1952).
14. Walker, F. Trans Edinburgh Geol. Soc. 15 (1952).
15. Wager, L. R. and R. L. Mitchell, Geochim et Cosmochim. Acta 3, No. 1 (1953).
16. Amstutz G. C. Geochim et Cosmochim Acta 3, No. 1 (1953).
17. Pinson, W. H., L. H. Ahrens, and others, Geochim. et Cosmochim. Acta 3, No. 1 (1953).
18. Fairbairn, H. W. and others, Geochim. et Cosmochim. Acta 3, 217 (1953).
19. Goldschmidt, V. M. Geochemistry, Oxford, 1954.
20. Patterson, E. M. and others, Proc. Roy. Irish Acad. 57 B (1955).
21. Hamilton, W. B. and G. Neuerburg, Am. Mineral. 41, No. 11-12 (1956).
22. Patterson, E. M. and D. L. Swaine, Trans. Proc. Roy. Soc. Edinburgh 63, No. 2 (1958).
23. Oftedal, I. Norsk geol. tidsskr. 23 (1943).
24. Ringwood, A. E. Geochim. et Cosmochim. Acta 7, (1954).
25. Daly, R. A. Igneous rocks and the depths of the Earth, New York, 1933.
26. Nockolds, S. R. and R. Allen, Geochemical observations. Izdeltsvo inostr. lit, 1958.

Received for publication
January 3, 1959

GEOCHEMISTRY OF RARE-METAL GRANITE PEGMATITES

N. A. SOLODOV
Institute of Mineralogy, Geochemistry,
and Crystal Chemistry of Rare Elements,
Academy of Sciences USSR, Moscow

(ABSTRACT)

According to the rock-forming minerals four types of rare-metal pegmatites are distinguished. Type I - microcline pegmatites, type II - albite-microcline pegmatites, type III - albite pegmatites, type IV - albite-spodumene pegmatites.

The content of alkaline and rare elements in these types is not always similar, usually ranging in rather narrow limits in well developed veins of the same types (table 2). The following elements are characteristic of the different types: type I - K, Be; type II - K, Na, Ta, Be, Cs, Rb, Tl, Li; type III - Na, Li, Be, Ta, Nb, Sn; type IV - Na, Li, sometimes Nb, Sn. The formation of the different types and the different degree of their enrichment by alkaline and rare elements may be explained by the initial geochemical specifity of the pegmatite melts.

On the basis of many years' study of the pegmatites of Altai and Kola Peninsula, the author separates the following four basic types of rare-metal granite pegmatites: type I -- microcline pegmatites, type II -- albite-microcline pegmatites, type III -- albite pegmatites and type IV -- albite-spodumene pegmatites.

In practice the type of pegmatite is determined by the abundance of three essential rock-forming minerals: microcline, albite and spodumene. Only those minerals which constitute more than 10-15% of the volume of the pegmatite are mentioned in the type name.

These minerals were chosen as the principal basis for classification of pegmatites, first, because they represent one of the main characteristics of pegmatites constituting, together with quartz, not less than 90-95% of any pegmatite vein, second, because they are easily identified in the field, and, third, because their content varies sharply from one pegmatite to another and makes it possible to use them for the purpose of classification.

Table 1

Main Features of the Principal Types of Rare Metal Pegmatites

		Type I. Microcline pegmatites	Type II. Albite-microcline pegmatites	Type III. Albite pegmatites	Type IV. Albite-spodumene pegmatites
Content of essential minerals, %	Microcline	60 - 70	25 - 35	up to 10	About 10
	Albite	up to 5	25 - 35	35 - 45	35 - 45
	Spodumene	0	up to 10	up to 10	15 - 25
	Quartz	23 - 26	25 - 30	30 - 40	30 - 35
Varietal and typomorphic minerals		Silvery muscovite, schlorlite, large prisms of beryl	Lepidolite, variegated and pink tourmaline, montebrasite, pink muscovite, beryl, vorobjevite, pollucite, tantalite, simpsonite, microlite, stibiotantalite	Blue-black tourmaline, bright green muscovite, lithiophilite, soda beryl, tantalite-columbite	Light green muscovite, soda-lithia beryl

Table 1 (Continued)

	Type I. Microcline pegmatites	Type II. Albite-microcline pegmatites	Type III. Albite pegmatites	Type IV. Albite-spodumene pegmatites
Structural zones of pegmatites. (Minerals of economic interest in parentheses. Some zones are usually absent or not separated from other zones. In this case combined zones are present: zone of blocky quartz-microcline etc. A brief characteristic of the zones was given earlier [15])	1. Zone of granite-pegmatite 2. Zone of graphic quartz-microcline 3. Zone of pegmatoid quartz-microcline 4. Zone of blocky microcline I (beryl between zones 4 and 5) 5. Zone of blocky quartz	1. Zone of granite pegmatite 2. Zone of graphic quartz-microcline 3. Zone of apographic quartz-albite-microcline (columbite) 4. Zone of fine-grained albite (beryl, columbite) 5. Zone of blocky microcline I 6. Zone of quartz-muscovite (beryl, columbite) 7. Zone of quartz-cleavelandite-spodumene (spodumene, beryl, tantalite-columbite) 8. Zone of fine platy albite (pollucite, tantalite, vorobjevite, spodumene)	1. Zone of apographic quartz-albite (columbite) 2. Zone of saccharoidal albite (columbite) 3. Zone of cleavelandite (beryl, tantalite-columbite) 3a. Zone of quartz-cleavelandite-spodumene (beryl, tantalite-columbite) 4. Zone of scaly muscovite (tantalite) 5. Zone of blocky microcline II 6. Zone of blocky quartz	1. Zone of fine-grained quartz-albite 2. Zone of quartz-albite-spodumene (spodumene, less often beryl and columbite) 3. Zone of blocky microcline II

Table 1 (Continued)

	Type I. Microcline pegmatites	Type II. Albite-microcline pegmatites	Type III. Albite pegmatites	Type IV. Albite-spodumene pegmatites
		9. Zone of scaly lepidolite (tantalite, lepidolite, rarely pollucite and cassiterite) 10. Zone of blocky microcline II 11. Zone of blocky quartz		
Distinctness of zonal structure	Average	Sharp	Very sharp	Poor
Texture of outer zones (structure of inner zones may be alike)	Granitic, graphic, pegmatoidal	Granitic, graphic, apographic	Apographic, saccharoidal	Fine-grained, saccharoidal
Form of pegmatite	Lenses and stocks	Lenses and veinlike bodies	Typical veins	Tabular veins
Size of pegmatite	Small, usually not over 100–200 m in length	Intermediate, 500–700 m long, less commonly up to 1 km	Small, usually not over 100–200 m in length, rarely up to 300 m	Large, up to 2 – 3 km in length

Table 1 (Continued)

	Type I. Microcline pegmatites	Type II. Albite-microcline pegmatites	Type III. Albite pegmatites	Type IV. Albite-spodumene pegmatites
Ratio of length to thickness	3 – 5, rarely up to 10	5 – 10, rarely more	20–30, sometimes up to 50	40–60 sometimes up to 80
Location with respect to parent granite	Nearest to granite	Near granite	Far from granite	Farthest from granite
Mutual cutting relations (after V. I. Kuznetsov [10])	Cut by all other types of pegmatites	Cut by the two following types only	Cut by albite-spodumene pegmatites	Cut all preceding types
Practical importance at present	Small projects. Yield coarse crystals of beryl, sometimes tantalite	Large complex deposits of beryl, pollucite, tantalite, often associated spodumene	Small projects. Yield beryl and tantalite-columbite	Largest economic spodumene deposits
Pegmatite type according to Fersman [17]	Beryl subtype of type 4	Lepidolite subtype of sodium-lithium type 5	Albite (or sodium-spodumene) subtype of sodium-lithium type 5	
Pegmatite type according to K. A. Vlasov [3]	Blocky and fully differentiated types	Rare metals replacement type		

Table 1 (Continued)

	Type I. Microcline pegmatites	Type II. Albite-microcline pegmatites	Type III. Albite pegmatites	Type IV. Albite-spodumene pegmatites
Pegmatite type according to A. A. Beus [2]	Blocky, muscovite-microcline with beryl	Lepidolite-albite replacement type	Muscovite-albite replacement type	Spodumene-albite replacement type
Pegmatite type according to A. I. Ginzburg [7]	Beryl-muscovite pegmatite	Spodumene-lepidolite pegmatite	Tantalo-beryllium pegmatite	Spodumene pegmatite

Classification on the basis of these minerals reflects also the geochemical character of a pegmatite, for the type name indicates immediately which one of the alkali metals, potassium, sodium, or lithium, is enriched in a given pegmatite.

Moreover, as will be shown below, each of the four types is characterized by the presence of certain rare metals, and this makes the classification useful in prospecting for pegmatites and in appraising them.

The geological and mineralogical characteristics of these pegmatite types are given in a brief form in Table 1. The present paper is devoted to a discussion of their geochemical characteristics. For this purpose, Table 2 has been constructed giving the usual content of the alkali metals

Table 2

Usual Content of Alkali Metals and Rare Elements in the Different Types of Rare Metal Pegmatites (%)

Components	I. Microcline pegmatites		II. Albite-microcline pegmatites with spodumene		III. Albite pegmatites		IV. Albite-spodumene pegmatites	
		from-to		from-to		from-to		from-to
Li_2O		(0,01—0,05)	10	0,1—0,6	7	0,1—0,9	19	1,10—1,50
Na_2O	12	2,70—3,50	4	3,0—4,0	3	3,0—4,0	2	about 4,5
Na_2O/Li_2O		about 100		40—7		30—5		4—3
K_2O	12	10,10—5,50	4	4,0—3,0	3	2,0—1,0	2	about 2,0
Rb_2O		~0,10	4	0,70—0,30	3	0,30—0,08	2	0,19—0,12
Cs_2O		~0,005	4	0,450—0,100	3	0,044—0,009	2	0,006—0,004
K_2O/Rb_2O				5—10		8—12		13—18
K_2O/Cs_2O				7—30		50—150		400—550
Rb_2O/Cs_2O				1,6—3		7—12		25—40
K_2O/Na_2O		3,3—2		about 1		0,5—0,3		about 0,5
BeO	40	0,005—0,010	4	0,040—0,080	7	0,100—0,200	2	0,035—0,012
Ta_2O_5			15	0,025—0,010	13	0,020—0,008	3	0,010—0,004
Nb_2O_5			15	0,020—0.009	13	0,015—0,010	3	0,012—0,010
$Ta_2O_5+Nb_2O_5$		~0,010		0,035—0,024		0,035—0,022		0,022—0,014
Ta_2O_5/Nb_2O_5		>1		3—0,9		1,3—0,7		0,8—0,4

Note: Comma represents decimal point.

and rare elements in pegmatites of different types. The content of the rare elements is given on the basis of sampling of pegmatite veins in the course of exploratory geological work, * on the basis of published data [6, 8, 12, 16, 19-24], and, in the case of low content of these elements, on the basis of chemical (tantalum, niobium, beryllium) or flame spectrophotometric

---

* The data of Ya. Kh. Eselev, V. P. Zueva, I. I. Kaupinen and S. I. Evenchik were used in addition to the author's.

analyses* (lithium, rubidium cesium) of group samples taken from characteristic veins of each type. Each group sample contained from 15 to 70 channel and core samples. The content of the principal alkalies, potassium and sodium, in pegmatites of types I, III and IV was also determined in group samples, either chemically (Table 3) or by flame photometry. Because of lack of material for preparation of representative group samples, the content of potassium and sodium in microcline pegmatites was taken from the works of Fersman [17] and Yu. Yu. Yurk [18]. All these data are presented in a generalized form on the graph.

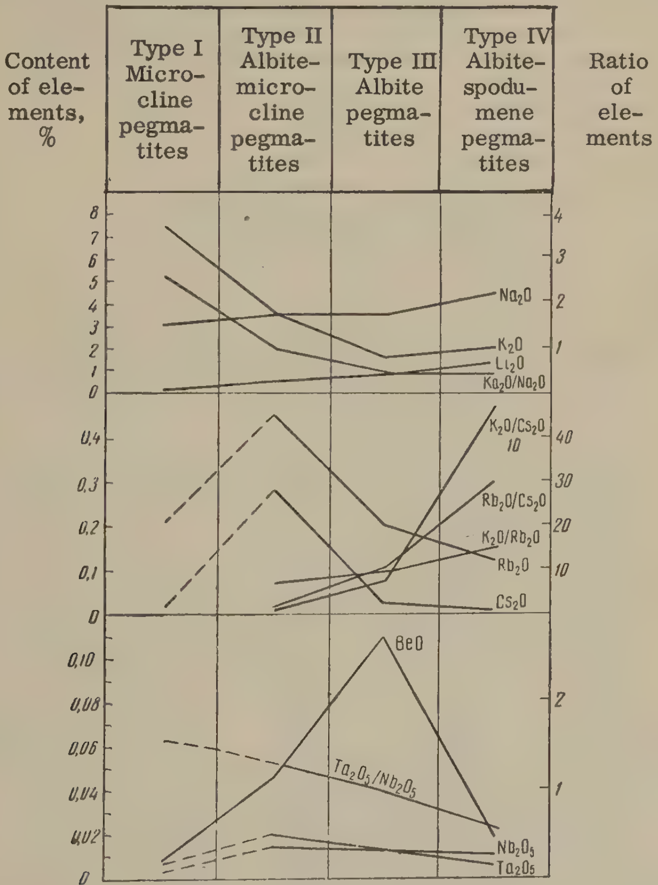

Variation in the content of rare elements and alkali metals in rare metal pegmatites

It will be seen from Table 2 and the graph that the K_2O content decreases harply from 10% in microcline pegmatites to 2% or less in albite and albite-spodumene pegmatites, and this is reflected in the decrease in microcline content from 60-70% to 5-15%. The Na_2O content increases in the same direction but although the albite content increases very considerably, the increase in sodium is rather slight, from 3 to 4.5%. The average sodium content in albite-spodumene pegmatites is only 1.3 - 1.5 times higher than in microcline pegmatites, and individual veins of any type may have the same soda content (Table 3). Therefore, it is more correct to speak of an increase from the first type to the fourth, not of the absolute but of the relative sodium content, for while in microcline pegmatites the content of sodium is 2-3 times less than that of potassium, in albite and albite-spodument pegmatites, there are 2-3 times as much sodium as potassium. It is important to note that the form of occurrence of sodium changes in the

---

*Analysts: E.A. Fabrikova and A. Manukhova (IMGRE AN SSSR).

Table 3

Chemical Analyses of Group Samples from Characteristic Veins of Different Pegmatite Types (%)

Components	I Microcline pegmatite*	II Albite-microcline pegmatite	III Albite pegmatite	IV Albite-spodumene pegmatite
SiO_2	70,62	69,68	79,22	73,33
TiO_2	0,00	0,02	trace	trace
Al_2O_3	14,61	20,15	12,25	16,92
Fe_2O_3	0,48	0,56	1,16	0,34
FeO	0,69	—	—	0,46
MnO	0,02	0,05	0,05	0,09
MgO	0,30	0,14	0,35	0,33
CaO	0,34	0,88	0,74	0,50
SrO	n. d.	0,01	—	n. d.
Na_2O	2,88	3,48	3,21	4,44
$(K,Rb,Cs)_2O$	9,49	3,76	1,07	2,32
Li_2O	n. d.	0,52	0,89	1,12
P_2O_5	0,17	0,25	n. d.	n. d.
SO_3	0,02	n. d.	n. d.	n. d.
BeO	n. d.	0,041	0,14	n. d.
H_2O^-	0,11	0,00	0,03	0,14
H_2O^+	0,48	0,47	0,90	0,11
Rest	n. d.	0.32	n. d.	0,25
Total	100,21	100,20	100,01	100,35
Analyst		O. Dorondova	T. Kapitonova	V. Shvets

*Analysis taken from Yu. Yu. Yurk's work [18].
Note: Comma represents decimal point.

same direction. In microcline pegmatites its main mass is in the perthite albite, which usually constitutes 20-25% of the potash feldspar crystals. In passing to albite-spodumene pegmatites not only the amount of microcline diminishes but also the content of perthitic albite diminishes practically to zero. Instead, sodium goes more and more into independent albite crystals and almost none of it is left for perthite. This explains the striking difference in the amount of albite in the extreme types (by a factor of 7 to 10) in spite of the insignificant change in the amount of sodium (by a factor of 1.3 to 1.5).

The content of all other essential elements (Si, Al, Fe, Ca, Mg, etc.) varies from type to type without discernible regularity.

The content of lithium oxide increases regularly from a few hundredths of one percent in the microcline pegmatites to 1.4 - 1.5% [19, 23], in albite spodumene pegmatites.[*] It should be mentioned that in albite-microcline and albite pegmatites the lithium content varies considerably from vein to vein, and each of these types may be divided into two subtypes: 1) the spodumene-bearing and spodumene-free albite-microcline pegmatites and 2) spodumene-bearing and spodumene-free albite pegmatites.

The maximum Rb_2O and Cs_2O contents are found in ablite-microcline pegmatites and in individual veins may reach 0.70 and 0.45%, respectively. It should be noted that the high concentration of cesium and rubidium is not found in all veins of type II but only in the spodumene-bearing subtype of albite-microcline pegmatites. Only these pegmatites contain lepidolite, pollucite, vorobjevite and rubellite. In all other types cesium is dispersed, while here, in some veins the amount of dispersed cesium diminishes to 25% [14] and the rest occurs in pollucite. The content of Rb_2O diminishes in the direction of albite-spodumene pegmatites to 0.12% and that of Cs_2O, to 0.004%. Because of the strong geochemical affinity between rubidium and potassium, the K_2O/Rb_2O ratio changes relatively little, from 5-10 in type II to 13-17 in type IV. The K_2O/Cs_2O ratio, on the other hand, increases from 7 to 500. Correspondingly, the Rb_2O/Cs_2O ratio also increases from 1.6 in albite-microcline pegmatites to 32 in albite-spodumene pegmatites. In the absence of representative samples of microcline pegmatites, their average content of Rb and Cs is known only approximately from a few analyses of individual specimens of microcline and may be estimated as 0.1% for Rb_2O and about 0.005% for Cs_2O[**]. Therefore the content of rubidium and cesium decreases from albite-microcline to microcline pegmatites.

The highest BeO content (0.10 - 0.20%) is characteristic of albite pegmatites. It diminishes in both directions, to 0.035-0.012% in albite-spodumene pegmatites and to 0.005-0.010% in microcline pegmatites. The Nb_2O_5 content diminishes from 0.020-0.009% in albite-microcline pegmatites to 0.015-0.010%, in albite pegmatites and is about the same, 0.012-0.010%, in albite-spodumene pegmatites. The Ta_2O_5 content decreases sharply from 0.025-0.010% in albite-microcline pegmatites to 0.010-0.004%

---

[*] The Li_2O content in albite-spodumene pegmatites usually varies between 1.10 and 1.50%. However, sometimes, because of the strong replacement of spodumene, it falls to 0.8 - 0.9%.

[**] According to N. N. Mart'yanov's data (oral communication) the barren pegmatites of southeastern Tuva similar to the microcline type contain 0.018-0.024% Rb_2O and 0.002-0.003% Cs_2O.

in albite-spodumene pegmatites. Hence the Ta_2O_5/Nb_2O_5 ratio also diminishes in this direction, from 3-0.9 to 0.8-0.4. The tantalum and niobium content of microcline pegmatites has not been studied, for they usually contain only negligible amounts of tantalate-niobates [15]. In any case, the Ta_2O_5-Nb_2O_5 content in these pegmatites is not likely to exceed 0.01%. In connection with the general geochemical tendency for the Ta_2O_5/Nb_2O_5 ratio to increase from type IV to type II, it may be expected that in type I it will be considerably greater than unity.

It will be seen from this analysis that the content of rare elements in each type is characterized by a certain level. The upper limit is especially instructive in this respect. For instance, in the microcline pegmatites, the BeO content usually does not exceed 0.01%, the author does not know a single albite-microcline vein with more than 0.08% BeO, while albite pegmatites average 0.20% BeO. In the same way, the Cs_2O content in the albite-spodumene pegmatites does not, as a rule, exceed thousandths of one percent, and in the albite-microcline pegmatites it reaches tenths of one percent. A similar pattern is observed for other rare elements.

Theoretically the lower limit of rare metal content in each type may drop to the clarke value (for pegmatites) or even lower, for in each type, because of the difference in texture, the structure of the ore body and other causes, all gradations are found from strongly mineralized veins to almost barren ones. Actually, however, the lower limit in pegmatites with a high upper limit is always higher than in pegmatites with a low upper limit.

On the whole, then, each pegmatite type is characterized by a fairly definite average content of rare elements (Table 2).

The differences in average content of elements in different types are very well shown in Table 4, which illustrates the degrees of relative enrichment of pegmatites in rare elements. The albite-microcline pegmatites are about 5 times as rich in beryllium as microcline pegmatites, and the albite pegmatites are 15 times as rich, but the albite-spodumene pegmatites are only 3 times as rich.

It is curious that niobium is very uniformly distributed among the pegmatite types and exhibits practically no maximum. It is followed by

Table 4

Approximate Degree of Enrichment of Different Pegmatite Types in Rare Elements
(Minimum content of rare elements is taken as unity)

Elements	I. Microcline pegmatites	II. Albite-microcline pegmatites	III. Albite pegmatites	IV. Albite-spodumene pegmatites
Li	1	15	25	45
Rb	1	3	1.5	1
Cs	1	50	5	1
Be	1	5	15	3
Ta	–	3	2	1
Nb	–	1	1	1

tantalum and rubidium, whose enrichment factor does not exceed three, while it is 15 for beryllium and 45 and 50 for lithium and cesium, respectively (Table 4).

The different degrees of enrichment of the different pegmatite types in rare elements directly affect their practical value. The possibility of profitable extraction of a rare element from a pegmatite depends not only on its average content in the vein but also on the character of distribution of the rare metal minerals in the pegmatitic bodies, the size of the veins and other geological, mineralogical, technological, and economic factors. For instance a considerable amount of beryl is obtained from microcline pegmatites although the average BeO content of the vein may be low, simply because beryl occurs in large prismatic crystals 1-2 m and more in length and can easily be extracted by hand. At the same time, although the lithium content in albite pegmatites is rather high, spodumene is not extracted from t, for the small size of the veins makes flotation uneconomic. At present he following elements are of practical interest in the different types of pegmatites: in type I--Be and rarely Ta; in type II--Ta, Be, Cs, Li, Rb, Nb; in type III--Be, Ta, Nb; and in type IV--Li (in the future some of these pegmatites will yield Be, Nb, Ta and Sn as a by-product, for veins of this type are usually huge, and these metals can be extracted economically even when their content is low).

For the sake of completeness, Table 5 gives the content in the pegmatites of some other rare and trace elements determined spectrographically N. V. Lizunov, analyst) on combined samples. As is to be expected, the content of thallium, which is geochemically very close to rubidium, is correspondingly high [1]. The pegmatites have also high concentrations of zirconium (0.05%) and sometimes of the rare earths, uranium, etc. On

Table 5

Content of Dispersed and Minor Elements in Group Samples from Characteristic Veins of Different Pegmatite Types (%)

Elements	II. Albite-microcline pegmatite	III. Albite pegmatite	IV. Albite-spodumene pegmatite
Te	0.001	-	-
Sn	0.001	0.01	0.001
Qa	0.01	0.005	0.01
Mo	-	-	0.005
V	-	0.01	0.005
Ti	-	-	0.05
Cu	0.005	0.005	0.001
Zn	-	0.005	-
Co	-	0.01	-
Ni	0.01	0.01	-
Zr	0.05	-	0.005
Sr	0.01	0.005	0.01
Cr	0.01	0.01	-
Ba	-	0.01	0.01

the whole, the albite-microcline pegmatites hold a somewhat exceptional position among the other types in containing a greater variety of rare metals. The microcline pegmatites, and, of the three albite-bearing pegmatites, the albite-spodumene pegmatites are poor in rare elements. The following paragenetic groups are observed in each of the pegmatite types:

Type I -- K, Be (Zr, RE, U)
Type II -- K, Na, Li, Rb, Cs, Be, Zr, Ta, RE, U, Tl
Type III -- Na, Li, Be, Ta, Nb, Sn
Type IV -- Na, Li, Nb, Sn

The reason for the existence of paragenetic groups among the alkali elements only is explainable by certain geochemical affinity between lithium and sodium and between rubidium, thallium, and cesium and potassium. But even this affinity is manifested in a one-sided way, for, while lithium does not occur in granite pegmatites without sodium, there are quite a few examples of sodium pegmatites without lithium (the albite pegmatite without spodumene, Type III). Again, concentrations of rubidium and cesium do not occur unless there are large amounts of potassium but potassium may be present without these rare alkalies as in the microcline pegmatites.

Basically, the appearance of a given paragenesis of elements and of a given pegmatite type depends on the geochemical characteristics of the initial pegmatitic melt*.

In discussing hydrothermal deposits, S. S. Smirnov [13], F. I. Vol'fson and V. A. Nevskii [5], A. V. Korolev [9], O. D. Levitskii and V. I. Smirnov [11] and others have repeatedly advanced the concept of spasmodic introduction of ore-bearing solutions of different composition from the magmatic hearth, i. e., the concept of successive separation of different elements from the magma. In the author's opinion, this idea serves also as an explanation of the appearance of different types of pegmatites and their unequal enrichment in rare elements.

An examination of the material presented above with this idea in mind suggests the following sequence of separation of alkali metals from the magmatic hearth: K → Na → Li. In reality this sequence represents successive pulsations of pegmatitic melt enriched to different degrees with this or that alkali element. The reality of such pulsations of different composition is confirmed by the existence of microcline pegmatites traversed by albite veins which, in their turn, are cut by albite-spodumene veins, as has been clearly shown by V. I. Kuznetsov [10]. It should be added that as far back as 1922, A. Lacroix [21], in studying the pegmatites of Madagascar, came to the conclusion that the sodium-lithium pegmatites are not related to potassium pegmatites and that the "lithium phase is the last one in the history of granitic magmas."

---

*If in the pegmatite types and subtypes separated by the author the rock-forming minerals are replaced by the corresponding alkalies, a geochemical classification of pegmatites will be closely approached:

Type I -- potassium pegmatites.

Type II -- potassium-sodium pegmatites: subtype 1 -- potassium-sodium pegmatites without lithium and cesium; subtype 2 -- potassium-sodium pegmatites with lithium and cesium.

Type III -- sodium pegmatites: subtype 1 -- sodium pegmatites without lithium; subtype 2 -- sodium pegmatites with lithium.

Type IV -- sodium-lithium pegmatites.

Naturally a given hearth or a given intrusive does not always produce the entire series of pegmatite melts of different composition. In some cases the separation occurs mainly at the moment when the melt has a specific potassium composition, in others, when the melt has essentially sodic or sodium-lithium composition. The concept of different degrees of maturing of pegmatitic sources which is being developed by K. A. Vlasov [4] is to be understood in precisely this way. This is the reason why individual deposits or pegmatite fields are characterized by the predominant development of one or several types and not of all four.

The following sequence of separation of rare elements from the magmatic hearth is observed in granitic pegmatites:

Zr → RE → U → Ta → Rb → Tl → Cs → Be → Nb → Li → Sn

The position of niobium in this sequence is tentative, for, so far as its absolute content is concerned, it is rather uniformly distributed between the early and late pulsations, but, as compared with Ta, it is strongly enriched in the late portions. This sequence shows that the early pegmatite types accumulate the first members of the series; the intermediate types, its middle members; and the late types, its last members. It should be nentioned that Zr, RE and U are most abundant in the still earlier oligoclase and oligoclase-microcline pegmatites and enter only incidentally into the microcline and albite-microcline pegmatites described here.

Summary

1. The content of rare elements in the different rare metal pegmatite ypes is not the same, but in well developed veins of a given type it varies vithin rather narrow limits (Table 2).

2. The formation of different types of pegmatites and the different degrees of their enrichment in alkalies and rare elements is explained by the nitial geochemical characteristics of the pegmatitic melt.

3. The first to separate from the magmatic hearth are the specifically otassium pegmatitic melts strongly impoverished in rare elements. They re followed by potassium-sodium melts rich in tantalum, cesium, rubidium and, to some extent, beryllium. Still later the specifically sodium nelts are separated which are enriched in beryllium and, to some extent, n tantalum and niobium. Finally, the concluding stage of pegmatitic activty of a magmatic hearth is characterized by sodium-lithium pulsations elatively rich in niobium and occasionally in tin.

REFERENCES

1. Ahrens, L. H. and W. R. Liebenberg (1952). Geokhimicheskoe issledovanie Redkikh Elementov Yuzhno-Afrikanskikh mineralov i Porod (Geochemical investigation of rare elements in South African minerals and rocks). Izd. inostr. lit., Moscow.
2. Beus, A. A. (1951). Izvestiya Akad. Nauk SSSR, ser. geol., No. 6.

3. Vlasov, K. A. (1952). Izvestiya Akad. Nauk SSSR, ser. geol., No. 2.
4. Vlasov, K. A. (1957). Izvestiya Akad. Nauk SSSR, ser. geol. No. 12.
5. Vol'fson, F. I. and V. A. Nevskii (1949). Izvestiya Akad. Nauk SSSR, ser. geol. No. 1.
6. Ginzburg, A. I. (1955). Tr. Mineralog. muzeya AN SSSR, No. 7.
7. Ginzburg, A. I. (1957). Razvedka i Okhrana nedr, No. 6.
8. Cameron, E. et al. (1951). Vnutrennee Stroenie Granitnykh Pegmatitov (Internal structure of granitic pegmatites). Izd. inostr. lit.
9. Korolev, A. V. (1949). Izvestiya Akad. Nauk SSSR, ser. geol., No. 1.
10. Kuznetsov, V. I. (1955). Tr. Inst. geol. nauk AN SSSR, No. 162.
11. Levitskii, O. D. and V. I. Smirnov (1959). Sovetskaya geologiya, No. 2.
12. Slepnev, Yu. S. (1959). Geokhimiya, No. 3.
13. Smirnov, S. S. (1937). Izvestiya Akad. Nauk SSSR, ser. geol., No. 6.
14. Solodov, N. A. (1958). Geokhimiya, No. 8.
15. Solodov, N. A. (1959). Geokhimiya, No. 4.
16. Strelkin, M. F. (1947). Olovonosnye Formatsii Pegmatitov, V kn. Geologiya Olova (Tin-bearing pegmatites. In the book: Geology of tin).
17. Fersman, A. E. (1940). Pegmatity, t. 1 (Pegmatites, v. 1). Izd. Akad. Nauk SSSR, Moscow.
18. Yurk, Yu. Yu. (1956). Granity i Pegmatity Ukrainskogo Kristallicheskogo Shchita (Granites and pegmatites of the Ukrainian crystalline shield). Izd. Ukr. Akad. Nauk.
19. Davies, J. F. (1956). Canad. Mining J., 77, No. 4.
20. Johnston, W. D. (1945). Bull. Geol. Soc. America, 56, No. 11.
21. Lacroix, A. (1922). Mineralogie de Madagascar, v. 1., Paris.
22. Pecora, W. T. and J. J. Fahey (1949). Amer. Mineralogist, 34, No. 12
23. Pye, E. G. (1956). Canad. Mining J., 77, No. 4.
24. Quensel, P. (1940-1941). Geol. Fören. Stockholm. förhandl. Bd. 62, h. 3, 1940; Bd. 62, h. 4, 1941.

Received for publication
April 29, 1959

THE USE OF PRIMARY DISPERSION HALOS OF MERCURY IN THE SEARCH FOR LEAD-ZINC DEPOSITS

N. A. OZEROVA
Institute of Geology of Ore Deposits,
Petrography, Mineralogy and Geochemistry,
Academy of Sciences USSR, Moscow

(ABSTRACT)

The primary dispersion halos of mercury were studied on the lead-zinc deposits of the Turkestan mountain range. It is established that the width of the mercury halos over this deposit is 1 — 2 km at a width of the ore zone of 50 — 100 m. The mercury content in the halos averages 5×10^{-6} - 5×10^{-5} per cent, increasing directly over the deposit till ten thousandths of a percent. The dispersion halos of mercury are considerably wider than the dispersion halos of lead.

Sphalerites and fahl ores are the richest in mercury among ore minerals as well as barytes are among the nonmetallic minerals.

The search for lead-zinc deposits is a vital problem at present and various geological, geophysical and geochemical methods are being used to solve it. Any new method which may help in the search is important. Among them, the method of prospecting for lead-zinc ores with the aid of primary dispersion halos of mercury deserves attention.

The mercury dispersion halos were first studied by A. A. Saukov [4] in Dagestan. Using theoretical postulates, he assumed that mercury halos form not only over a quicksilver deposits but over other sulfide deposits as well. Here are some of these theoretical postulates. The chalcophile nature of mercury is indicated, according to Fersman, by its position among the elements of sulfide deposits and on the atomic volume curve and it must, therefore, be concentrated in sulfide deposits. The relatively high mercury content in sulfide minerals and barite cited in Saukov's works

[4, 5] and later in the works of other investigators [1, 2, 11-15] confirms this proposition. Mercury has an exceptionally high vapor pressure and forms a gas phase over hydrothermal solutions. The capacity of mercury vapor to penetrate into surrounding rocks is considerably greater than that of the solutions, and mercury dispersion halso must therefore be much broader than those of the other chalcophile elements of sulfide deposits [4].

The presence of mercury dispersion halos over lead-zinc deposits was mentioned by E. A. Sergeev and A. P. Solovov [7-9]. The investigations by V. Z. Fursov [10] and by the author [3], made under Saukov's supervision, confirm this phenomenon.

The author has studied mercury dispersion halos sinze 1955 at the lead-zinc deposits in the Fergana Karatau and Lyakan districts on the northern slopes of the Turkestan Range.

In most samples mercury was determined by the semiquantitative spectrographic method developed by E. A. Sergeev and A. P. Stepanov at the VITRe [8]. This method determines (3-5) $\cdot 10^{-5}\%$ Hg in a 0.4 g sample and (1-2) $\cdot 10^{-6}\%$ Hg in a 10 g sample. This very sensitive spectrographic method requires a little more time than the less sensitive methods. In a number of monomineralic samples and sulfide ores, mercury was determined by the rapid chemical method devised by A. A. Saukov and N. Kh. Aidin'yan [6]. The samples were analyzed for other elements by the semiquantitative spectrographic method of A. F. Novikova and T. S. Reshetina, in the spectrographic laboratory of the IGEM, Academy of Sciences USSR and in other laboratories.

The geological setting of the Fergana Karatau and Lyakan deposits should be briefly described. The deposits are located in Middle Paleozoic dolomite-limestone and sandstone-conglomerate strata. The dolomite-limestone beds form the anticlinal structures of the Kok-Tyube, Karatau and Guzan mountains; the sandstone-conglomerate beds from the synclinal folds. The ore deposits occur in both the anticlines and synclines.

The Fergana Karatau district contains the Karaotek and Bezymyannoe deposits, and Kok-Tyube, Berkutuyassy, Pereval'noe and Yaryk-tash mineralized areas; the Lyakan district contains the Eski-kan and Kizyl-bel' deposits and the Chil'gazy, Ak-tash, Kumysh-tash and Rudnyi-sai mineralized areas. The mineralization and the localization of the ores was controlled mainly by faults. The ore bodies lie along the faults in small separate lenses and nests. Some of them outcrop, and others have been discovered by exploratory work at depths down to 100 m.

The most abundant ore minerals are galena and sphalerite, with realgar, tetrahedrite, bournonite and pyrite occurring in subordinate amounts. The gangue minerals are barite, calcite, siderite and, less commonly, quartz.

Seventeen composite samples were taken from all of the deposits and prospects of Fergana Karatau and Lyakan. Composite samples were used to determine the average content of mercury and other elements in the ores. The samples were prepared by mixing a large number of channel samples if duplicates of samples for chemical analysis were available; otherwise, they were prepared from bulk samples weighing about 30 kg. The mercury in the composite samples ranged from 4 $\cdot 10^{-4}\%$ to 0.02%, with twelve samples containing thousandths of one percent of mercury (Table 1). To determine the distribution of mercury among ore and gangue minerals, 34 monomineralic samples of ore minerals and 29 samples of gangue minerals were analyzed.

The ore minerals subjected to analysis were galena, sphalerite,

Table 1

Mercury Content in Composite Samples of Ore Taken at Intervals at the Deposits and in Mineralized Areas of the Fergana Karatau and Lyakan Districts

Number in sequence	Deposits and mineralized areas	Number of samples in the composite sample	Mercury content, %
	Fergana Karatau		
1	Karaotek	75*	$3.6 \cdot 10^{-3}$
2	Bezymyannoe	226*	$2 \cdot 10^{-2}$
3	Berkutuyassy	112*	$8.5 \cdot 10^{-3}$
4	Peraval'noe	109*	$1 \cdot 10^{-2}$
5	Yaryk-tash	32*	$3 \cdot 10^{-3}$
6	Kok-tyube, northern area	56*	$3 \cdot 10^{-3}$
7	Kok-tyube, central area	125*	$5 \cdot 10^{-3}$
8	Kok-tyube, southern area	50*	$3 \cdot 10^{-3}$
	Lyakana group		
9	Eski-kan	106*	$4.4 \cdot 10^{-4}$
10	Kizyl-bel', western area	108**	$9.5 \cdot 10^{-3}$
11	Kizyl-bel', eastern area	101**	$3 \cdot 10^{-3}$
12	Zakan	125*	$3 \cdot 10^{-4}$
13	Shor-tang	92**	$7 \cdot 10^{-3}$
14	Ak-tash	79**	$2 \cdot 10^{-3}$
15	Chil'gazy	83**	$9.5 \cdot 10^{-4}$
16	Kumysh-tash	86**	$4 \cdot 10^{-3}$
17	Rudnyi sai	97**	$1 \cdot 10^{-3}$

*Channel samples.
**Bulk samples.

bournonite, tetrahedrite and pyrite (Table 2).* The results of analyses are given in Table 2.

In galenas (10 samples) the mercury content ranges from less than $5 \cdot 10^{-5}$% to hundredths of one percent, and the samples are rather uniformly distributed according to content.

The sphalerites (11 samples) contain from ten thousandths of one percent to 0.03% of mercury, and in five samples mercury constitutes hundredths of one percent. According to V. N. Petrov's data, the mercury

---

*The number of samples of each mineral analyzed for mercury was not he same because the distribution of the minerals in the ores is very irregular and because it is very difficult to obtain pure monomineralic frac- ions of some of the minerals (for example pyrite and tetrahedrite).

Table 2

Mercury Content in Monomineralic Samples of Ore Minerals from Ore Deposits and Mineralized Areas of the Fergana Karatau and Lyakan Districts

Number in sequence	Mineral	Locality	Mercury content, %
1	Galena	Karaotek	0.01
2	"	Bezymyannoe	0.02
3	"	"	0.005
4	"	"	0.00007
5	"	Berkutuyassy	<0.00005
6	"	Yaryk-tash	0.0003
7	"	Kok-tyube, northern area	0.0001
8	"	" southern area	<0.00005
9	"	Eski-kan	0.0004
10	"	Kizyl-bel', eastern area	0.03
11	Sphalerite	Karaotek	0.34*
12	"	Bezymyannoe	0.23*
13	"	" central area	0.02
14	"	" "	0.01
15	"	" "	0.002
16	"	" western area	0.015
17	"	Peraval'noe	0.0005
18	"	Kok-tyube, central area	0.1*
19	"	" "	0.002
20	"	Kizyl-bel', western area	0.01
21	"	" eastern area	0.03
22	Realgar	Bezymyannoe, western area	0.05
23	"	" "	0.0001
24	"	" "	0.00001
25	Bournonite	Kizyl-bel', eastern area	0.0005
26	"	" "	0.0004
27	"	" "	0.0002
28	"	Rudnyi sai	0.00001
29	"	"	0.00001
30	Tetrahedrite	Yaryk-tash	0.01
31	"	Shor-tang	>0.01
32	Pyrite	Karaotek	0.0003
33	"	Eski-kan	0.001
34	"	Zakan	<0.00005

*According to data of V.N. Petrov.

content in the sphalerites of Fergana Karatau is higher, reaching tenths of one percent in three of his samples.

Mercury is very irregularly distributed in realgar. Three samples taken from the same segregation contain from one hundred thousandths to five hundredths of one percent.

Table 3

Mercury Content in Monomineralic Samples of Gangue Minerals from Deposits and Mineralized Areas of Fegana Karatau and Lyakan

Number in sequence	Mineral	Locality	Mercury content, %
1	Barite	Bezymyannoe, central area	0.0004
2	"	" "	0.0004
3	"	" "	0.0002
4	"	" "	0.00003
5	"	" eastern area	0.0003
6	"	Berkutuyassy	0.00005
7	"	"	0.000003
8	Siderite	Kizyl-bel', western area	0.0005
9	"	" "	0.0001
10	"	" "	0.00006
11	"	" "	0.000001
12	Calcite	Karaotek	0.00004
13	"	"	<0.00005
14	"	Bezymyannoe, central area	0.000004
15	"	" western area	0.000001
16	"	" eastern area	0.000003
17	"	Kok-tyube, central area	<0.00005
18	"	Eski-kan	0.00001
19	"	"	0.000004
20	"	Kizyl-bel'	0.0006
21	"	"	0.0001
22	"	"	0.0001
23	"	"	0.00005
24	"	"	0.00003
25	"	"	0.00002
26	"	"	<0.00005
27	"	"	<0.00005
28	"	"	<0.00005
29	"	"	<0.00005

In five analyzed bournonites, mercury content is from ten thousandths to hundred thousandths of one percent.

In tetrahedrites (2 samples) mercury content is one hundredth of one percent and more.

In three pyrite samples the concentration of mercury ranges from less than $5 \cdot 10^{-5}$% to one thousandth of one percent.

Of the gangue minerals, barite, calcite and siderite were analyzed (Table 3).

In barite (7 samples) mercury content ranges from millionths to ten thousandths of one percent, with half of the samples having the latter content.

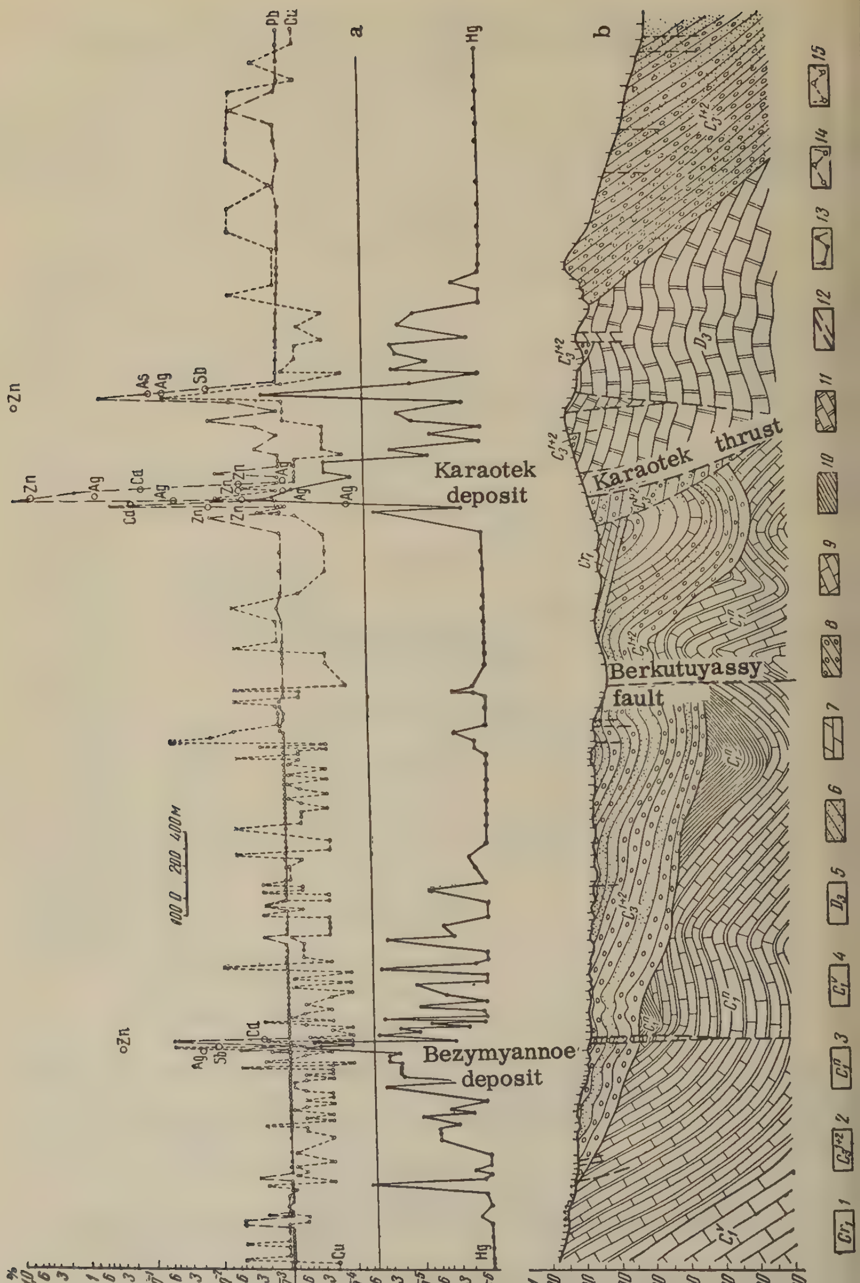
a
b
Karaotek deposit
Bezymyannoe deposit
Karaotek thrust
Berkutuyassy fault
Pb
Cu
Hg
Zn
Ag
Cd
Sb
As
100 0 200 400 м
%
1,0
1·10⁻¹
1·10⁻²
1·10⁻³
1·10⁻⁴
1·10⁻⁵
1·10⁻⁶
м
1600
1400
1200
1000
800
600
400
200
C_3^{1+2}
D_3
C_1^n
C_1^v
Cr_1
1
2
3
4
5
6
7
8
9
10
11
12
13
14
15

Of four siderite samples, two contain ten thousandths of one percent Hg and two, hundred thousandths and millionths of one percent.

Among 18 calcite samples, only three contained ten thousandths of one percent mercury; the rest, hundred thousandths and millionths.

Thus, of the analyzed minerals, the richest in mercury are the sphalerites and tetrahedrites among the ore minerals, and barite among the gangue minerals. In all of these minerals, mercury is probably present as a diadochic substitute, but this is certain only for tetrahedrite and barite [4, 5]. In view of the experimentally demonstrated substitution of Hg^{2+} for Ca^{2+} in fluorite [4], it may be assumed that the high mercury content in calcite also is due to diadochic replacement of calcium by mercury. This hypothesis must be checked experimentally for calcite and other minerals.

Let us turn now to a concrete example of a mercury dispersion halo over a lead-zinc deposit. As an illustration, a section through two deposits in the Fergana Karatau may be used (see drawing). The section cuts across the strike of the main structures. Its length is 7.4 km. Samples were taken at 10 to 100 m intervals, depending on the distance from the deposit, the intervals becoming shorter with approach to it. Altogether, 195 samples were taken along the profile. The samples weighed 50 g, on the average. All samples were analyzed spectrographically for mercury, lead, zinc, copper, silver, arsenic, antimony and a number of other elements.

A study of halos showed that lead halos over the deposits are not extensive. Over the Bezymyannoe deposit in the sandstone-conglomerate beds, the lead halo coincides with the ore zone and is 50-70 m in length along the section. The lead content in the halo is low, varying from a few thousandths to several hundredths of one percent. Over the Karaotek deposit, lying in the limestones, the lead halo is more extensive and measures 800 m, the width of the deposit being about 100 m. Most of the samples from this halo contain thousandths of one percent Pb and only occasionally hundredths and tenths of one percent. Beyond the boundaries of the deposit, lead content is below the sensitivity of analysis, i.e., below one or two thousandths of one percent. Zinc, silver, cadmium, antimony and arsenic occur sporadically in some samples. Copper presents a very complex picture, and although individual samples over the deposit have relatively high copper content (high in the thousandths of one percent and even hundredths of one percent) similar copper concentrations are found beyond the boundaries of the deposit.

Mercury forms the most extensive and clear-cut dispersion halos. Over

---

Graph of distribution of Hg, Pb, Cu and other elements along a section through the Bezymyannoe and Karaotek deposits (Fergana Karatau). Compiled by N.A. Ozerova.

a - limit of sensitivity of spectrographic analysis with small electrodes;
b - geological section based on the data of A.A. Seskutov.

1 - Lower Createaceous sediments; 2 - Upper Carboniferous sediments; 3 - Lower Carboniferous sediments, Namurian stage; 4 - Lower Carboniferous sediments, Visean stage; 5 - Upper Devonian sediments; 6 - sandstones; 7 - marlstones; 8 - conglomerates; 9 - thick-bedded limestones; 10 - argillaceous shales; 11 - dolomites with beds of limestone; 12 - faults; 13 - Hg, 14 - Pb; 15 - Cu

the Bezymyannyi deposit the width of the mercury halo is 1.8 km; over the Karaotek deposit it is 1.2 km; i.e., in the first case it is more than 30 times as wide as the ore zone and its lead halo and in the second, 15 times as wide as the ore zone and 1.5 times as wide as the lead halo. The mercury content in the halos ranges from $5 \cdot 10^{-6}\%$ to $5 \cdot 10^{-5}\%$, rising to $10^{-4}\%$ directly over the deposit and exceptionally to thousandths of one percent.

To determine the normal mercury content in limestones and sandstones, 69 samples were analyzed, taken along the section far from the deposit and beyond its boundaries on the southern slope of the Fergana Karatau Range. Mercury was found in only 15 of the analyzed samples. The mercury content in most of them was $2 \cdot 10^{-6}\%$ and in only a few samples $(3\text{–}4) \cdot 10^{-6}\%$.

It was pointed out by Saukov [4], on the basis of his own data and those of Stock, that the mercury content in limestones and sandstones is below the clarke value. In nine analyses cited by him the mercury content is $1.9 \cdot 10^{-6}\%$ to $4 \cdot 10^{-6}\%$, and in one sample only does it attain the clarke value. Evidently low mercury content is characteristic of limestones and sandstones.

It will be noticed in comparing the data on the mercury halos and those of other elements (see drawing) that there is a direct correlation between high concentrations of mercury and lead and mercury and zinc. This correlation and the relatively high mercury content in the sulfides and in barite indicate that, in the halos, mercury is associated with these minerals. But the high mercury content in rocks is not always accompanied by high concentrations of the other metals. In such cases mercury is not associated with the sulfides in rocks. This is confirmed by a comparison of the mercury content in the rocks and in their heavy fractions*, which consist mainly of pyrite and contain from five to ten times less mercury than the light fractions. Therefore, mercury not only may be associated with sulfides and barite but may permeate the entire rock mass.

In conclusion it is necessary to say a few words about the significance of the sensitivity of the analytical method to be used at lead-zinc deposits, where mercury occurs in small amounts as compared with mercury-bearing minerals.

If the data of spectrographic analyses with sensitivity of $3 \cdot 10^{-5}\%$, which in practice is often reduced to $5 \cdot 10^{-5}\%$, are used, then the mercury halos almost entirely coincide with the lead halos; i.e., they are not extensive, are almost completely confined to the mineralized zone and are of little use in prospecting. In using spectrographic analysis of greater sensitivity, $(1.5\text{–}2) \cdot 10^{-6}\%$, a broad (1–2 km) halo is revealed which may aid in the search for ore (see drawing). To illustrate, among 62 samples taken within the mercury halo over Bezymyannyi, only 7, or 11% of the total samples, have mercury content over $5 \cdot 10^{-5}\%$. When the sensitivity of analysis is increased to $2 \cdot 10^{-6}\%$, the number of samples showing relatively high mercury content increases to 41, i.e., to 66%. This explains why low sensitivity analyses of rocks collected by V. Z. Fursov [10] over concealed ore bodies of the Achisai district disclosed mercury in only 13 of 460 samples. The use of the high sensitivity method at such an extensive deposit would probably have revealed much broader mercury halos and would have aided more effectively in exploration.

---

*Heavy fractions were separated from samples weighing one kilogram. Altogether 84 samples were analyzed and the same number of heavy fractions.

Summary

1. Primary dispersion halos of mercury over lead-zinc deposits may be used in prospecting for new and concealed deposits, for they are tens of times as extensive as the mineralized zones and are delimited from the barren zones by mercury content approximately ten times as high. Mercury halos have a considerable advantage over lead halos, because they are more extensive, a circumstance very important in prospecting.

2. In studying the distribution of mercury in the regions of lead-zinc deposits, it is necessary to use high sensitivity spectrographic analysis capable of detecting $(1-2) \cdot 10^{-6}\%$ Hg. Only this degree of sensitivity will reveal a broad halo over a deposit. When the sensitivity is reduced to $(3-5) \cdot 10^{-5}\%$, the mercury halo narrows to the size of lead halo and sometimes to the size of the deposit itself and thus loses its advantage.

REFERENCES

1. Lazarenko, E. K. (1956). O Bleklykh Rudakh (Gray copper ores). Mineralog. sb. L'vovsk. geol. o-va pri un-te, No. 10.
2. Novokhatskii, I. P. and S. K. Kalinin (1952). O Soderzhanii Rtuti v Nekotorykh Sul'fidnykh Mineralakh (Mercury content in some sulfides), Vestn. AN KazSSR, No. 9.
3. Ozerova, N. A. (1958). O Pervichnykh Oreolakh Rasseyaniya Rtuti nad Mestorozhdeniyami Khaidarkan, Kadamdzhai i Mestorozhdeniyami Ferganskogo Karatau. Materialy Konferentsii Molodykh Uchenykh Posvyashchennoi 40-letiyu Leninskogo Komsomola (On the primary mercury dispersion halos over the Khaidarkan, Kadamdzhai and Fergana Karatau ore deposits. Transactions of the Conference of Young Scientists on the 40th anniversary of the Lenin Komsomol), No. IV.
4. Saukov, A. A. (1946). Geokhimiya Rtuti (Geochemistry of mercury). Tr. In-ta geol. nauk AN SSSR, No. 78, ser. min.-geol., No. 17.
5. Saukov, A. A. (1939). Doklady Akad. Nauk SSSR, 22, No. 5.
6. Saukov, A. A. and N. Kh. Aidin'yan (1941). Zavodsk. laboratoriya, No. 2.
7. Sergeev, E. A. (1957). Metodika Rtutnometricheskikh Issledovanii, v. kn. "Geokhimicheskie Poiski Rudnykh Mestorozhdenii". Tr. Perv. Vsesoyuzn. Soveshchaniya po Geokhimicheskim Metodam Poiskov Rudnykh Mestorozhdenii (Method of prospecting by mercury halos. In the book: Geochemical prospecting for ores. Proceedings of the 1st All-Union Conference on Geochemical Methods of Prospecting).
8. Sergeev, E. A. and P. A. Stepanov (1957). Metodika Spektral'nogo Analiza Metallometricheskikh Prob na Rtut' (Method of spectrographic analysis of metallometric samples for mercury). Izd. VITR, BNTI, L.

9. Solovov, A. P. (1957). Teoriya i Praktika Metallometricheskikh S'emok, v. kn. "Geokhimicheskie Poiski Rudnykh Mestorozhdenii." Tr. Perv. Vsesouyzn. soveshchaniya po Geokhimicheskim Metodam Poiskov Rudnykh Mestorozhdenii (Theory and practice of metallometric surveys. In the book: Geochemical prospecting for ores. Proceedings of the 1st All-Union Conference on Geochemical Methods of Prospecting).

10. Fursov, V. Z. (1958). Geokhimiya, No. 3.

11. Bonska, V. (1956). Změna mřižkové konstanty Hg tetraedritů vlivem různého chemického složeni. Výzkum nerostů tetraedritové skupini, II, Rozpr. ČSAV, Rada, MPV, 66.

12. Cotelo Neiva, J. J. (1956). Considérations sur la géochimie de blendes at de galènes portugaises. Estud. notas e trab. serv. fomentomineiro, N 11.

13. Haberlandt, H. (1953). Die systematische Grundlage und die Fortschritte in der Erforschung der Spurenelemente als geochemische Leitelelemente in Mineralien und Erzen. Fortschr., Mineral 31.

14. Nazmy, A. I. (1957). Beitrag zur Kenntnis ostalpiner Fahlerze, II. Tschermaks mineral. und petrogr. Mitt., 6, N 3.

15. Schroll, E. (1955). Über das Vorkommen einger Spurenmetalle in Blei-Zink-Erzen der ostalpinen Metallprovinz. Tschermaks mineral. und petrogr. Mitt., 3-te Folge, 5, N 3.

Received for publication
May 7, 1959

ON THE GEOCHEMISTRY OF NIOBIUM AND TANTALUM IN THE LOVOZERO ALKALIC MASSIF

V. I. GERASIMOVSKII, M. M. KAKHANA, L. M. RODIONOVA,
and V. A. VENKINA
Vernadskii Institute of Geochemistry
and Analytical Chemistry,
Academy of Sciences, U. S. S. R., Moscow

(ABSTRACT)

In the nepheline syenites of the Lovozero massif (Kola Peninsula), niobium and tantalum are concentrated in minerals which contain titanium and zirconium and isomorphously replaces these elements in them. In the process of formation of rocks of the massif, which, compared to other types of magmatic rocks, is enriched in niobium and tantalum, a separation of niobium from tantalum does not occur. The niobium-tantalum ratio for nepheline syenites is the same (~ 12) for different intrusive phases. An increase of tantalum with respect to niobium is not even observed in rocks considerably enriched in zirconium. Towards the end of the magmatic process an accumulation of niobium and tantalum takes place; their relative concentration compared to titanium increases simultaneously.

As is known, the concentrations of niobium and tantalum in nepheline syenites are high by comparison with other types of magmatic rocks. Attention was first paid to this by V. M. Goldschmidt [1], who gave 0.02% Nb_2O_5 for nepheline syenites.

The content is nepheline syenites, not only of niobium, but simultaneously of tantalum, was given in the work of Rankama and Sahama [2]. According to their data, these rocks have 0.031% Nb and 0.00008 Ta, and the ratio Nb/Ta = 387.5. To clarify the explanation of the authenticity of the contents of tantalum in nepheline syenites and the ratio in them of niobium to tantalum, the authors carried out determinations of Nb and Ta in foyaites, eudialyte- and loparite-lujavrites of the Lovozero massif [3]. They showed that these rocks are enriched not only in niobium, but also in tantalum, and that the ratio Nb/Ta is 11.0-11.8, that is much lower than the above-mentioned figures of Rankama and Sahama. Our data on the lower magnitude of the ratio niobium-tantalum were soon confirmed by the studies of E. M. Es'kova [4] on nepheline syenites (miaskites) of Vishnevy Mt. (Urals). They led for the miaskites to the average magnitude for the ratio Nb/Ta = 11.8 (limits of variation 6.9-21.3).

Below in our paper are discussed new data on the distribution of niobium and tantalum in rocks of the Lovozero massif, which occupies an area of about 650 sq. km. The massif consists of complex bodies, formed in four intrusive phases.

To the first phase are referred the equigranular, porphyritic, poikilitic, and other nepheline syenites; to the second the complex lujavrites, foyaites, and urtites; to the third the eudialyte-bearing lujavrites and the associated porphyritic lujavrites, poikilitic sodalite syenites and tavites; and to the fourth, the complex vein rocks (monchiquites, tinguaites, etc.)

The rocks of the first complex are about 2% of the volume of the massif, the second 80%, the third 18%, the fourth probably not more than 0.01%.

The most widely distributed rocks of the second complex (lujavrites, foyaites, urtites, etc.) form the lower part of the massive with thicknesses up to 1.6 km. They form seams (layers), or, as they are often called, horizons of various thicknesses from some tens of centimeters to some tens of meters, repeatedly alternating with one another, and lying nearly horizontal or at small angles up to 30°. In this rock complex, the lujavrites comprise about 60%, the foyaites 35-36%, and the urtites 4-5%.

In different parts of the massif there are found one and the same layers of rocks of the second complex, arranged in one and the same sequence (usually urtites, foyaite, lujavrite, etc.) varying only in their thicknesses and insignificantly in their stratification [5]. Such exposures of sections of this complex in the whole massif are one of the remarkable features of the constitution of the Lovozero massif.

The rocks of the third complex comprise the upper part of the massif with thicknesses up to 0.45 km. Of them the most widely distributed are eudialyte lujavrites (about 94% of the volume of the rocks of third complex) and less porphyritic lujavrite (5%), poikilitic sodalite syenites and tavites (about 1%).

Among the rocks of the second and third complexes there occur small xenoliths composed of rocks of the first complex. The vein rocks of the fourth intrusive phase are very rare; the thickness of the vein usually does not exceed one meter.

The rocks comprising the massif are in most cases characterized by an excess of alkalies over aluminum. The coefficient of agpaitization of the rocks of the first intrusive phase varies from 0.83 to 1.20, those of the second from 0.84 (urtites) to 2.54 (lujavrites with loparite), of the third from 1.13 to 1.88.

The deficiency of aluminum in relation to the alkalies during the formation of the rock is covered in the first place by iron, which was associated with part of the sodium to form the alkali pyroxene (aegirine) and the rare alkali amphibole (arfvedsonite), which is a rock-forming mineral. The iron content in the rocks is usually very high; from 2.21 to 15.46% FeO + Fe_2O_3, with trivalent iron in most cases greatly predominating over divalent (from 1.2 to 20).

The deficiency of aluminum is compensated for not only by iron, but also by zirconium and titanium with the formation in the rocks of the massif of many zircono-and titano-silicates (eudialyte, lovozerite, lomonosovite, murmanite, lamprophyllite, ramsayite, etc.).

The geochemical fate of niobium and tantalum in the rocks of the massif is closely associated with titanium and zirconium. Independent minerals of niobium and tantalum are not found, with the exception of the rarely encountered pyrochlore. Niboium and tantalum are found in those minerals that contain titanium (loparite, lomonosovite-murmanite, lamprophyllite, ramsayite, etc.) or zirconium (eudialyte, lovozerite, etc.). This is explained by the fact that titanium and zirconium generally greatly predominate over niobium and tantalum in quantitative ratio (see Table 1). Because the ionic radii of niobium (Nb^{+5} 0.69Å) and of tantalum (Ta^{+5} 0.69Å) are close to those of titanium (Ti^{+4} 0.64Å) and also of zirconium (Zr^{+4} 0.87Å), niobium and tantalum during the formation of agpaitic rocks do not form independent minerals, but are concentrated in the minerals of titanium and zirconium, replacing them isomorphously. For example, in loparite there is 39.65-40.78% TiO_2, 8.04-9.74% Nb_2O_5, and 0.62-0.75% Ta_2O_5; in murmanite 29.51-30.40% TiO_2, 6.56-7.71% Nb_2O_5, and 0.50-0.56% Ta_2O_5; in eudialyte 12-14% ZrO_2 and 0.60-1.16% $(Nb, Ta)_2O_5$. The replacement of titanium and zirconium by niobium and tantalum probably is by the scheme $(Nb, Ta)^{+5} + Na^{+1} \rightarrow Ti^{+4} + Ca^{+2}$, or $(Nb, Ta)^{+5} + 2\,Na^{+1} + TR^{+3} \rightarrow Ti^{+4} + 3Ca^{+2}$, or $Nb^{+5} + Na^{+1} \rightarrow Zr^{+4} + Ca^{+2}$, or $Nb^{+5} + TR^{+3} \rightarrow 2Zr^{+4}$.

Our results on the contents of niobium and tantalum in the rocks of the massif are given in Table 1.

The determination of niobium and tantalum was carried out by two methods - chemical and x-ray spectral. The chemical determinations of the elements were made colorimetrically; Niobium was determined by the thiocyanate method, based on the reaction of niobium with sulfocyanic acid in hydrochloric acid solution. Thereby there is formed a complex compound, niobium oxo-thiocyanate, $H[NbO(SCN)_4]$, which is extracted from aqueous solutions by ether. This method was developed and studied by I. P. Alimarin and R. L. Podval'naya [6]. A rapid variation of this was given by N. S. Poluektov [7].

Tantalum was determined with para-dimethyl-amino-phenylfluorone by the method of V. I. Nazarenko, which is based on the extraction of tantalum by a mixture of acetone and isobutanol from solutions containing hydrofluoric and sulfuric acids and ammonium sulfate. After tantalum is extracted, it is determined by the colorimetric method with paradimethylaminophenylfluorone.

The x-ray spectral analyses of the studied samples were carried out with preliminary chemical enrichment, which was done in two stages: the first-enrichment with phenylarsonic acid, the second by tannin [7].

The x-ray spectral determinations of Nb and Ta were carried out by the method of primary excitation with the help of a short-wave spectrograph of the Koshua type with x-ray tubes, described previously [8]. The concentrations of niobium and tantalum were determined by comparison of the intensities of the lines $TaL\alpha_1$ and $NbK\alpha_{1,2}$ in the studied samples and in standard mixtures. The analytical lines mentioned were recorded, corresponding to the first and second series of reflections, by the photographic method. To carry out the analysis, a group of three samples and a standard mixture, being brought to the four faces of the anticathode of the x-ray tube, were exposed in turn on a single spectrogram under strictly constant experimental conditions, with 40 kV, 15 mA, duration 15-30 minutes. We used X-ray photofilm of type XX.

Table 1

Contents of Nb, Ta, Ti, and Zr in rocks of the Lovozero massif

No. Sample	Name of rock	Locality	Content in %						Ratio $\frac{Nb}{Ta}$		Ratios		
			Chemical analyses				X-ray Spec. anal.		Chem. anal.	X-ray Spec. anal.	$\frac{Ti}{Nb+Ta}$	$\frac{Zr+Hf}{Nb+Ta}$	$\frac{Zr+Hf+Ti}{Nb+Ta}$
			Zr+Hf	Ti	Nb $n \cdot 10^{-2}$	Ta $n \cdot 10^{-3}$	Nb $n \cdot 10^{-2}$	Ta $n \cdot 10^{-3}$					
	Rocks of the first intrusive phase												
139	Equigranular nepheline syenite	Ninchurt Mt.	0,215	0,845	—	—	3,17	1,68	—	18,8	25,6	6,5	32,1
69	" " "	" "		0,612	2,4	2,8	2,8	2,1	8,5	13,5	22,8—20,3		
183	Porphyritic nepheline syenite	Alluaiv Mt.	0,102	0,69			3,6	1,93		18,7	18,15	4,2	22,35
186a	" " "	" "		0,66	3,5	3,1	3,8	3,3	11,1	11,6	17,3—16,0		
193	" " "	" "		0,683	3,5	3,5	3,0	2,0	10,0	14,2	16,7—21,3		
188a	" " "	" "		0,46	3,5	3,1	3,9	2,8	11,1	14,0	12,2		
66	Poikilitic nepheline-hydrosodalite syenite	Suoluaiv Mt.	0,152	0,61			2,77	2,25		15,5	21,04	5,05	26,09
431	Poikilitic "hydrosodalite" syenite	Tavaiok R.		0,623	1,47		1,76	1,4		13,0	32,8		
196	" " "	Alluaiv Mt.	0,074	0,59			2,25	1,7		13,0	24,2	3,08	27,28
	Rocks of the second intrusive phase												
276	Urtite	Alluaiv Mt.		0,384	4,0	3,4	4,4	3,5	11,6	13,5	8,95—8,08		
132	Ijolite-urtite	" "		0,30	4,2	4,6	3,1	2,2	9,0	14,0	6,55—9,01		
187	" "	" "	0,099	0,396			4,74	3,4		13,89	7,77	1,98	9,75
14b	" "	Karnasurt Mt.	0,094	0,24			0,9	0,56		16,0	25,1	9,8	34,9
143	Foyaite	" "	0,360	0,55	4,4	4,0	4,78	2,16	11,0	22,1	11,5—11,0	7,2	18,7
144	"	" "	0,320	0,65	2,6	2,0	3,2	2,1	13,0	15,24	22,9—18,57	9,4	31,13
182b	"	Alluaiv Mt.		0,41	5,8	6,1	5,5	3,0	9,7	18,6	6,4—7,03		
272	"	" "		0,587	3,5	3,3	3,7	1,8	10,6	21,6	15,2—17,57		
130	"	" "		0,62	4,4	4,2	5,7	3,8	10,2	15,2	12,9—10,2		
26b	Lujavrite leucocratic	Karnasurt Mt.	0,0925	0,62			7,2	5,3		13,56	8,02	1,2	9,22
26	" mesocratic	" "	0,268	0,80			6,6	5,5		12,0	11,3	3,72	15,02
8	" amphibolitic	" "	0,203	0,83			5,2	2,97		17,2	15,1	3,7	18,8

Table 1 (Continued)

No. Sample	Name of rock	Locality	Content in %						Ratio $\frac{Nb}{Ta}$ X-ray		Ratios		
			Chemical analyses				X-ray Spec. anal.		Chem. anal.	Spec. anal.	$\frac{Ti}{Nb+Ta}$	$\frac{Zr+Hf}{Nb+Ta}$	$\frac{Zr+Hf+Ti}{Nb+Ta}$
			Zr+Hf	Ti	Nb	Ta	Nb	Ta					
124	Lujavrite amphibolitic	Alluaiv Mt.		0,77	6,4	4,1	6,1	4,0	16,0	16,0	11,3—11,8		
19	" "	Karnasurt Mt.		0,70	4,2	3,4	3,7	2,6	12,3	14,5	15,5—17,6		
362	" with loparite	Parguaiv Mt.		1,04	13,4	13,5	12,0	8,6	10,0		6,8		
264	" " "	Alluaiv Mt.	0,481	1,16			12,0	8,67		13,3	8,92	3,7	12,62
190	" and eudialyte	" "		0,995	10,5	10,5	12,0	10,9	10,0	11,9	9,1—7,64		
Rocks of the third intrusive phase													
168a	Lujavrite with eudialyte	Alluaiv Mt.		0,74	8,75	7,4	9,6	7,2	11,75	13,3	7,8—7,23		
168b	" " "	" "		0,49	8,4	9,0	11,0	9,3	9,3	11,8	5,3		
170	Porphyritic lujavrite	" "		0,25	3,25	3,25	3,5	3,0	10,0	11.4	7,0		
249	" with murmanite	" "		0,66	9,8	10,0	9,5	7,0	9,8	14,5	6,2		
106	Porphyritic with lovozerite	Vavnbed Mt.	0,114	1,32			16,0	9,2		17,0	7,77	6,72	14,49
141	Poikilitic sodalite syenite	Chinglusuai R.	0,203	0,74			5,9	3,2		18,6	11,94	3,15	15,09
266	" " "	Tulbnynai R.	0,108	0,58			3,65	2,0		18,2	15,26	2,85	18,11
92	" " "	Uelkuai R.		0,44	3,5	3,2			10,8		11,6		
430	Tavite	Tavaiok R.	0,195	0,59	4,0	5,0			8,0		13,1	5,93	18,93
Rocks of the fourth intrusive phase													
1393	Monchiquite	Karnasarf Mt.		1,68	1,1	1,1			10,0		140		
XXII	"	Alluaiv Mt.		1,72	0,87	1,22	1,1	1,1	7,2	10,0	172		

Average of the massif: 0,71% Ti; $7{,}014\cdot10^{-2}$% Nb; $5{,}85\cdot10^{-3}$% Ta; $\frac{Nb}{Ta}=12$; $\frac{Ti}{Nb+Ta}=9{,}2$; $\frac{Zr+Hf}{Nb+Ta}=4{,}4$

Note: Comma represents decimal point.

Calculation of the concentrations of the elements analyzed for is comparatively simple with this type of film, because it has a sufficiently large interval of blackening, with a straight-line course of the dependence of blackening to the magnitude of the intensity of the emission. For the copper lines $CuK\alpha_1$ ($\lambda = 1534.40X$), and consequently also for the nearby line of tantalum $L\alpha$ ($\lambda = 1518.80X$), the linear part of the curve $S = S\ (I)$ extends approximately to $S = \sim 1$, in consequence of which the calculation of the concentration of tantalum is carried out in this interval without conversion of the scale of blackening. For the radiation used for niobium, $K\alpha_1$ ($\lambda = 744.65X$), the curve $S = S\ (I)$ is linear only up to magnitudes of blackening approximating 0.5–0.6. To determine the contents of niobium and tantalum in the samples, the intensities of the analytical lines were calculated by the method of interpolation, based on the measured ratios of blackening of the doublet $K\alpha_{1,2}$ of niobium. On each individual photograph there was found the magnitude of the ratio $SNb\alpha_1 : SNb\alpha_2 = q$ (where $S = S_{peak} - S_{background}$). The magnitude q may thus represent the distortion in the process of photographing the relative intensities of any two lines, if the true ratio of intensities equals 2.02 ($INb\alpha_1 : INb\alpha_2 = 2.02$). In our case, the small distortion we assume for the latter increases linearly from the point $I_1 : I_2 = 1$, where $S_1 : S_2 = 1$, up to the point $I_1 : I_2 = 2.02$, corresponding to our measurement $Sa_1 : Sa_2 = q$. In this assumption we use the interpolation linear correction $K = \frac{I_1 : I_2}{S_1 : S_2} = f(S_1 : S_2)$, suitable between the points $K = 1$ to $K = 2.02/q$ for some possible magnitudes of the parameter q (see illustration.)

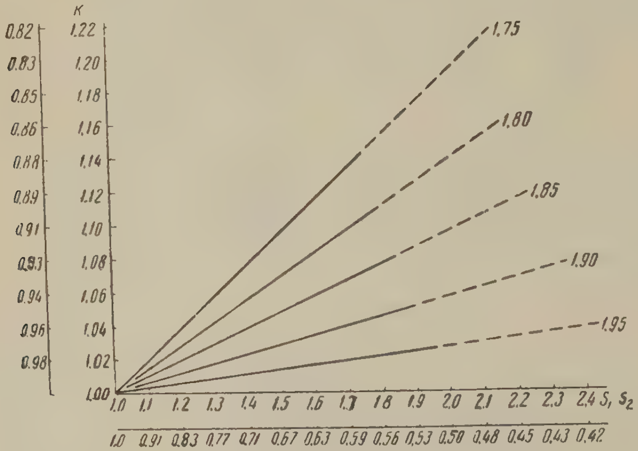

Graph of correction for the calculation of relative intensities of analytical lines. (for convenience the correction is entered on the inner scale if $S_1 > S_2$ and on the outer if $S_1 < S_2$, where S_1 and S_2 correspond to the blackening of the analytical lines of the element in samples and the standard mixture.

Note: Comma represents decimal point.

The corrections necessary in conducting analyses for the calculation of the relative intensities of any two lines are found easily by means of this graph. For the axes of the latter, for convenience we have also plotted the reverse magnitudes corresponding to the case $S_1 < S_2$. Tests showed that the graph of corrections may be used practically for magnitudes of $S_1 : S_2$ somewhat exceeding q (dotted extensions of the straight lines). To determine the contents of niobium, where both components of the doublet may be used, this implies the possibility of comparison of the analytical lines up to a five - or six-fold ratio of the concentration of the element.

The given method for the calculation of intensities by work with the x-ray film of type XX gives excellent agreement with results obtained by analysis of samples on the basis of different analytical lines, and also by using standard mixtures differing in composition (see Table 2.)

The data given in Table 1 show that the contents of niobium and tantalum in nepheline syenites of the massif range within the wide limits from 0.009 to 0.160% Nb and from 0.0006 to 0.013% Ta, and sometimes more.

The massif on the whole is undoubtedly characterized by its high contents of niobium and tantalum, both as compared to nepheline syenites of other areas and to other types of magmatic rocks.

The average contents of niobium and tantalum in the Lovozero massif equal 0.070% Nb and 0.00395% Ta, whereas that of nepheline syenites as given by Goldschmidt [1] is 0.02% Nb_2O_5, according to Sahama and Rankama [2] 0.031% Nb, Borodin [9] 0.008-0.030% Nb_2O_5, and in the miaskites of Vishnevy Mts., according to Es'kova [4] 0.25% Nb and 0.0021% Ta. According to Vinogradov [10], the average contents of niobium and tantalum in acid rocks equals 0.002% Nb and 0.00035% Ta, and in the ultrabasic 0.0015% Nb and 0.000075% Ta.

Table 2

No. of Photograph	Sample	Compared lines of Nb K_1 and K_2		$S_1 : S_2$	q	Correction K	Result of analysis (% Nb)	
		Sample	Standard				Without correction	Corrected
1417	123/2	α_1 α_2	α_1 α_2	1,51 0,84	1,80	0,07 0,97	2,26 2,52	2,42 2,44
1420	249/1	α_1 α_2	α_2 α_2	0,85 1,95	1,80	0,98 0,89	0,64 0,77	0,63 0,68
1659	21/49	α_1 α_2	α_1 1	1,43 0,84	1,65	1,11 0,95	14,3 16,8	15,9 16,0
1414	123/1	α_2 α_2	α_1 α_2	0,74 1,28	1,70	0,93 0,07	4,44 3,84	4,12 4,10
1514	U-21	α_1 α_2 α_1	$\left.\begin{matrix}\alpha_1\\\alpha_2\end{matrix}\right\}$ α_2	0,86 1,52	1,80	0,98 1,07	2,58 2,28	2,52 2,44

Note: Comma represents decimal point.

In the Lovozero massif there has occurred accumulation of niobium and tantalum at the end of the magmatic process. For example, the average content of niobium and tantalum in the rocks of the first intrusive phase euqals 0.0296% Nb, 0.00228% Ta; in the second phase 0.0630% Nb, 0.0052% Ta; and in the third phase 0.1064% Nb, 0.0090% Ta. The ratio niobium/tantalum in the rocks of the massif varies from 8 to 21.6; for the massif as a whole it equals 12.

The analogous number 11.8 was obtained for the miaskites of the Vishnevy Mts. [4]. The ratio found for niobium to tantalum in the rocks of the Lovozero massif is analogous to those for the main types of magmatic rocks. They range, according to Rankama and Sahama [2] from 4.8 (granite) to 17.3 (gabbro).

In the process of formation of the Lovozero massif, the separation of niobium and tantalum did not occur, as is clearly seen from comparison of the magnitudes of the niobium/tantalum ratios in rocks of the various intrusive phases, see Table 1. This is not even reflected in the pegmatic phase. For example, in eudialyte from pegmatite, there is 0.30% Nb and 0.0295% Ta, Nb/Ta = 10, murmanite has 5.40% Nb, 0.41% Ta, Nb/Ta = 13, Ti/Nb + Ta = 3.0; in segirine 0.0846% Nb, 0.0065% Ta, 0.89% Ti, Nb/Ta = 13, Ti/Nb + Ta = 9.8; loparite 6.19% Nb, 0.56% Ta, Nb/Ta = 11.1, Ti/Nb + Ta = 3.6.

In most cases there is observed a dependence of the Nb and Ta contents on those of Ti or Zr. This is expressed in the fact that there is more titanium and zirconium in the rock than niobium and tantalum.

The magnitude of the ratio of titanium to the sum of niobium and tantalum in the rocks ranges from 5.3 to 32.8, averaging about 9.2; that of $\frac{Zr + Hf}{Nb + Ta}$ from 1.2 to 9.8, averaging 4.4. The average magnitude of the ratio $\frac{Ti}{Nb + Ta}$ in rocks of the third phase is about 6.0, whereas it is 21.2 in the rocks of the first phase. This shows that there is an increase of niobium and tantalum with respect to titanium at the end of the magmatic process, the more so, because the content of titanium in the rocks of the third phase is higher (0.92% Ti) than in the rocks of the first phase (0.64%).

The highest relative concentration of niobium and tantalum with respect to titanium in the rocks of the third phase leads to this: in them niobium and tantalum enter not only into the crystal lattices of titanium-containing minerals, but also into zirconium minerals (eudialyte, lovozerite) in which the content of niobium and tantalum reaches 1.16% $(Nb, Ta)_2O_5$. One must note that zirconium in the rocks of the third complex is somewhat higher (0.96% Zr + Hf) than titanium (0.92% Ti).

The highest absolute concentrations of niobium and tantalum, as mentioned above, are generally observed in minerals with high contents of titanium (loparite, lomonosovite-murmanite, etc.). In these minerals there occurs concentration of Nb and Ta with respect to titanium. For example, the magnitude of the ratio Ti/Nb + Ta varies from 3 to 4 in loparite, and is about 3 in murmanite.

Despite the high absolute concentrations of niobium and tantalum, and also their relative concentration with respect to titanium and zirconium, independent minerals of niobium and tantalum are absent in the rocks of the Lovozero massif, with the exception of the rarely found pyrochlore, genetically associated with rocks of the first complex. The latter are characterized by low coefficients of agpaitization, low contents of Nb and Ta, and high magnitudes of the ratio Ti/Nb + Ta.

The question arises, why in the rocks of the third complex, enriched in Nb and Ta and characterized by low magnitudes of the ratio Ti/Nb + Ta, there is absent any independent mineral of niobium and tantalum, but in the rocks of the first phase, poor in these elements and having a high magnitude of the ratio Ti/Nb(Nb + Ta), pyrochlore appears. The explanation of this, probably, must be sought in the composition of the melt from which these rocks are formed, and, in the first place, in the ratios of the alkalies and alumina. The rocks of the second and third complexes are characterized by high coefficients of agpaitization. In them the deficiency of aluminum is covered by titanium and zirconium, with the formation of titanozirconosilicates, in the crystal structure of which niobium and tantalum enter, ismorphously replacing Ti and Zr in them. This is aided by the alkalies, especially Na. The latter enters into the composition of all zircono-and titano-silicates. During the replacement of quadrivalent titanium and zirconium by quinquevalent niobium and tantalum, it is necessary to have a corresponding compensation of charge, which may occur, for example, by the simultaneous replacement of Ca^{+2} by Na^{+1}, as mentioned above, according to the scheme $(Nb, Ta)^{+5} + Na^{+1} = Ti(Zr)^{+4} + Ca^{+2}$, or $(Nb, Ta)^{+5} + 2\,Na^{+1} + TR^{+3} = Ti(Zr)^{+4} + 3\,Ca^{+2}$. These schemes of replacement in agpaitic rocks are very probable, because they have an excess of alkalies over aluminum, unfavorable for miaskitic rocks. In the latter, because of the lack of an excess of alkalies, the ismorphous entry of niobium and tantalum into the crystal structure of titanium-containing minerals is less favorable, which leads to the concentration of Nb and Ta at the end of the magmatic process and the formation of an independent niobium mineral, pyrochlore. In miaskitic rocks, with the absence of enrichment of an excess of alkalies over aluminum, the role of zirconium and titanium is different.

In them in place of eudialyte and lovozerite, zircon appears; in place of the titanosilicates, usually containing Na and rare earths, there are formed calcium titano-silicates (sphene, ilmenite, titanomagnetite, etc.)

In the rocks of the massif there occurs an accumulation at the end of the magmatic process not only of niobium and tantalum, but also of zirconium and hafnium. In the rocks of the first complex, the average content of zirconium and hafnium equals 0.167% $(Zr, Hf)O_2$; of the second complex, 0.285%, and of the third 1.30%. The magnitude of the niobium: tantalum ratio is analogous in rocks with high and in rocks with low contents of zirconium and hafnium. Even in eudialyte with a content of 8.2% ZrO_2 the magnitude of the ratio Nb/Ta is 11.2 (x) ray spectral analysis)-12.2 (chemical analysis, entirely similar to that for the majority of the rocks of the massif (see Table 1). Separation of niobium from tantalum does not occur even in rocks greatly enriched in zirconium.

Determinations of niobium and tantalum were made on monchiquites - vein rocks belonging to the fourth intrusive phase. They contain more titanium and less niobium and tantalum than the nepheline syenites.

Titanium greatly predominates (140-170 fold) over the sum of Nb and Ta, although the magnitude of the ratio Nb/Ta is the same as for the series (about 10) as for the nepheline syenites (averaging 12).

Conclusions

1. Niobium and tantalum in the massif have a geochemical history in common with titanium and zirconium, which they replace isomorphously in

titanium- and zirconium-containing minerals. The highest concentrations of niobium and tantalum occur in titanium minerals. In most cases, a dependence is observed between the contents of Nb and Ta with Ti or Zr, so that the more Ti and Zr are in the rock, the more niobium and tantalum in them.

2. The contents of niobium and tantalum in the nepheline syenites of the massif are higher than in the same rocks from other regions, or in other types of magmatic rocks (acid and basic).

3. Accumulation of niobium and tantalum occurs at the end of the magmatic process. The rocks of the third phase are enriched in this element over the rocks of the first or secondary phases. There was also observed the relative accumulation of Nb and Ta with respect to titanium. In the rocks of the first phase, the ratio Ti/Nb(Nb ± Ta) = 21; in those of the third phase, about 6.

4. In the process of formation of the rocks of the Lovozero massif, there occurred no separation of niobium from tantalum, because the ratio Nb/Ta is the same for rocks of the various intrusive phases. In the minerals from pegmatites, the magnitude of this ratio is the same as in the rocks.

5. In rocks both with high and with low contents of zirconium, the magnitude of the Nb/Ta ratio is nearly the same. There is no increase in tantalum relative to niobium in rocks considerably enriched in zirconium.

In conclusion, the authors express thanks to Yu B. Kholina, who carried out the determinations of titanium in the rocks of the Lovozero massif.

REFERENCES

1. Goldschmidt, V. M. Principles of the distribution of the chemical elements in minerals and rocks. Collected works on the geochemistry of rare elements, GONTI NKTP, U. S. S. R., 1938.
2. Rankama, K., and Th. Sahama. Geochemistry, Chicago, 1950.
3. Gerasimovskii, V. I., M. M. Kakhana, and L. M. Rodionova, Geokhimiya 1957, No. 5.
4. Es'kova, E. M. Geokhimiya 1959, No. 2
5. Gerasimovskii, V. I. Doklady Akad. Nauk SSSR 56, No. 9 (1947).
6. Alimarin, I. P., and R. P. Podvelnaya. Zh. analyt. Khim. 1, 30 (1946).
7. Analysis of mineral ores, Goskhimizdat, 1959.
8. Pavlenko, A. S., E. E. Vainshtein, and M. M. Kakhana. Geokhimiya 1958, No. 6.
9. Borodin, L. S. Doklady Akad. Nauk SSSR 103, No. 6 (1955).
10. Vinogradov, A. P. Geokhimiya 1956, No. 1.

Received for publication
June 11, 1959

DISCUSSION

DISCUSSION OF THE POSITION OF ALKALI METALS IN THE STRUCTURE OF BERYL

V. A. FRANK-KAMENETSKII
Department of Crystallography, University of Leningrad

A paper by A. A. Beus [1], in Geokhimiya, No. 3, 1959, discusses the position of the alkali metal ions in the structure of beryl. The author comes to the conclusion that the entry of the alkali ions into beryl is accompanied by the transfer of a part of the aluminum ions from octahedral into tetrahedral coordination, the 4-coordinated Al ions replacing beryllium in the tetrahedra. According to Beus, the smaller alkali ions (Li, Na) take the place of the 6-coordinated aluminum, while the larger ones (Cs, K) occupy the hollow channels in the structure of beryl.

The incorrectness of this interpretation of diadochy in alkali beryls was clearly pointed out by N. V. Belov [2] on the basis of the chemical data (the constant number of Al and Si ions, 2 and 6, respectively, and the constant sum of the alkali ions and Be, equaling 3), cited by Beus as the starting point for his discussion of diadochy, and on the basis of general crystallochemical considerations permitting the diadochic replacement of Be by Li in the tetrahedral coordination. Agreeing entirely with Belov's arguments, I consider it my duty to comment on the problem, because the data on the diadochy in alkali beryls based on x-ray analysis, published by myself and T. A. Sosedko [3], were inaccurately interpreted in Beus' paper [1] and our conclusions about the position of the alkali metals in beryl were pronounced incorrect without justification.

It should be noted at the outset that the regular increase of parameter c in the beryl lattice with increase in the content of alkali metals and the constancy of parameter a, first established by us, provides a more solid basis for interpretation of the position of the alkali metals in the beryl structure than the data from chemical analyses used for this purpose before [1, 4]. The correlation between the compositions of beryls and the dimensions of the corresponding unit cells given in our work ([3], Fig. 1, Table 2) indicate quite definitely that the increase in lattice parameter c is connected with the increase in the average thickness of the Al-Be layer in the beryl structure, and this, together with the chemical relationships, leads to the conclusion that it is beryllium that is replaced by the alkali ions. The artificiality of Beus's idea of the transfer of a part of Al into tetrahedral positions to replace Be has been adequately discussed by Belov [2], and it is only necessary to mention here that our data ([3], Table 2) also contradict Beus's hypothesis.

In discussing the position of the alkali metals in the beryl structure, we suggested [3] that the diadochic substitution here is of the type involving replacement and change of position. The alkali metals crowd Be from the tetrahedra and become distributed in the Al-Be layers in the channels bounded at top and bottom by the hexagonal silicon-oxygen rings. Having abandoned the idea of transfer of a part of the Al ions into tetrahedral positions, we must exclude also the second part of Beus's scheme of diadochy in beryl, which requires that the smaller alkali ions (Li, Na) replace Al in octahedral positions. It should be mentioned in connection with Belov's [2] hypothesis, adequately documented by geochemical considerations, that the smallest of the alkali ions, Li, unlike the larger alkali ions (Na, Cs), may assume the "acid" function and replace Be in the tetrahedra rather than enter the hollow channels in the beryl structure, and this does not in any way contradict our data.

In the light of our data on diadochy in alkali beryls derived from x-ray analysis which provide information on the variation in the lattice parameters, the scheme of diadochic substitutions proposed by Beus [1] is invalid. His objections ([1], pp. 278-279) to our interpretation of this phenomenon seems to us to be without basis, and his statement that our views are identical with those of A.I. Ginzburg is not quite correct.

As for the refinement introduced into our scheme by Belov [2] concerning the position of the smallest alkali ion, Li, in the structure of beryl, this concept, although tempting, at present has no other basis than crystallochemical analogy. As a matter of fact, our analyses of alkali beryls do not show equality between atomic amounts of Li and (Na + Cs) as they "normally" should if Belov's point of view were accepted [2, 5]. In some cases the smaller alkali ions are fewer than the larger ones (Na, Cs); in other cases they are in excess. It seems to us that the ideal vorobjevite with the formula $CsLiBe_2Al_2[Si_6O_{18}]$ is an exception rather than the rule.

REFERENCES

1. Beus, A.A. Geokhimiya, No. 3, (1959).
2. Belov, N.V. Geokhimiya, No. 3, (1959).
3. Frank-Kamenetskii, V.A., and T.A. Sosedko. Doklady, Akad. Nauk SSSR, 118, No. 4 (1957).
4. Ginzburg, A.I. K Voprosu o Khimicheskom Sostave Berilla (On the chemical composition of beryl). Trudy Mineral. Muzeya, Akad. Nauk SSSR, No. 7 (1955).
5. Belov, N.V. Ocherki po Strukturnoi Mineralogii. IX, 54. O Kislotnou Funktsii Litiya (Essays in structural mineralogy. IX, 54. On the "acid" function of lithium). Sb. Lvov Geol. Soc. No. 12 (1958).

Received for publication
August 12, 1959

Geokhimiya began publication in 1956 under the able editorship of A. P. Vinogradov. It is the Soviet counterpart of Geochimica et Cosmochimica Acta, having practically identical fields of interest and coverage and publishing approximately the same number of pages per year. With the great increase in geochemical research in the U. S. S. R., there have come into being a number of highly specialized journals in geochemistry and related fields. It is probably better to begin translating this more general journal first and follow with some of the more specialized ones if interest appears to justify this course of action and if the financial arrangements can be made.

An initial grant from the National Science Foundation in 1958 enabled the Geochemical Society to translate and publish the eight issues for that calendar year. These issues have been very well received by a growing list of subscribers in most of the countries of the Western world.

The issues for 1956 and 1957 have been translated and may be ordered from the Society, c/o Translation Editor, at current subscription prices (see inside front cover).

The National Science Foundation has continued to be most cooperative in this venture. They are continuing support of the project although subscriptions are too few to make it anything like self supporting thus far. It is hoped that subscribers will call attention of other interested workers to the availability of the translation of Geokhimiya so that these important research papers can be made more generally available to those interested in geochemical and related investigations.

Earl Ingerson
Translation Editor
Department of Geology
The University of Texas
Austin 12, Texas

In matters of subscription for Geokhimiya refer to: Moskva K-104, Pushkinskaya, 23, Akademkniga. Chief Editor: A. P. Vinogradov. Editorial Council: V. I. Baranov, K. A. Vlasov, V. I. Gerasimovskii, D. S. Korzhinskii, A. A. Saukov, N. I. Khitarov (Responsible Secretary), V. V. Shcherbina (Deputy Chief Editor).

Geochemical News is an informal bi-monthly newsletter published by the Geochemical Society and sent without charge to all of its members. It contains news of the activities of the Society, such as summaries of Council Meetings, reports of committees and plans for the future. It also includes announcements of forthcoming meetings and symposia of interest to geochemists, personalia, announcements or short reviews of books of geochemical interest, information on translations and translation services, letters and short notes by members, etc.

Subscriptions are available to institutions at $2.00 per year. Orders should be sent to the Treasurer:

Dr. George T. Faust
U. S. Geological Survey
Washington 25, D. C.

Individuals who wish to receive the *News* should join the Geochemical Society. Application blanks are available on request from the Secretary, Dr. F. R. Boyd, Geophysical Laboratory, 2801 Upton Street, N. W., Washington 8, D. C. Dues are $2.00 per year.

Geochimica et Cosmochimica Acta is the official journal of the Geochemical Society. It is an international journal interested in the broad aspects of geochemistry, both geographically and subject-wise; articles have been received from contributors from all of the (inhabited) continents.

New chemical data and interpretations involving chemical principles are emphasized. For example, papers in chemical mineralogy, petrology, oceanography and volcanology are acceptable, as are those in the chemistry of meteorites, whereas it would be suggested that those in descriptive mineralogy and volcanology, petrography, physical and biological oceanography and physical meteoritics, be sent to other journals specializing in these subjects.

Thus, the subject coverage is closely similar to that of *Geokhimiya*. Also, the number of pages published per year is of the same order of magnitude. Subscription prices are as follows:

To members of the Geochemical Society----- $10.00 per year
To other individual subscribers ------------ $20.00 per year
To libraries, laboratories, and other institutional subscribers
------------ $46.50 per year

Orders for subscriptions should be sent to: Pergamon Press, 122 E. 55th Street, New York 22, New York or Headington Hill Hall, Oxford, England.